



LUND UNIVERSITY

The polar protein α -synuclein - An electrifying journey from chaos to order

Pálmadóttir, Tinna

2024

Document Version:
Other version

[Link to publication](#)

Citation for published version (APA):

Pálmadóttir, T. (2024). *The polar protein α -synuclein - An electrifying journey from chaos to order*. Lund University.

Total number of authors:

1

General rights

Unless other specific re-use rights are stated the following general rights apply:

Copyright and moral rights for the publications made accessible in the public portal are retained by the authors and/or other copyright owners and it is a condition of accessing publications that users recognise and abide by the legal requirements associated with these rights.

- Users may download and print one copy of any publication from the public portal for the purpose of private study or research.
- You may not further distribute the material or use it for any profit-making activity or commercial gain
- You may freely distribute the URL identifying the publication in the public portal

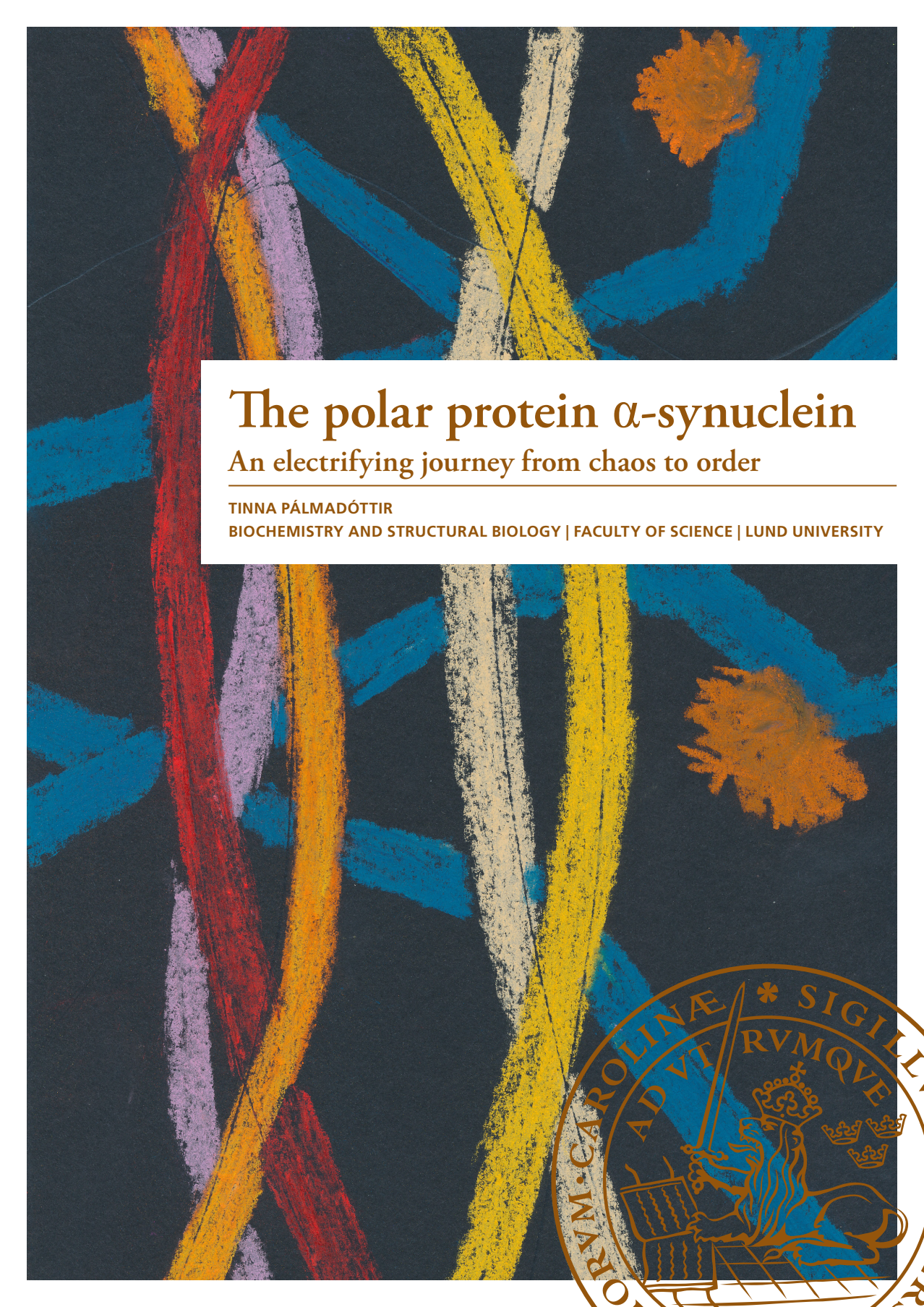
Read more about Creative commons licenses: <https://creativecommons.org/licenses/>

Take down policy

If you believe that this document breaches copyright please contact us providing details, and we will remove access to the work immediately and investigate your claim.

LUND UNIVERSITY

PO Box 117
221 00 Lund
+46 46-222 00 00



The polar protein α -synuclein

An electrifying journey from chaos to order

TINNA PÁLMADÓTTIR

BIOCHEMISTRY AND STRUCTURAL BIOLOGY | FACULTY OF SCIENCE | LUND UNIVERSITY



The polar protein α -synuclein

An electrifying journey from chaos to order

Tinna Pálmadóttir



LUND
UNIVERSITY

Thesis for the degree of Doctor of Philosophy

Thesis advisors:

Prof. Sara Linse, Assoc. Prof. Anders Malmendal, Thom Leiding

Faculty opponent:

Prof. Pernilla Wittung-Stafshede

To be presented, with the permission of the Faculty of Science of Lund University, for public criticism in lecture hall A, Kemicentrum on Wednesday, the 29th of January 2025 at 09:15.

Organization LUND UNIVERSITY Biochemistry and Structural Biology Box 124 SE-221 00 LUND Sweden		Document name LICENTIATE THESIS	
		Date of disputation 2025-01-29	
Author(s) Tinna Pálmadóttir		Sponsoring organization	
Title and subtitle The polar protein α -synuclein-An electrifying journey from chaos to order			
Abstract <p>The accumulation of amyloid fibrils from the protein α-synuclein is a pathological hallmark of Parkinson's disease. α-synuclein is a highly polar protein with a remarkable primary structure that can be divided into three regions: the slightly basic N-terminal region, a central hydrophobic region, and a highly acidic C-terminal tail. The C-terminal tail is of specific focus in this thesis. A change in pH of almost one unit was measured upon fibril formation, indicating upshifts in the pK_a values of monomers in fibrils compared to monomers in solution. This can be related to the proximity of the charges in and between different tails surrounding the fibril core. The number of acidic residues significantly altered the rate and pH dependence of α-synuclein amyloid formation. A decrease in the number of acidic residues within the tail was found to shift the optimal pH range for secondary nucleation to lower pH. These results can be related to a smaller increase in the pK_a values upon fibril formation for the mutants in comparison to the wild-type, resulting in a downshift in the pI value and thus affecting the relative contribution of various intra- and inter-molecular interactions. Furthermore, the interaction of free monomers with the fibril surface of two chemically identical but structurally distinct morphologies was studied. The two morphologies formed under identical conditions, presumably due to similar kinetic barriers. In both cases, the positively charged N-terminus was found to be attracted to the negatively charged fibril surface, to what extent differed between the two morphologies. These results further emphasize the role of electrostatic interactions in the amyloid formation, with particular relevance for secondary nucleation. The solubility and, thus, the stability varied between the two fibril morphologies. However, with time, the samples will become dominated by the more stable fibril morphology. The aggregation of α-synuclein in the presence of the molecular chaperone DNAJB6b was studied under mildly acidic conditions, showing a retardation effect at sub-stoichiometric ratios. The results show strong indications of the formation of α-synuclein-DNAJB6b co-aggregates. The co-aggregates were found to have higher apparent solubility, which may be related to the high chemical potential of the chaperone alone. The free energy of the system as a whole may thus be lower for co-aggregates compared to α-synuclein fibrils co-existing with free chaperone in solution. Lastly, the method "photo-induced cross-linking of unmodified proteins" was optimized for studying α-synuclein oligomers. We find that good control of the reaction time is crucial.</p>			
Key words α -synuclein, amyloid formation, protein aggregation, electrostatic interactions, pKa values, pKa perturbations, C-terminal tail, solubility, stability, fibril morphology, DNAJB6, co-aggregates			
Classification system and/or index terms (if any)			
Supplementary bibliographical information		Language English	
ISSN and key title		ISBN 978-91-8104-333-4 (print) 978-91-8104-334-1 (pdf)	
Recipient's notes		Number of pages 326	Price
		Security classification	

I, the undersigned, being the copyright owner of the abstract of the above-mentioned dissertation, hereby grant to all reference sources the permission to publish and disseminate the abstract of the above-mentioned dissertation.

Signature _____

Date 2024-11-26 _____

The polar protein α -synuclein

An electrifying journey from chaos to order

Tinna Pálmadóttir



LUND
UNIVERSITY

Cover illustration front: by my father Pálmi Hinriksson. An abstract representation of my work

Cover illustration back: by my children Mitra Ísold (purple) and Rökkvi Kian (blue)

Pages 1-126 © Tinna Pálmadóttir 2025

Paper I © American Chemical Society

Paper II © MDPI

Paper III © by the authors (manuscript unpublished)

Paper IV © American Chemical Society

Paper V © by the authors (manuscript unpublished)

Faculty of Science, Biochemistry and Structural Biology

ISBN: 978-91-8104-333-4 (print)

ISBN: 978-91-8104-334-1 (pdf)

Printed in Sweden by Media-Tryck, Lund University, Lund 2024



Media-Tryck is a Nordic Swan Ecolabel certified provider of printed material. Read more about our environmental work at www.mediatryck.lu.se

MADE IN SWEDEN 

*Dedicated to
Mitra Ísold and Rökkvi Kian*

Contents

List of publications	ii
My contributions to papers	v
Popular science summary	vi
Á mannamáli	viii
Acknowledgements	xi
Abbreviations	xiv
Preface	xvi
1 From proteins to amyloids	1
1.1 Proteins	1
1.2 Protein folding and misfolding	2
1.3 Amyloid fibrils	3
1.4 Amyloid fibril morphologies	5
2 Amyloid fibril formation	7
2.1 Mechanism and kinetics of amyloid formation	7
2.1.1 The microscopic kinetic processes	9
2.2 Pre-nucleation species	11
2.2.1 Oligomers	12
2.2.2 Liquid like condensates	13
2.3 Amyloid formation in the presence of chaperones	14
2.3.1 The molecular chaperone DNAJB6b	14
3 α-synuclein	17
3.1 The sequence of α -synuclein	19
3.2 The structure of α -synuclein	19
3.3 The formation of α -synuclein fibrils	21
4 The role of electrostatic interactions in α-synuclein fibril formation	23
4.1 The fundamentals of pH and pK_a values	25
4.1.1 Acid-base equilibrium	25
4.1.2 Auto-ionization of water	26
4.1.3 pH values	26
4.1.4 The relationship between pH, K_a and pK_a	27

4.1.5	pK_a values of amino acid residues	29
4.1.6	pK_a perturbations	29
4.2	Electrostatic interactions and α -synuclein fibril formation . . .	32
4.2.1	The C-terminal tail	32
4.2.2	Electrostatic effects on the aggregation mechanism . .	33
4.2.3	pK_a upshift of acidic residues of α -synuclein	34
4.2.4	Transient intra- and inter-molecular interactions of the C-terminal tail	35
5	Stability and solubility of amyloid fibrils	37
5.1	Relationship between solubility and stability	37
5.2	Kinetic versus thermodynamic stability	40
5.3	Relationship between solubility and reversibility	41
5.4	Effect of chaperones on solubility	43
6	Methodology	47
6.1	Preparation of α -synuclein samples	47
6.2	Formation of amyloid fibrils	49
6.3	Aggregation kinetics	49
6.4	Confirming the presence of fibrils	51
6.5	Determining pK_a shifts upon fibril formation	53
6.6	Detecting differences in morphology	57
6.7	Measuring apparent solubility	59
6.8	Photo-induced cross-linking of unmodified proteins	60
7	Summary of thesis work	65
7.1	Paper I	65
7.2	Paper II	71
7.3	Paper III	78
7.4	Paper IV	83
7.5	Paper V	88
8	Conclusion	93
	References	97
	Scientific publications	127

List of publications

This thesis is based on the following publications, referred to by their Roman numerals:

- I **Charge Regulation during Amyloid Formation of α -Synuclein**
Tinna Pálmadóttir, Anders Malmendal, Thom Leiding, Mikael Lund, Sara Linse
Journal of the American Chemical Society, 2021, 143(20)
- II **Morphology-Dependent Interactions between α -Synuclein Monomers and Fibrils**
Tinna Pálmadóttir, Christopher A. Waudby, Katja Bernfur, John Christodoulou, Sara Linse, Anders Malmendal
International Journal of Molecular Sciences, 2023, 24(6)
- III **The Role of α -Synuclein-DNAJB6b Coaggregation in Amyloid Suppression**
Tinna Pálmadóttir, Josef Getaschew, Dev Thacker, Johan Wallerstein, Ulf Olsson, Cecilia Emanuelsson, Sara Linse
to be submitted
- IV **Photo-Induced Cross-Linking of Unmodified α -Synuclein Oligomers**
Lei Ortigosa-Pascual, Thom Leiding, Sara Linse, Tinna Pálmadóttir
ACS Chemical Neuroscience, 2023, 14(17)
- V **On the Role of α -Synuclein C-terminal Acidic Residues**
Tinna Pálmadóttir, Monika Szewczyk, Ricardo Gaspar, Sara Linse
to be submitted

All papers are reproduced with permission of their respective publishers.

Publications not included in this thesis:

I **On the Reversibility of Amyloid Fibril Formation**

Tinna Pálmadóttir, Josef Getachew, Lei Ortigosa-Pascual, Emill Axell, Jiapeng Wei, Ulf Olsson, Tuomas PJ Knowles, Sara Linse
in review

II **Single-vesicle intensity and colocalization fluorescence microscopy to study lipid vesicle fusion, fission, and lipid exchange**

Alexandra Andersson, Marco Fornasier, Katarzyna Makasewicz, **Tinna Pálmadóttir**, Sara Linse, Emma Sparr, Peter Jönsson
Frontiers in Molecular Neuroscience, 2022, 15

My contributions to papers

Paper I

I designed the study together with the co-authors. I expressed and purified non-labelled and ^{15}N -labelled wild-type α -synuclein, performed potentiometric pH measurements, pH indicator experiments, fibril formation kinetics, CD spectroscopy, ANS-fluorescence measurements, and measurements of concentrations at the end of the fibril formation. I prepared the samples for NMR spectroscopy and Cryo-TEM. I did calculations together with my supervisor. I took part in data-analysis. I wrote the first draft of the manuscript and revised the manuscript with input from all co-authors.

Paper II

I designed the study together with AM and SL. I expressed and purified non-labelled and ^{15}N -labelled wild-type α -synuclein. I prepared all monomeric and fibrillar samples for all experiments, performed CD spectroscopy experiments, ThT-titrations experiments, solubility measurements, SDS-PAGE. I prepared the samples for NMR spectroscopy, Cryo-TEM and MS experiments. I took part in data-analysis. I wrote the first draft of the manuscript and revised the manuscript with input from co-authors.

Paper III

I designed the study together with co-authors. I took part in expression and purification of α -synuclein. I took part in aggregation kinetics experiments and in solubility measurements (involving SDS-PAGE and absorbance), and scattering experiments of DNAJB6. I took part in preparing samples for cryo-TEM and analyzed the images. I took part in data-analysis. I wrote the first draft of the manuscript and revised the manuscript with input from co-authors.

Paper IV

I designed the study together with co-authors and supervised the project. I took part in expression and purification of α -synuclein. I performed preliminary experiments with PICUP and took part in designing the reaction chamber. I took part in the writing and the revision of the manuscript.

Paper V

I took part in the design of the study together with co-authors. I expressed and purified wild-type α -synuclein. I prepared all samples for the kinetic experiments within the manuscript. I performed the kinetic experiments and data analysis presented within the manuscript. I wrote the first draft of the manuscript and revised the manuscript with input from my supervisor.

Popular science summary

Proteins are our bodies' tiny workers. Everything we do, from taking a deep breath to blinking our eyes or swallowing our favorite food, involves proteins. Some proteins are like miniature machines, carrying oxygen or pumping water. Others support our body and give us strength, like our muscles. We also have guardian proteins that protect us from diseases. All of these proteins work hard to keep our bodies alive and healthy.

Where do the proteins come from? It all starts with nature's tiniest building blocks, atoms! Similar to LEGO pieces, atoms can be joined together in different ways to form structures called molecules. One group of those structures are the building blocks of proteins, called amino acids. In our bodies, we have 20 different kinds of amino acids, each with a unique character! These 20 amino acids, like beads on a string, can be combined in countless ways to form proteins.

The assembly of those beads is not a random process. Like a modern LEGO box comes with an instruction manual, every cell in our body carries nature's instruction manual: DNA. DNA contains information on how to combine the amino acids into the correct sequence to form proteins.

Similarly, as each origami pattern creates a specific structure, each unique string of beads (amino acids) usually folds into a defined 3D structure, determined by the amino acid sequence itself. This 3D structure is the functional form of most proteins, allowing it to do the work for which it has evolved. The protein at heart in my studies is an exception and belongs to a group of proteins with no 3D structure. Instead, such proteins remain unfolded, like silk ribbons dancing through the air. These proteins are called intrinsically disordered proteins, and their flexibility is crucial for their tasks.

Although most proteins have their own unique 'origami' shape, under certain conditions, they can lose that structure and converge into another kind of structure called amyloids. Amyloids are remarkable structures that are highly stable and large on a molecular level. Despite being considered large structures, the diameter of one amyloid structure can be about 10,000 times smaller than the diameter of your hair - it is all relative! All amyloids have the same overall structure, each formed from thousands of identical proteins stacked on top of each other, like a stack of pancakes. Amyloids can also be visualized as long twisting ropes. However, although amyloids share the same overall structure, they can vary on the atomic level and how they are organized inside the rope.

The formation of amyloids can be a toxic process that can result in cell death

and lead to several serious diseases. For example, in Parkinson's disease and Alzheimer's disease, it can lead to death of neuronal cells within our brain. As life expectancy increases, these diseases become more prevalent, making it crucial to understand the process underlying the formation of these fascinating yet very dangerous structures, amyloids.

The key player in my research is the intrinsically disordered protein α -synuclein. Under certain conditions, this protein forms amyloid structures in the brain, which is the hallmark of Parkinson's disease. The protein consists of 140 connected beads (amino acids). Their arrangement is quite particular, where one end of the protein has a net positive charge while the other end is very negatively charged. The protein is thus said to be polar, similar to a rod battery, with one positive and one negative end.

In my doctoral project, we have worked towards increased understanding of the behavior of the protein and which factors affect the formation of those large stable structures, amyloids. From the results, one can conclude that the polarity of the protein has a significant influence on its behavior, both on its tendency to form fibrils and on the formation process itself. The project includes studies on how individual protein molecules and their different ends are attracted to the surface of fibrils, which can significantly impact their multiplication.

Studies were also conducted to obtain information on differences in the solubility and stability of different fibrils. The results show that with increasing time, the systems will consist of the most stable structure. The project also includes studies on the effects of other proteins, called chaperones, on amyloid formation. Chaperones are like tiny guardians, and when they are present, α -synuclein amyloids form more slowly and form different types of structures. The project also involved developing and optimizing methods for studying fibrils, as well as small toxic structures that form during the process of amyloid formation.

Á mannamáli

Prótein vinna verkin í líkama okkar. Allt sem við gerum felur í sér vinnu próteina, eins og t.d. að anda, blikka augunum, taka bita af mat og að hugsa. Prótein eru eins og agnarsmáir vinnumenn, þar sem hver og einn hefur sitt hlutverk. Sumum próteinum má líkja við litlar fullkomnar vélar sem sjá til dæmis um að flytja súrefni um líkamann eða dæla vatni yfir himnur. Önnur gefa líkama okkar stuðning og hreyfigetu og enn önnur vernda okkur gegn sjúkdómum. Próteinin í líkama okkar vinna hörðum höndum að því að halda okkur lifandi og heilbrigðum, öllum stundum.

En hvernig verða prótein til? Hvaðan koma þau? Það má rekja til minnstu byggingareininga náttúrunnar, atóma! Á svipaðan hátt og LEGO-kubbar, geta atóm tengst saman á mismunandi hátt og myndað byggingar sem við köllum sameindir. Ein gerð af þessum sameindum eru byggingareiningar próteina, sem kallast amínósýrur. Í líkama okkar finnast 20 mismunandi amínósýrur, og hver og ein hefur sitt sérkenni. Þessar mismundi amínósýrur geta svo tengst saman á nánast óendanlega marga vegu, eins og perlur á þræði, og myndað það sem við köllum prótein.

Röðin á perlunum (uppröðun amínósýra) er ekki tilviljunarkennt ferli. Rétt eins og hver LEGO-kassi kemur með leiðbeiningum, inniheldur hver fruma í líkama okkar leiðbeiningar, sem við þekkjum sem DNA. DNA-ið inniheldur upplýsingar um hvaða og hversu margar amínósýrur eigi að tengja saman til að mynda ákveðið prótein.

Hver einstaka amínósýru röð þakast svo saman í ákveðna þrívíddarbyggingu sem er ákvörðuð af amínósýruröðinni sjálfri. Þessi þrívíddarbygging er hið virka form flestra próteina og gerir þeim kleift að vinna þau verk sem þau hafa þróast til að leysa af hendi. Próteinið sem ég vinn með í verkefninu mínu er hins vegar undantekning frá þessu og tilheyrir hópi próteina sem hafa ekki neina ákveðna þrívíddarbyggingu og má því líkja við silkiborða sem sveigist um í loftinu. Þessi prótein kallast edlislega óregluleg (e. intrinsically disordered) prótein og er sveigjanleiki þeirra nauðsynlegur fyrir þau verk sem þau sinna.

Þrátt fyrir að flest prótein hafi sína sérstæðu byggingu, þá geta flest öll undir ákveðnum aðstæðum tapað þessari edlislægu byggingu og í staðin farið að þakast saman á rangan hátt og myndað gerð af byggingu sem kallast mýlildi (e. amyloids). Mýlildi eru stórfenglegar byggingar, sem eru einstaklega stöðugar og stórar á sameindastigi (e. molecular level). Þrátt fyrir að mýlildi séu talin stór, þá getur þvermálið á hárinu okkar verið um 10.000 sinnum stærra en

Þvermálið á einu mýlildi. Heildarbygging allra mýlilda er mjög sambærileg, þar sem hvert mýlildi er myndað úr þúsundum eins próteina sem raðast hvort ofaná hvort annað, á svipaðan hátt og bunki af amerískum pönnukökum. Við getum líka séð mýlildi fyrir okkur sem löng snúin reipi. Þrátt fyrir að heildarbygging þeirra sé í megindráttum eins, þá getur bygging mýlilda verið mismunandi á frumeindastigi.

Myndun mýlilda er eitrað ferli og getur leitt til frumudauða. Sem dæmi má taka að ferlið getur leitt til dauða á taugafrumum í heila okkar og valdið alvarlegum sjúkdómum eins og t.d. Parkinsonsjúkdómi og Alzheimersjúkdómi. Með hækkandi meðalaldri eykst tíðni þessara sjúkdóma og það verður sífellt nauðsynlegra að skilja ferlið sem liggur að baki myndun þessara heillandi, en á sama tíma stórhættulegu, bygginga.

Próteinið sem fer með aðalhlutverkið í doktorsverkefni mínu heitir α -synuclein. α -synuclein getur myndað mýlildi í heilanum okkar. Myndun α -synuclein mýlilda getur leitt til Parkinson sjúkdóms. Próteinið samanstendur af 140 aminósýrum og er uppröðun þeirra heldur sértæk, þar sem annar endi próteinsins hefur jákvæða hleðslu, á meðan hinn endinn er mjög neikvætt hlaðinn. Próteinið er því sagt vera skautað (e. polar).

Í doktorsverkefninu mínu hef ég unnið að því að auka skilning á því hvaða þættir hafa áhrif á myndun α -synuclein mýlilda. Verkefnið inniheldur rannsóknir á því hvernig einstakar próteinsameindir og mismunandi endar þeirra dragast að yfirborði mýlilda, sem getur haft mikil áhrif á fjölgun þeirra. Út frá niðurstöðunum má draga þá ályktun að skautun próteinsins hafi mikil áhrif á hegðun þess, bæði á tilhneigingu þess til þess að mynda mýlildi og á myndunarferlið sjálft. Rannsóknir voru einnig gerðar á stöðugleika mismunandi mýlilda, og niðurstöðurnar sýna að með auknum tíma munu kerfin alltaf samanstanda af þeirri byggingu sem hefur hæsta stöðugleikann. Verkefnið inniheldur einnig rannsóknir á áhrifum annarra próteina, svokallaðra siðgæsluvarða (e. chaperones), á myndun mýlilda. Niðurstöðurnar hafa leitt í ljós að í návist þessara siðgæsluvarða myndast α -synuclein mýlildi hægar og mynda einnig annars konar byggingar. Verkefnið felur líka í sér þróun og bestun aðferða til að rannsaka mýlildi, sem og litlar eitraða byggingar sem myndast á sama tíma og mýlildin.

Acknowledgements

This thesis would never have been completed without the support and help from all the precious people that surround me.

Sara, since I first met you I have been inspired by your love for science. You are, without a doubt, the best supervisor I could ever have wished for. I've tried every trick in the book to extend my time as your PhD student, but I suppose even the best things must come to an end. Thank you for everything you have taught me, for your understanding, and for patiently listening and discussing countless number of questions. I am so enormously thankful and privileged for the opportunity you have given me, and how you have allowed me to explore science and follow my curiosity. You have always been by my side, both in science and life, through fun and exciting times, but also through harder and more challenging times. You are very valuable to me, and I am lucky that you are a part of my life.

Anders, you have been a very important person in my PhD studies. Our paths crossed early in my PhD journey, and for that I am forever grateful! Thank you for all the honest discussion, and sharing your deep insights and wisdom about both science and life. Thank you for all the NMR experiments across Sweden, UK, and Denmark and for bringing me along to different institutes and labs. Your mentorship has meant so much to me, thank you for being my co-supervisor. To my co-supervisor **Thom**, thank you for trusting me with one of the very first versions of your Probe-Drum instrument. Your passion for bringing new ideas to life and your courage to follow your scientific dreams are truly inspiring. **Mikael Lund**, thank you for what you have taught me about simulations and the fun talks about music. **Ulf**, Thank you for so generously sharing your vast knowledge and patiently explaining colloidal chemistry to me. **Cecilia**, thank you for introducing me to DNAJB6, your kindness, and your delicious långkål recipe. **Peter Jönsson** and **Alexandra**, thank you for all the time we spent with the TIRF microscope. **John Christodoulou**, thank you for welcoming me to your lab in UCL. **Chris Waudby** thank you for your collaboration. **Yun-Ru Chen**, thank you for the generous opportunity to work in your laboratory in Academia Sinica, and thanks to your group for the guidance in lab and teaching me about PICUP, with special thanks to **Shih-Han**. **Anna** and **Crispin**, thank you for your help with Cryo-TEM.

Thanks to all past and present members of Sara Linse's research group. **Kalyani**, you are one of the greatest treasures the PhD journey brought into my life. You have taught me what a true friendship is and for that I am forever thankful.

Thank you for all your support. You are a diamond. **Stefán**, this journey would have been so different without you, I really value our friendship. The office still feels empty, and I miss our everyday talks about all and nothing. My dear friend **Xiaoting**, there is only one Xiaoting. Thank you for all the precious memories in lab and around the world! You are such a loyal person. I miss having you close by. Thank you **Diana** for our fun times in lab, all the girls-nights and later, all the mom-chats. **Tania**, I still think about our girl's times, the concerts, late night dancing and long nights in the lab. **Elodie**, thank you for the hikes in Iceland, party preparations in Sweden and the time shared in India, thank you for caring. **Mattias**, thank you for all the fun conference or course adventures, and for the meaningful conversations and laughter we've shared throughout this journey. **Rebecca**, thank you for our lovely walks and conversations, for sharing life's special moments - I miss having my go-to person in the office for all those unwritten rules of PhD life. **Tanja**, you've been such a caring presence and a good listener - I'm especially grateful that we got to share a office space again during the final months of this journey. **Dev**, thank you for being a good friend, I hope we can work on something fun together. **Veronica**, dancing in the lab late nights and laughing as well as deep talks about life is what comes to mind when I think of you. **Lei**, thank you for all the PICUP work and all the fun conversations the last years. **Josef**, it has been a lot of fun working with you on the JB6 project, I look forward to working more together. **Katja**, you are one of those rare people who make everyone feel welcome when asking for help - thank you for all your expertise with mass spec and α -synuclein purifications. **Johan**, thank you for fun chats and the NMR work. **Ricardo**, thank you for teaching me how to purify α -synuclein, that has been so valuable. **Egle**, I miss your warm presence and our conversations in the office. **Martin**, thank you for all the work you do for us in the group and all the help. **Karin Åkerfeldt**, thank you for bringing such as positive energy to the lab everytime you visit. **Birgitta**, **Eimantas** and **Erik**, thank you for all the work you have done with maintaining the lab and making it function so well. **Andreas**, thank you for the chats and making sure I would not collapse at my desk the last months. **Ewelina**, I am glad we got to share office for a while, thank you for the octopuses you made for Mitra and Rökkvi, that was very special. I would like to thank **Emil**, for believing in my Swedish skills. **Max**, it has been nice to have someone to share the last sprint of this journey with. **Elin** and **Karolina**, I look forward to work more with you, your positive spirits are so refreshing.

Thanks to all the past and present members of CMPS. **Jennifer**, thank you for being so caring person and loyal friend, I will soon visit Göteborg more often. I specially want to thank, **Magnus** and **Maryam**. Magnus thank you for all your support with computer and technology. Maryam, thank you for all the

important work you do for the department and all the good times. **Tommy** and **Susanna**, thank you for your excellent leadership at CMPS. **Ingemar** and **Kristine**, thank you for all the good conversations and your kindness. Thanks to **LINXS** for allowing me to hijack Daniel's office and **Shandana** for being so sweet and encouraging.

I want to thank all my close friends outside of the department. **Safiya!** when I first met you, I immediately felt in my heart that you were a person I wanted to have in my life. Since then we have been in sync and now 10 years later, we are finishing our PhD at the exact same time with two children each in our arms. **Kena**, **Jason**, **Katarina**, **Milos**, **Linnéa**, and **Fredrik**, and your beautiful children, how lucky I am to have you all as friends, to spend time playing in parks, having dinners together and watching our children develop and play. My dear friends **Snædís**, **Ólöf**, **Likki**, **Valeria**, **Josefine**, **Sinéad**, **Suman** and **Li** thank you for being such good friends and I hope you know how much you matter to me. **Malin**, I can't wait to get more time to create and play music with you - and just talking and being!

Stjærnan, **Mánen** and **Himlagalaxen**. Thank you for taking so well care of Mitra and Rökki during the daytime, so I could work and finish this thesis with peace of mind. I appreciate you.

Mamma og **pabbi**, ég er heppnasta dóttir veraldar. Takk fyrir að vera til staðar fyrir mig öllum stundum, takk fyrir að styðja mig í því að fylgja draumum mínum, takk fyrir að sýna því áhuga sem ég tek mér fyrir hendur, takk fyrir að vera besta amma og afi fyrir Mitru og Rökkva. Takk fyrir að tala við mig í lok hvers einasta dags og hlusta á hvernig allt gengur. Ég elska ykkur. **Birkir** bróðir minn og **Kristín** systir mín, ég veit ekki hvar ég væri án ykkar, þið eruð mér óendanlega verðmæt, einfaldlega lang best. **Vaka**, **Morten**, **Ísak**, **Emilía**, **Hrólfur** og **Unnsteinn** you all matter so much to me. **Niki** och **Askar**, tack för att ni finns här för oss och för all er hjälp. Jag uppskattar er.

While this book represents years of scientific work, my partner and children are the most precious gifts these years have given me. My love and my best friend, **Daniel**, I am forever grateful for you and our life together. Thank you for the immense support, for being there for me every second and loving me for whom I am. Our beautiful children **Mitra Ísold** and **Rökkvi Kian**, það eru ekki til orð sem lýsa því hversu heppin mamma ég er. Þið eruð allt sem ég gæti óskað mér og svo miklu meira en það. Thank you for being you, you mean the world to me. I love you endlessly.

Abbreviations

Here follows a list of the different abbreviations used within the thesis.

$A\beta$	amyloid β
ANS	8-Anilino-1-naphthalenesulfonic acid
APS	ammonium persulfate
CD	circular dichroism
Cryo-TEM	cryogenic transmission electron microscopy
DOSY	diffusion order NMR spectroscopy
<i>E. coli</i>	<i>Escherichia coli</i>
HPLC	high-performance liquid chromatography
HSQC	heteronuclear single quantum coherence
IEX	ion-exchange chromatography
JB6	DNAJB6b
MS	mass spectrometry
NAC	non- $A\beta$ component
NMR	nuclear magnetic resonance
PAGE	polyacrylamide gel electrophoresis
PICUP	photo-induced cross-linking of unmodified proteins
$\text{Ru(II)(bpy)}_3^{2+}$	ruthenium (II) tris-bipyridyldication
SDS	sodium dodecyl sulfate
SEC	size-exclusion chromatography
ThT	thioflavin T
UV	ultraviolet
wt	wild-type

Amino Acid		
Alanine	Ala	A
Arginine	Arg	R
Asparagine	Asn	N
Aspartic acid	Asp	D
Cysteine	Cys	C
Glutamic acid	Glu	E
Glutamine	Gln	Q
Glycine	Gly	G
Histidine	His	H
Isoleucine	Ile	I
Leucine	Leu	L
Lysine	Lys	K
Methionine	Met	M
Phenylalanine	Phe	F
Proline	Pro	P
Serine	Ser	S
Threonine	Thr	T
Tryptophan	Trp	W
Tyrosine	Tyr	Y
Valine	Val	V

Preface

Looking back, my fascination with amyloids can be traced to my high-school years when I studied biochemistry. While walking the corridors of the nursing home where I worked, taking care of people with dementia, I formulated some of the questions that would later shape my scientific path. *Why do some people get Alzheimer's disease? Why do others get Parkinson's disease? What is underlying these diseases?* I did not get the answers I hoped for. The mechanisms behind the diseases were not fully understood.

This wasn't satisfactory for someone as deeply curious as I am. I wanted to understand.

These questions began guiding me toward my bachelor's in biochemistry, where protein science and, more specifically, protein folding and unfolding captured my interest. During this time, I was introduced to amyloids. Those remarkably stable structures fascinated me. How could different proteins converge to form such similar structures? From this point, there was no way back. My next step was a master's in protein science, which brought me here to Sara Linse's research group, where I have been fortunate to spend several years working on the projects presented in this thesis. Along the way, I've begun the long process of answering some of the questions that went unanswered in the nursing home. The path to completing this thesis has been challenging and rewarding, and I can say without doubt that it has been an electrifying journey.

This thesis presents the findings of my doctoral research in Biochemistry. To guide the reader, I would like to outline the structure of the thesis. The thesis starts with giving an **introduction** to my research work. The introduction is divided into five chapters: **Chapter 1** introduces the journey from proteins to amyloids through folding and misfolding. This chapter ends by describing the common structure of amyloids as well as the variations between different amyloid fibril morphologies.

The aim of **chapter 2** is to give an overview of the mechanism and kinetics behind amyloid formation. The different microscopic kinetic processes and the formation of pre-nucleation species during the nucleation processes are described. The chapter ends by exploring the roles chaperones may play in amyloid assembly, with special emphasis on the molecular chaperone DNAJB6.

Chapter 3 introduces α -synuclein, the protein at the heart of all studies within this thesis. An insight into the polar nature of the primary structure is provided, followed by a description of the structure of the protein in solute and solid

phases. This chapter concludes by giving a brief introduction to the formation of α -synuclein fibrils.

Electrostatic interactions, crucial to a large part of my work, are the focus of **chapter 4**. The chapter starts by giving an overview of some fundamental and core concepts, such as pH, pK_a values, and pK_a perturbations. After that, we explore the effect of electrostatic interactions on amyloid fibril formation and how the acidic C-terminal tail may play a crucial role.

The aim of **chapter 5** is to give a more detailed insight into the relationship between solubility and stability of amyloid fibrils. The difference between kinetic and thermodynamic stability is covered. Furthermore, the solubility and stability of different morphologies are introduced, as well as how the solubility and stability of aggregated structures may change in the presence of chaperones.

The aim of **chapter 6** is to give an overview of the developed and applied methodology within the thesis, focusing on experimental approaches applied to address the research questions.

The main findings of this thesis are summarized in **chapter 7**. This thesis is composed of 5 papers. **Paper I** focuses on measuring the change in apparent pK_a values upon fibril formation and demonstrates that the pK_a values of the acidic residues become upshifted for α -synuclein. **Paper II** presents studies of two α -synuclein fibril morphologies of different solubility and stability formed under identical conditions. It includes studies of the interaction of monomers with the fibrils and shows that with time, the samples will become dominated by the more stable morphology. In **paper III**, we study the role of α -synuclein-DNAJB6 co-aggregation in amyloid suppression. The focus of **paper IV** is to improve and optimize the cross-linking method PICUP that can be used in the studies of oligomers. In **paper V**, we study the effect of the high number of acidic residues within the C-terminal tail on α -synuclein aggregation, aiming to better understand the pH dependence of the aggregation mechanisms. The thesis ends with **chapter 8**, where the findings are synthesized.

This thesis follows a top-down structure, starting with broader concepts and moving to increasingly detailed analysis both within and across chapters. Although the chapters are interconnected, they can more or less stand-alone, allowing readers to focus on specific concepts of interest.

I hope this overview helps you navigate through the journey of my work.

Chapter 1

From proteins to amyloids

1.1 Proteins

Proteins, the miniature workhorses of life, were first named in 1838 by the Swedish scientist Berzelius, after the Greek word "proteios," meaning "of first rank"^{1,2}. These fundamental components of life are crucial for the structure, regulation, and function of all living organisms. Protein molecules continuously work to sustain our existence. They have evolved under selective pressure to fulfill myriad unique functions, including catalyzing biochemical reactions, regulating their own production through gene expression, facilitating transportation, signaling, participating in immune responses, providing structural support, and enabling muscle contraction¹.

Proteins are composed of one to several linear and non-branched heteromolecular chains, termed polypeptide chains. These chains are constructed from building blocks known as amino acid residues. There are 20 main amino acids, each with distinct chemical properties. Amino acids are commonly grouped into: polar-charged, polar-non-charged, and hydrophobic residues. They can be arranged into diverse sequences of different lengths. Despite the seemingly modest number, the combinations of these building blocks can produce an astonishing variety of polypeptide chains. These linear chains of amino acid residues is referred to as the primary structure of the proteins^{1,3,4}

1.2 Protein folding and misfolding

Protein folding is a process where the primary structure of a protein, i.e., its amino acid sequence, dictates the intricate arrangement of its polypeptide chain into its native tertiary structure^{1,3-5}. Different segments of the polypeptide chain either locally fold into secondary structures, such as α -helices and β -sheets, or remain largely unstructured (loops or random coils)^{1,3,4}. While the native three-dimensional structure is the functional form of most proteins, some proteins do not fold into well-defined structures and instead stay predominantly unfolded and unstructured. Such proteins are classified as intrinsically disordered proteins (IDPs) and are commonly found to play important roles in various essential cellular functions such as signaling and regulation⁶.

Protein folding is a reversible process, where folded proteins may unfold or denature under specific conditions⁷⁻¹³. Studying the denaturing propensities of proteins provides insights into the stability of the protein structure relative to the unfolded state⁵. Proteins can also misfold and transit into a separate solid phase consisting of aggregates, such as amorphous aggregates and amyloids^{14,15}.

The complex process of protein folding can be conceptually visualized by the schematic representations of protein folding funnels, where the depth of the funnel - y-axis - represents the free energy, and the width of the funnel (x-axis) represents the entropy. This energy landscape contains many energy minimum of varying stabilities, where the proteins pass through various local minima on their way toward the energy minima of a native structure. When proteins fold, they travel from the top of the funnel, from an unfolded conformation with high free energy and high entropy, down to lower energy minima with narrower wells, representing lower free energy and entropy^{14,16,17}.

Aggregated states, such as amorphous aggregates and amyloids, are highly stable and represent separate energy minima from the native structure. At concentration above the critical aggregation concentration, they can be visualized as a separate but connected energy funnel, known as the aggregation funnel^{14,16-18}. The energy minima of the aggregation funnel can be lower than that of the folding funnel and may consist of several local minima, representing aggregates of different structures (different morphologies) of different stabilities¹⁸.

1.3 Amyloid fibrils

Misfolding of proteins into amyloid fibrils is linked to several pathological conditions, such as α -synuclein in Parkinson's disease, amyloid- β -peptide (A β) and tau in Alzheimer's disease, polyQ in Huntington's disease and Islet amyloids polypeptide (IAPP) in type II diabetes^{18–25}. The word amyloid originates from early studies on pathologically associated protein aggregates that showed similar staining properties to starch (amylose, or in Greek amylon)^{26–28}. As life expectancy rises, neurological diseases linked to the pathological formation of amyloid structures are becoming more prevalent. Therefore, an increased understanding of the mechanisms and factors underlying these diseases has become more crucial than ever.

The formation of amyloid fibrils is a reversible, non-covalent, self-assembly process. Amyloid fibrils are highly stable, linear, non-branched, and hierarchical structures^{14,18,29–39}. The characteristic of amyloid fibrils is their cross- β X-ray diffraction pattern that originates from its highly ordered core⁴⁰. The core is comprised of monomers that misfold into β -strands oriented perpendicular to the fibril axis, which, through intermolecular hydrogen bonding form β -sheets aligning parallel to the fibril axis (figure 1.1)^{18,29–39}. The ability to form this characteristic cross- β fibril core has been suggested to be a common inherent property shared between proteins, and thus independent of the amino acid sequence^{28,41}.

Amyloid structures can be visualized as long single stranded "ropes" twisted around each other. Each individual "rope" is built from stacking of identical planes, where the number of molecules per plane can vary. Stacking the planes on top of each other generally results in a slight twist with its handedness governed by the peptide chirality, resulting in an overall helical structure⁴². The arrangement of molecules within these "ropes" can vary between different amyloid proteins. For instance for α -synuclein amyloids, each plane usually consist of one molecule^{35,36,43} while for instance A β amyloids often consist of two molecules per plane^{44–46}. Within the literature, the terms "filament" and "protofilament" are used interchangeably to describe these single-stranded rope-like structures. A single fibril is most commonly built up by packing of more than one "rope" twisting around each other^{33–36,38,42,43,47}. However, single-stranded fibrils (only one rope or filament) have been documented⁴³. The diameter thus varies and depends on the type of proteins, how the monomer folds within a filament, the number of monomers within each plane of a filament, and how different filaments arrange together into the amyloid fibrils. The diameter of amyloid fibrils is commonly found to be between 5–20 nm and the fibrils can

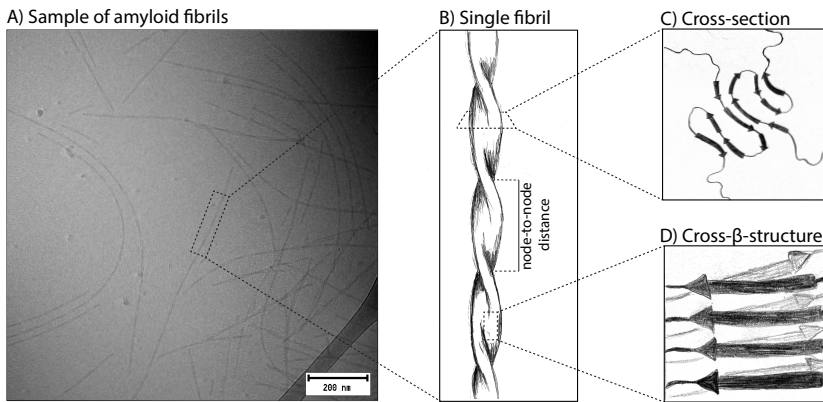


Figure 1.1: Schematic illustration of amyloid fibrils, emphasizing their linear, non-branched and hierarchical structures. A) Cryo-TEM images of a sample consisting of amyloid fibrils. B) Schematic illustration of a single amyloid fibril. C) Illustration showing a cross-section of a fibril consisting of two filaments (view from the top). D) Illustration of the cross- β -structure in the fibril core. The monomers within a fibril misfold into β -strands oriented perpendicular to the fibril axis. Through intermolecular hydrogen bonding, the β -strands from neighbouring monomers form β -sheets running parallel to the fibril axis.

comprise thousands of monomers and have a length of several micrometers⁴².

The interior of amyloid fibrils is generally dominated by hydrophobic and polar-noncharged residues^{33,36,37,39,42}. In literature, hydrophobic interactions and hydrogen bonding have been predominantly reported as the two main stabilizing interactions involved in amyloid fibril formation^{48,49}. However, energy contributions from hydrogen bonds most likely remain relatively unchanged between the monomeric and fibrillar states as long as the potential hydrogen bonding sites are satisfied through hydrogen bonding with water or other hydrogen bonding groups in the same or neighboring peptides. Charged and polar residues are, on the other hand, commonly situated at the fibril surface, where electrostatic interactions have been found to modulate fibril stability and interactions with the fibril surface (introduced further in chapter 4)⁵⁰⁻⁵⁶.

1.4 Amyloid fibril morphologies

Over the last decade, the number of solved structural models of amyloid fibrils has increased drastically due to advances within structural biology, particularly in solid state NMR spectroscopy and cryo-electron microscopy^{33,35-37,43,45,46,57}. Despite the shared characteristics of amyloid fibrils, an enormous conformational diversity exists among different amyloid structures. This diversity is observed between fibrils originating from different proteins/peptides and among those formed by the same protein/peptide (figure 1.2). These different amyloid fibril structures can be referred to as different fibril **morphologies**⁴². The formation of the different fibril morphologies is dependent on solution conditions such as pH, ionic strength, temperature, type of buffer, and presence of other molecules^{18,33,34,43,58}.

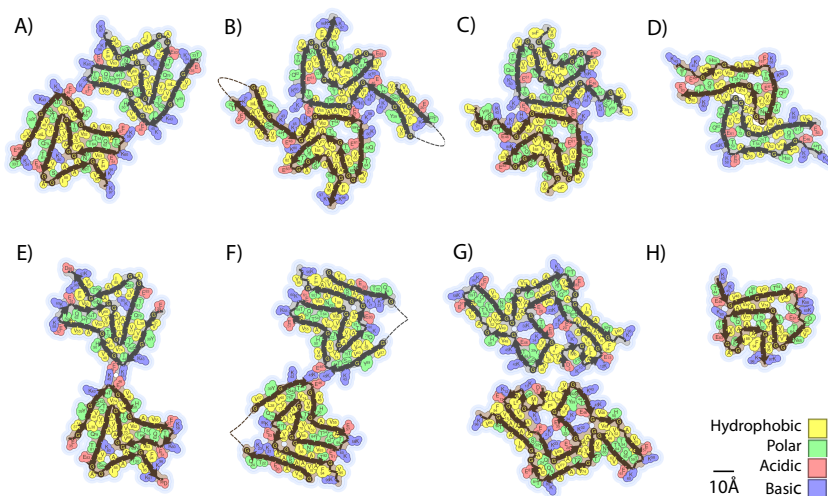


Figure 1.2: Comparison of solved high-resolution structural models of α -synuclein amyloid fibrils. Examples of the variability within different fibril morphologies of recombinant α -synuclein are shown. PDB-IDs: A) 8pix (ordered residues: 33-97) B) 9ck3 (ordered residues:15-22, 36-97) C) 6h6b (ordered residues: 38-95) D) 6cu8 (ordered residues: 48-83) E) 9fyp (ordered residues: 35-98) F) 6sst (ordered residues: 14-25, 36-98), G) 8pk4 (ordered residues: 2-96), H) 2noa (ordered residues:(27-30, 43-97). All models were solved using cryo-electron microscopy except for model H that was solved using solid state NMR spectroscopy and only shows a single filament. All structures are of a full-length α -synuclein, except for C that is of a 1-121 mutant. All illustrations are obtained from the Amyloid Atlas 2024^{42,57}.

Different morphologies may have different intra- and/or inter-molecular contacts, which can be seen by differences in packing of the monomer into filaments (on an atomic level) and/or by differences in packing of filaments into the mature fibrils (figure 1.2)^{18,34,42,43,57,59}. Such differences may result in fibril structures with different characteristics, which can be seen as differences in the node-to-node distance (e.g., straight or curly), length, filament packing, and the number of filaments within the mature fibrils (diameter)^{18,34,58,60,61}. Amyloid fibrils of different morphology can thus have different surface properties; this was documented in **paper II**.

The formation of different morphologies from identical proteins can also occur under identical conditions, in cases of similar nucleation barriers for the morphologies. Samples consisting of more than one morphology are termed **polymorphic (paper II)**^{33,34,43,59,61,62}.

Chapter 2

Amyloid fibril formation

Extensive research has been done in the last decades to understand the microscopic processes underlying amyloid fibril formation^{63–66}. The focus of this chapter is to introduce the different macroscopic and microscopic kinetic processes that may exist, as well as introducing the formation of pre-nucleation species during amyloid fibril formation. The effect of molecular chaperones on the aggregation of amyloidogenic proteins will also be covered, with a specific focus on DNAJB6b.

2.1 Mechanism and kinetics of amyloid formation

Kinetic analyses provide a fundamental framework to conceptualize and mechanistically understand the self-assembly process of amyloid fibril formation^{66,67}. Using various *in vitro* bulk measurement techniques, such as fluorescence and NMR spectroscopy, the accumulation of fibril mass or decrease in free monomer concentration can be monitored over time. A macroscopic characterization of the aggregation can be obtained from such measurements. The formation of amyloid fibrils generally follows a sigmoidal curve, which can, on a macroscopic level, be divided into a **lag phase**, a **growth phase**, and a **plateau phase** (figure 2.1). The midpoint of the sigmoidal curve corresponds to the **half-time** ($t_{1/2}$) and can be defined as the time it takes to reach 50% of the total signal change. This is, in principle, the same as the time point at which the concentration of monomers incorporated into fibrils reaches 50% of the total change in monomer concentration between the initial state and the final plateau.^{65,66,68} (figure 2.1). Throughout the aggregation process, the system is predominantly

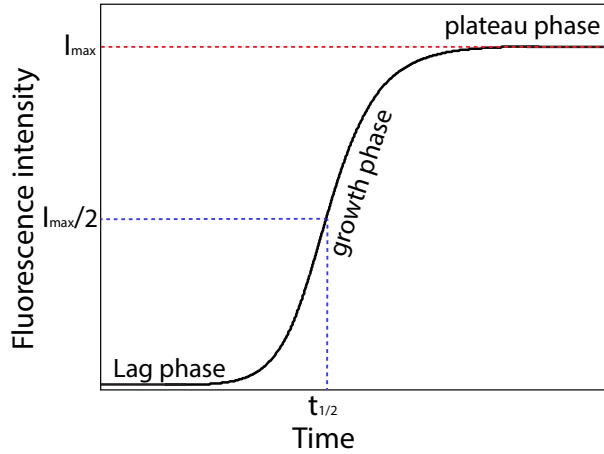


Figure 2.1: Schematic representation of a sigmoidal aggregation curve that reports on the accumulation of fibril mass. Such an aggregation curve can be obtained for example by monitoring a change in the fluorescence of a reporter dye, e.g., Thioflavin T (ThT). In such case, the monomer concentration at each given time point is proportional to the inverse of the fluorescence intensity, relative to the initial signal, plus the solubility. The y-axis represents the fluorescence intensity, where I_{\max} corresponds to the fluorescence intensity at the plateau phase (the maximum amplitude). The x-axis represents the time, where $t_{1/2}$ corresponds to the time it takes to reach 50% of the maximum amplitude signal relative to the initial signal.

populated by monomers and fibrils, while the concentration of other species, such as oligomers, is much lower⁶⁵.

The formation of amyloid fibrils involves several dynamic microscopic processes that can be divided into primary nucleation, secondary nucleation, fragmentation, and elongation (figure 2.2). The different microscopic processes can occur simultaneously during all three different macroscopic phases of amyloid formation, i.e., all the microscopic processes can co-occur from the initial formation of the first nucleus⁶⁹. The different macroscopic kinetic parameters, e.g., lag-time, maximal growth rate, and half-time, therefore, depend on the rate constants of the different microscopic processes. The extent (rates) to which each microscopic process occurs varies across the macroscopic phases of the aggregation^{64,65}. Kinetic analysis is a valuable tool for studying the effect of intrinsic and extrinsic factors on the aggregation mechanism. Some examples of extrinsic factors include pH, temperature, ionic strength, small molecules, chaperones, nanoparticles, and other surfaces. Intrinsic factors involve aspects regarding the protein sequence itself, like truncation and mutations^{65,70}.

Amyloid fibril formation is a linear non-covalent self-assembly process and can be viewed as a **phase transition**, where the protein or the peptides transition from a solution phase (monomers) to a solid phase (fibrils)^{15,71}.

2.1.1 The microscopic kinetic processes

The nucleation process involves the formation of a **critical nucleus**, defined as the smallest nucleated unit that can further grow into mesoscopic structures. Nucleation occurs when a system is put into a non-equilibrium state; for instance, a protein solution becomes unstable at conditions where the total monomer concentration exceeds the **solubility (S)** - the critical concentration (c_c) - of the protein molecule. Above the solubility limit, the most stable state consists of monomers in solution, at the critical concentration, coexisting with aggregated species (fibrils) (introduced further in chapter 5)^{68,72}. This section focuses on introducing the different nucleation and growth processes involved in amyloid fibril formation, when the total concentration of the amyloidogenic protein is above its solubility limit.

Primary nucleation involves the spontaneous formation of stable critical nuclei from monomers, where the addition of monomers is more favorable than dissociation of the monomers. Primary nucleation depends on the monomer concentration⁶⁶ and can be either **homogeneous** or **heterogeneous**. Homogeneous primary nucleation occurs in bulk, and heterogeneous primary nucleation occurs on external surfaces or interfaces, such as liquid-air interfaces, liquid-liquid interfaces, lipid membranes, sample container surfaces, and fibril surfaces originating from other proteins^{68,73-82}.

Another type of homogeneous nucleation process is **secondary nucleation**. It occurs on the surface of existing fibrils formed from identical monomers. Secondary nucleation is dependent on both the monomer concentration and the fibril concentration. Due to the increase in fibril concentration throughout the aggregation process, secondary nucleation becomes an auto-catalytic process, resulting in a close to exponential growth^{66,69,83}. This is in contrast to heterogeneous primary nucleation that occurs on an external surface and is not an auto-catalytic process^{66,68,76,84,85}. Another secondary process is the **fragmentation** of already existing fibrils, resulting in an increased number of fibril-ends. Fragmentation is only dependent on the fibril mass⁶⁶. Lastly, the fibril growth process, **elongation**, involves the addition of monomers to fibril ends and is therefore dependent on both the monomer concentration and the concentration of fibril ends⁶⁶.

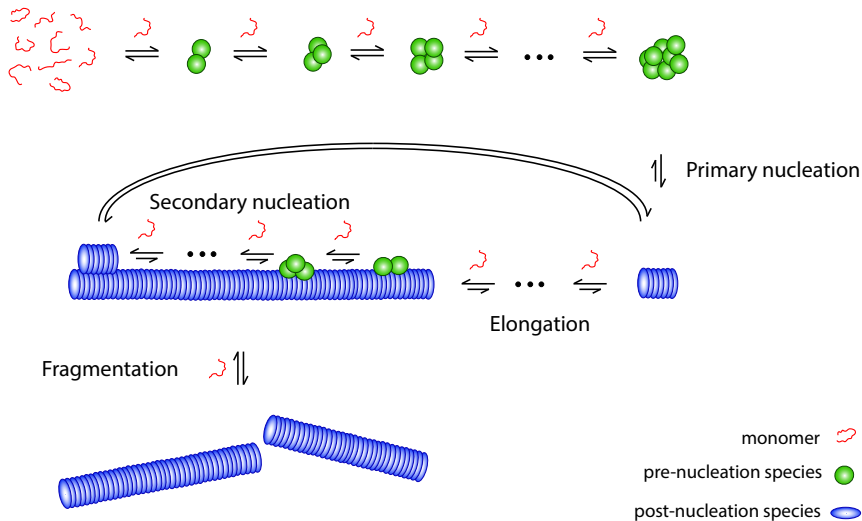


Figure 2.2: A schematic illustration of the microscopic kinetic processes of amyloid fibril formation: primary nucleation, secondary nucleation, elongation, and fragmentation. Monomers free in solution are represented by red curved lines, monomers within pre-nucleation species (such as oligomers and liquid condensates) are represented as green spheres, and blue ellipsoids represent monomers within post-nucleation species (amyloid fibrils).

Primary nucleation and elongation are the two microscopic processes that are essential for fibril formation to occur from a pure monomeric sample (Figure 2.2). However, secondary processes significantly enhance the rate of amyloid fibril formation by affecting the number of existing fibrils, and thereby increasing the fibril surface and fibril ends⁶⁵.

Due to the secondary nucleation aggregation mechanism being an autocatalytic process, the generation of nuclei from secondary nucleation can quickly exceed the number of nuclei generated through primary nucleation. A consequence of this is that the addition of pre-formed fibrils, referred to as seeds, to a supersaturated monomeric solution *in vitro* bypasses the need for primary nucleation to happen, as the seeds serve as templates, which can lead to exponential growth through secondary nucleation^{19,86}. This can be further explained by the energy barriers for primary nucleation being higher than for secondary nucleation and elongation (figure 2.3)⁸⁷.

There is strong evidence that secondary nucleation also occurs *in vivo*^{76,88,89}, which thus can lead to an exponential increase of pathological amyloids within

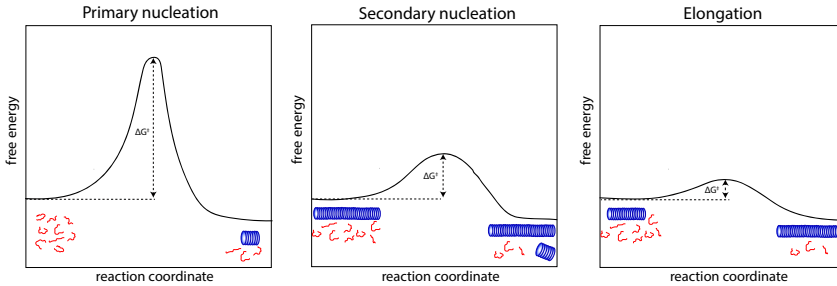


Figure 2.3: Schematic illustration showing the energy barriers of the individual molecular mechanisms. The energy barriers differ, where the activation energy for primary nucleation is higher than for secondary nucleation and elongation.

living systems. Increased knowledge of ways to slow down and inhibit secondary nucleation is therefore crucial for drug development.

2.2 Pre-nucleation species

As mentioned earlier, amyloid fibril formation can be viewed as a **phase transition**, where protein or peptides transition from a solution phase (monomers) to a solid phase (fibrils)^{15,71}. Nucleation is the first step in the transition of the monomers from a solution phase to a solid phase. We have all witnessed phase transitions in our everyday lives. A common example of a gas-liquid phase transition is the water droplets we see on our windows after a cold night. The water droplets result from a phase transition of water vapor in the air to a liquid phase due to cooling at night. The liquid water can then further transit into a solid phase during freezing. The nucleation of water molecules into water droplets is a one-step process that follows the classical nucleation theory, where the energy landscape has only one transition state, and the molecules are, thus, either in the gas phase or a part of the liquid phase^{68,90}.

However, the nucleation of amyloid proteins is more complex and does not follow the classical nucleation theory. It follows a non-classical nucleation theory where the energy landscape is characterized by multiple transition states, involving the formation of various transient intermediates or pre-nucleated species, such as **oligomers** and **liquid condensates**⁶⁸. These intermediates modify the free energy landscape so that the free-energy barriers for nucleation become lower, leading to a phase transition of monomers from a solution phase into a solid phase via the formation of a critical nucleus. However, not all intermedi-

ates do promote an easier way of nucleation. These concepts will be introduced further in the following paragraphs.

2.2.1 Oligomers

Studies suggest that oligomers play a significant role as intermediate species in the nucleation processes (figure 2.2). Oligomers form through the self-assembly of monomers into various structures that are transient in nature as well as smaller and structurally distinct from the amyloid fibrils^{85,91-96}. Compared to amyloid fibrils, oligomers are usually less structured, consisting of fewer β -sheets and having more hydrophobic surface^{85,94,97}. The lifetime or the kinetic stability differs over oligomeric species where the relative values of the association and dissociation rate varies⁹⁶. Oligomers are heterogeneous species, and different oligomeric structures with distinct characteristics are found within the same system^{93,95,96}.

Oligomers can be viewed as pre-nucleation species where structural conversion steps are essential in order for them to nucleate into a critical nucleus. The structure of a critical nucleus is compatible with amyloid fibrils and can thus further grow through elongation⁹³. The growth rate of oligomers is lower than for the post-nucleated species, and the concentration of oligomers relative to monomers and fibrils is low^{93,96}. The likelihood of structural conversion to occur varies between the different oligomeric structures^{95,96,98}. This phenomenon has recently been described by a new quantitative framework where different oligomeric structures can be given a value (pathway index) on the scale of 0 to 1, representing how much they contribute to amyloid fibril formation⁹⁵. The monomers found within oligomeric structures with a low chance of undergoing structural conversions are thus more likely to end up within an amyloid fibril structure through dissociation from such oligomeric structures and the formation of new oligomeric structures with a higher propensity of structural conversion. The structural conversion of oligomers in solution into more ordered and stable amyloid structures can be viewed as a liquid-solid phase transition, where the oligomeric structures transit from solution into a solid phase⁶⁸.

Oligomers can form within the process of both homogeneous and heterogeneous primary nucleation as well as secondary nucleation. As secondary nucleation is an auto-catalytic process, the number of oligomers formed through secondary nucleation can be many times the number of oligomers originating from primary nucleation^{83,85,87,98,99}.

In contrast to monomers and fibrils, oligomers are believed to be central to the

pathology of amyloid diseases where they have been identified as the primary toxic species in amyloid aggregation^{91,99–104}. The different oligomeric structures have been found to differ in toxicity. Properties such as the hydrophobic nature of oligomers have been found to disrupt membranes and thus are a potential cause of their toxicity^{101,104,105}. An increased understanding of oligomers and their link to cell toxicity is, thus, essential. Ways to suppress the number of oligomers formed through, for example, secondary nucleation, are, thus, important for limiting disease progression. However, the detection and characterization of oligomers are challenged by their transient nature and low abundance relative to monomers and fibrils (chapter 6.8)^{83,93,97}. Differences in the lifetime of the various oligomeric species can result in oligomeric species of higher stability and longer lifetime being more accessible and thus more easily examined by the experimental method, causing a bias towards such oligomers⁹⁷. Methods that can be used for capturing the different oligomeric structures are thus necessary (see more chapter 6.8). Utilizing various methods within the study of oligomers can be helpful as established methods could report on distinct groups of oligomers⁹³. This concept is central to **paper IV**, where we optimized and improved a previously established method that can be used to study oligomers formed during the process of amyloid fibril formation. This method is named Photo-Induced-Crosslinking of Unmodified Proteins (PICUP)^{106,107}.

2.2.2 Liquid like condensates

The formation of liquid condensates is an example of a **liquid-liquid phase separation** of a dilute liquid phase and a dense liquid phase^{108–111}. In recent years, such phase separation has more frequently been found to be involved in numerous cellular functions; for example, liquid condensates play a role in the organization of intracellular spaces within the cell and function as non-membrane bound organelles^{112–115}. Liquid condensates are dynamic and transient self-assemblies, and within the cell, they can consist of various bio-molecules, such as protein and RNA^{109,112–114}.

Lately, liquid condensates have also been associated with human diseases, where they have, for example, been recognized as playing a part in the nucleation process of amyloidogenic proteins^{114,116,117}. Proteins with intrinsically disordered regions have been found to be prone to undergo liquid-liquid phase separation, and many of these proteins are linked to amyloid diseases, such as tau in Alzheimer's and α -synuclein in Parkinson's disease^{79,112,114,116,118–120}. This development brings a fresh perspective to the amyloid field, where the formation of liquid condensates is associated with nucleation and phase transition of amy-

loidogenic proteins, reshaping how we think about the underlying processes involved in nucleation.

Compared with the dilute phase (bulk), the increase in local protein concentration within the liquid condensates leads to an increased chance of protein-protein interaction. Liquid condensates of high concentrations of amyloidogenic proteins can, therefore, increase the chance of liquid-to-solid phase transition - nucleation^{68,79}. The interactions between the molecules at an interface differ from those in the dilute phase (bulk). The presence of liquid condensate provides an interface that can serve as new heterogeneous nucleation points by affecting the orientation of the molecules and thereby promoting conformational changes and inducing nucleation^{68,79}. Similar phenomena have been seen for amyloidogenic proteins at fibril and lipid-vesicle surfaces, where particular orientation is preferred and interaction of the molecules are affected^{78,121-126}. There is evidence that the nucleation of amyloidogenic proteins is prone to start at the interface of the condensates and then grow towards the middle of the condensate, giving rise to an in-homogeneous phase of liquid (monomers) and solid species (fibrils) (until the condensate becomes a gel)¹⁰⁹. By that said, condensates have also been found to suppress aggregation and stabilize amyloidogenic proteins^{68,79}.

2.3 Amyloid formation in the presence of chaperones

Molecular chaperones are a group of proteins that play an essential role within the protein quality system by promoting protein folding and preventing misfolding and protein aggregation¹²⁷⁻¹³¹. Molecular chaperones have also been found to slow down the process of amyloid fibril formation *in vitro* and *in vivo*^{130,132-144}. Which microscopic steps are predominantly affected is dependent on both the type of the chaperone and the type of the amyloid protein, and which species along the reaction pathway the chaperone binds to^{136-139,142-145}. Chaperones can also affect the solubility of the amyloid proteins as well as contributing to the dissociation of already formed amyloid fibrils^{130,144-149}.

2.3.1 The molecular chaperone DNAJB6b

DNAJB6b (JB6) belongs to the family of DNAJ/Hsp40 molecular chaperones^{135,150}. In the human body, JB6 is present within multiple organs, including brain neurons, where it has been found within the cytosol and the nucleus¹⁵¹⁻¹⁵³.

JB6 has been identified as a promiscuous inhibitor of amyloid fibril formation, and *in vitro* it has been found to suppress the aggregation of several amyloidogenic proteins, including A β peptide^{138,139,142–144,154,155} and polyglutamine peptide^{140,143}, by both decreasing the rate of aggregation and affecting the apparent solubility¹⁴⁴. JB6 has been found to both interfere with the primary nucleation and the secondary nucleation^{140,142–145}. The decreased rate of primary nucleation has been linked to the interaction between JB6 and oligomers of amyloidogenic proteins. These interactions may stabilize the oligomers and hinder or slow down the structural conversion steps of primary nucleation^{138,142,145}. The potential effect of the chaperone JB6 on the stability and solubility of amyloidogenic proteins will be further introduced in chapter 5.4.

JB6 has been found to form large polydisperse oligomers at concentrations above its critical aggregation concentration^{143,156}. Its smallest subunits (monomers or dimers) have been found to exhibit the capacity to suppress amyloid fibril formation^{138,154,156}. The sequence and structure of JB6 can be divided into three domains: the N-terminal domain (J-domain, residues 1–71), a flexible linker (residues 72–184) and the C-terminal domain (residues 185–241)^{139,143,157,158}. The structure of the α -helical N-terminal domain and the β -sheet rich C-terminal tail have been determined by NMR spectroscopy¹⁵⁷. On the other hand, the linker is less structured and has low sequence complexity. A region corresponding to residues 155–195 contains a high number of serine and threonine residues and is referred to as the S/T-rich region^{144,158}. Previous *in vitro* studies of JB6 have revealed that the elimination of serine and threonine residues from this region reduces its ability to suppress the amyloid formation of A β ₄₀, A β ₄₂ and polyglutamine peptides^{138,144,159}.

JB6 has been linked to reduced risk of Parkinson's disease, with studies showing reduced disease pathology and cell death in mouse and cellular models^{132,160,161}. JB6 has been identified as a component within the core of Lewy bodies, and its expression levels have been found to be elevated in Parkinson's disease patients¹⁵¹. The effect of the molecular chaperone JB6 on the aggregation of the amyloidogenic protein α -synuclein, linked to Parkinson's disease (see chapter 3) was studied in **paper III**. We compare the effect of the wild-type to that of a mutant, where 18 serine and threonine residues have been substituted with alanine residues. Furthermore, we study the effect of the chaperone on the apparent solubility of α -synuclein and detect the presence of co-aggregates of α -synuclein and JB6.

Chapter 3

α -synuclein

The human α -synuclein is the protein of interest in this thesis. It is widely distributed within the nervous system, with a particularly high concentration in the presynaptic terminals. α -synuclein has been found to interact with lipid membranes, synaptic proteins, and synaptic vesicles^{162–166}. This is in accordance with *in vivo* studies of α -synuclein, suggesting an involvement in diverse functions, such as synaptic plasticity, neurotransmitter release, and regulation of synaptic vesicle recycling.^{162,167–171} The sequence of α -synuclein is highly conserved within vertebrates; however, studies indicate that α -synuclein is not essential for basal neuronal activity but instead plays an important role in maintaining long-term normal neuronal function^{162,172}.

Apart from its normal functions, the protein can also misfold, forming amyloid fibrils and toxic oligomers. Within the nervous system, α -synuclein amyloid fibrils tend to accumulate into intracellular inclusion bodies, called Lewy bodies, which are the pathological hallmark of synucleinopathies, such as Parkinson's disease^{162,169}. A progressive depletion of dopaminergic neurons in the substantia nigra is characteristic of Parkinson's disease, leading to a decrease in dopamine production. The symptoms include decreased motor system function, such as muscular rigidity and tremors. Examples of symptoms that do not regard the motor system are sleep problems, reduced sense of smell, depression, and dementia^{168,173}.

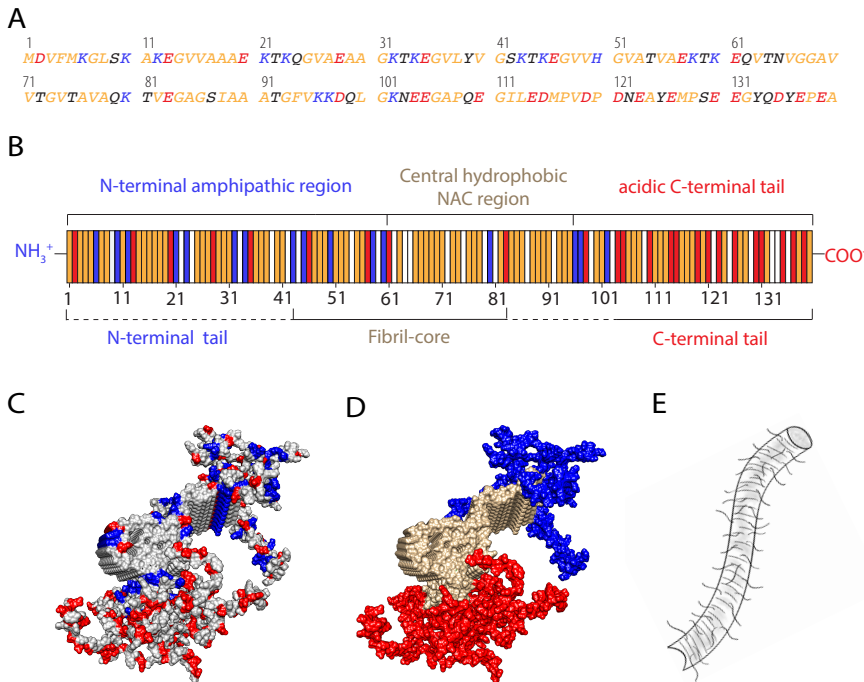


Figure 3.1: Sequence and structure of α -synuclein. A) amino acid sequence, where acidic residues are shown in red, basic in blue, hydrophobic in orange, and polar-non-charged in black. B) Schematic representation of the distribution of the acidic (red), basic (blue), hydrophobic (orange), and non-charged-polar residues (white). Above the residue-illustration, the sequence is divided into three regions according to the properties and residue distribution within the sequence: The N-terminal amphipathic region, the central hydrophobic NAC region, and the C-terminal tail. At the bottom of the residue-illustration, the sequence is divided into three regions according to how the monomer misfolds into the fibril structure: the N-terminal tail, the fibril core, and the C-terminal tail. The part of the sequence corresponding to the fibril core varies between solved structures, ranging from residue 2 to 104. The C-terminal tail remains unstructured in all solved structures (written at the end of 2024). C) A filament structure (PDB: 2noa) colored according to the distribution of acidic (red: Glu and Asp) and basic (blue: Lys and His) residues. D) A filament structure is colored according to the three different regions: N-terminal tail (blue), fibrils core (gold), and C-terminal tail (red). E) The Schematic illustration of α -synuclein fibrils shows the tails forming a fuzzy coat around the fibril core.

3.1 The sequence of α -synuclein

α -synuclein consists of 140 residues and has a molecular weight of 14.5 kDa¹⁷². The primary structure of α -synuclein is characterized by its asymmetric charge distribution. Accordingly, the sequence can be divided into three regions: a basic N-terminal amphipathic region (residues 1-65), a hydrophobic central NAC (non-amyloid β component) region (residues 66-95) and the acidic C-terminal tail (residues 96-140) (figure 3.1)^{172,174,175}. The positive residues of the sequence are mainly found within the N-terminal region, giving the region a net positive charge (at pH below 9.5). There is a historical reason for the name of the NAC region. A peptide with the corresponding sequence was found within amyloid plaques purified from Alzheimer's disease patients, and as not being part of the A β sequence, it was thus consequently given the name non-A β component (NAC)¹⁷⁶. The central NAC region mainly consists of hydrophobic and non-charged polar residues, making it on overall hydrophobic. The C-terminal tail, on the other hand, has a high number of acidic residues, or 15 acidic group (including the C-terminal end). This gives the C-terminal tail a high negative charge at neutral pH, or -14. Even at pH 3.5, the net charge of the tail is still slightly negative (see figure 4.2). The C-terminal tail has been found to contribute significantly to charge regulation upon fibril formation, modulating pH dependence and rate of aggregation, and to play an important role in intra- and intermolecular interactions of α -synuclein (discussed further in chapter 4, and paper I, II and V)^{31,32,50,52,53,56,122,123,177-184}. The distinct charge distribution within the sequence, and thus the different net charge of the individual regions, makes the protein highly polar.

Another characteristic feature of the α -synuclein sequence is that it consists of seven imperfect repeats of eleven residues. The repeats span the N-terminal and NAC region and are linked to the ability of α -synuclein to bind to lipid membranes^{164,170,185}.

3.2 The structure of α -synuclein

In its monomeric form, free in solution, the protein is intrinsically disordered¹⁸⁶. In contrast, when bound to membranes, a large part of the protein (or up to the first ca. 95 residues) folds into an amphipathic α -helix^{124,126,164,185,187,188}. Interaction and binding of α -synuclein to membranes is believed to both play a role in its normal and abnormal functions^{162,164,165,170,189-192}.

When considering α -synuclein in its fibrillar form, it is logical to divide the sequence based not only on its primary structure but also on how the monomers assemble into fibrils or into the N-terminal tail, the fibril core, and the C-terminal tail (figure 3.1)^{32,37,42,43}. This makes it easier to refer to the different parts of the protein in its fibrillar form. The hydrophobic core has the structural characteristic of amyloid fibrils described in chapter 1, with a cross- β -structure.

The structure of the fibrils can vary between different morphologies, where the exact packing of the monomers into the filaments (figure 1.2), as well as the higher-order arrangement of the filaments into the mature fibrils, is dependent on solution conditions, such as pH and ionic strength^{32,35-37}.

The comparison of reported α -synuclein structural models (when this thesis was written) reveals significant variability in the extension of the ordered fibril core (figure 1.2)^{42,57}. The starting residue can range from residue 2 to residue 43, demonstrating considerable polymorphism among different fibril morphologies. The length of the N-terminal tail, thus, differs between reported structural models but most commonly comprises residues 1 to ca. 37 (in recombinant structures). In contrast, the C-terminal tail remains disordered and excluded from the fibril core in all reported structural models. The exclusion of the highly acidic C-terminal tail from the core appears to be a recurring feature. The exact start of the C-terminal tail varies only slightly, and it is most commonly found to start around residue 97-99. Figure 3.1 illustrates these variations, with dashed lines representing the range of each region observed between different structures.

To sum up, from reported structural models of α -synuclein fibrils it can be seen that the highly acidic C-terminal tail, and most often a part of the slightly basic N-terminal domain, are not a part of the ordered fibril core and instead form a fuzzy coat around the fibril core^{32,35-37,57}. The acidic C-terminal tail is of particular interest in this thesis (**papers I, II, and V**), as it is believed to contribute significantly to electrostatic interactions during the amyloid formation of α -synuclein. The contribution of the C-terminal tail to electrostatic interactions and its different interaction modes will be introduced in further detail in chapter 4, focusing on its role in electrostatic interactions in α -synuclein amyloid fibril formation.

3.3 The formation of α -synuclein fibrils

The rates of heterogeneous nucleation and homogeneous secondary nucleation are much higher than the rate of primary nucleation. The rate of homogeneous primary nucleation of α -synuclein is so extremely low^{50,73,80} that spontaneous nucleation of α -synuclein in bulk has up to my knowledge only been detected at extreme conditions: such as at high ionic strength (400 mM sodium phosphate)¹⁹³ or high concentrations of α -synuclein within liquid condensates (in the mM range)¹²⁰. On the other hand, heterogeneous primary nucleation and homogeneous secondary nucleation has been well documented, where the presence of heterogeneous surfaces (e.g., nano-particles⁷⁵, liquid-liquid and air-water interfaces^{73,79,80}, and lipid membranes^{81,82,194}) and existing fibril surface (seeds)^{50,53,195} has been found to catalyze nucleation.

Elongation and secondary nucleation are the main microscopic processes present at quiescent conditions. The aggregation kinetics of α -synuclein is highly dependent on solution conditions, where the secondary nucleation rate is strongly dependent on pH. In contrast, the rate of elongation is altered to a lesser extent^{50,53,195,196}. The pH dependence of fibril formation of α -synuclein will be addressed further in chapter 4, focusing on the role of electrostatic interactions.

Chapter 4

The role of electrostatic interactions in α -synuclein fibril formation

Electrostatic interactions are essential in protein studies. Although hydrophobic interactions are the most significant contributors to protein folding and stability, electrostatic contributions can be crucial for the solubility of proteins and intrinsic and extrinsic protein interactions, modulating their stability, structure, flexibility, and function^{197–202}.

“Since proteins are only marginally stable at room temperature, no type of molecular interaction is unimportant, and even small interactions can contribute significantly (positively or negatively) to stability⁵” (Dill, 1990).

Electrostatic interactions are manifested in different ways, and are highly dependent on pH and ionic strength by affecting the charge state of interacting species and modulating the strength of the interactions⁵. In the context of proteins, charges are usually found on the surface⁵. Electrostatic interactions can be long-range, short-range, attractive and repulsive. Long-range electrostatic interactions depend more on the net charge of the protein while short-range electrostatic interactions depend more on the charge distribution of the protein. Electrostatic interactions have been found to have a significant role in the stability and formation of large self-assembled protein structures, such as amyloid fibrils and virus capsids^{50,54,202}.

Long-range repulsive and non-specific electrostatic interactions (Coulombic interactions) between like charges can be essential for the solubility and stability of proteins in opposite means. Increased electrostatic repulsions within a protein molecule most often destabilize the folded protein, promoting unfolding. At the same time, increased electrostatic repulsions between protein molecules stabilize the protein towards aggregation. In other words, increased electrostatic repulsions counterbalance attractive interactions between protein molecules, decreasing their propensity to aggregate and thus increase their solubility^{5,200}. In the case of amyloid fibrils, increased electrostatic repulsions may both decrease the chance of monomer-monomer association as well as decrease the stability of the amyloid structure, shifting the monomer-fibril equilibrium towards free monomers, and thus increasing the solubility.

Electrostatic interactions can be crucial for protein function^{5,200}. For example, enzyme activity and ligand binding can be modulated by changes in electrostatic interactions^{200,203}. The formation of ion pairs (e.g., salt bridges) between oppositely charged amino acid residues is an example of short range interactions²⁰⁰. The contribution of short-range charge-charge interactions to protein stability is debated. However, studies have shown that an increased number of favorable charge-charge interactions (salt bridges) are generally found within proteins from thermophiles (organisms adapted to higher temperatures) compared to proteins from mesophiles (organisms adapted to moderate temperatures), contributing to higher stability^{200,202,204,205}. Attractive patchy protein-protein interactions are another example of attractive electrostatic interactions^{206–208}.

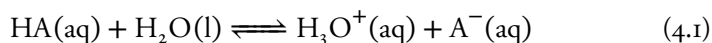
Electrostatic interactions between protein molecules can also be highly directional²⁰⁷. Such directionality can, for example, be seen in the case of α -synuclein, where preferential interactions have been found between the N-terminal region of the monomers with the negatively charged fibril surface and vesicles^{53,121–123}. The highly segregated primary structure and polarized nature of α -synuclein, thus, results in a complex combination of electrostatic interactions that affect the misfolding of the protein into amyloid fibrils. A fundamental understanding of those interactions can thus be crucial for understanding the amyloid formation of α -synuclein. In this thesis, the role of electrostatic interaction in the amyloid fibril formation of α -synuclein is of particular interest.

4.1 The fundamentals of pH and pK_a values

In this part of this chapter, fundamental concepts for understanding electrostatic interactions will be introduced. This includes a general description of acid-base equilibrium, auto-ionization of water, the definition of pH, pK_a values of amino acid residues and pK_a perturbations.

4.1.1 Acid-base equilibrium

According to the definition of acids and bases given by the Swedish scientist Svante Arrhenius in 1880, the concentration of H^+ increases while acids are dissolved in water and the concentration of OH^- increases while bases are dissolved in water. Later, or in 1923, a more general definition of acids and bases was given by the Danish scientist Johannes Brønsted and the English scientist Thomas Lowry. The Brønsted-Lowry theory describes that acid-base reactions involve a transfer of protons between compounds, where an acid is the proton donor and a base is the proton acceptor:^{209,210}



Equation 4.1 is a simple example of such an acid-base reaction where the acid HA (proton donor) reacts with water (proton acceptor) and forms the conjugated base A^- (proton acceptor) and hydronium ion (proton donor). The equilibrium of a chemical reaction is given by its equilibrium constant, K , which gives the amount of each reaction component at equilibrium and is a measure of the tendency of a compound to donate or accept a proton. In the case of acids and bases, the equilibrium constant is referred to as the **acidic dissociation constant**, K_a , and the **basic dissociation constant**, K_b . The equilibrium of the acid-base reaction shown in equation 4.1 is described as^{209,210}:

$$K_a^T = \frac{\{H_3O^+(aq)\}\{A^-(aq)\}}{\{HA(aq)\}} \quad (4.2)$$

where K_a^T is the **thermodynamic acid dissociation constant** and $\{ \}$ denotes activities. Calculating the equilibrium constants from activities corrects for interactions between ionic groups and incomplete hydration that can occur at higher concentrations. However, with dilution the system approaches ideal behavior and the **concentration-based acid dissociation constant**, K_a^C , approaches the

thermodynamic acid dissociation constant, K_a^T ^{211,212}. At infinite dilution the concentration-based constant is equal to the thermodynamic constant:

$$K_a^T = K_a^C = \frac{[\text{H}_3\text{O}^+(\text{aq})][\text{A}^-(\text{aq})]}{[\text{HA}(\text{aq})]} \quad (4.3)$$

where [] denotes concentrations.

4.1.2 Auto-ionization of water

Water is an amphiprotic solvent, meaning it can behave as an acid and a base (see equation 4.1. This property makes water the most common acid and base in living systems. Water can thus "react" with itself - which is referred to as the auto-ionization of water:



The equilibrium constant for the auto-ionization reaction of water, referred to as K_w can be described as:

$$K_w = [\text{H}_3\text{O}^+][\text{OH}^-] = 1.008 \times 10^{-14} \quad (\text{at } 25^\circ\text{C}) \quad (4.5)$$

The equilibrium constant, K_w , is very low, which means that a very low fraction of water is ionized. This means that in pure water (55.5 M) at neutral pH, the concentration of H_3O^+ equals 1.0×10^{-7} M. Despite this low molar ratio, this is a critical phenomenon (see 4.1.3)^{209,210,213}.

4.1.3 pH values

The equilibrium constant for auto-ionization of water is the foundation of the pH scale. The pH is the negative logarithm of the concentration/activity of hydronium ions [H_3O^+]:

$$\text{pH} = -\log_{10}[\text{H}_3\text{O}^+] \quad (4.6)$$

In neutral solutions, where the concentration/activity of H_3O^+ and OH^- is equal, the pH is 7:

$$\text{pH} = -\log_{10}[1.0 \times 10^{-7}] = 7 \quad (4.7)$$

The concentration of hydronium ions increases while weak acids are dissolved in water, opposite to when weak bases are dissolved in water. The concentration of $[\text{H}_3\text{O}^+]$ in a system is determined by the dissociation constants of all ionizable groups in a system^{4,209,213}.

Hydronium ions and hydroxide ions move extremely fast in solution. Their movement has been described as "proton" hopping. Individual ions do not move; instead, the protons "jump" and are relayed over the hydrogen-bonded water network, making the net movement over a long distance very fast. Due to this fast movement, acid-base equilibrium in solution is reached very fast, and pH can thus be described as a system property⁴.

4.1.4 The relationship between pH, K_a and pK_a

The pK_a values of ionizable groups are defined as the negative logarithm of the acid-dissociation constant, K_a ;

$$pK_a = -\log_{10}[K_a] \quad (4.8)$$

Acids and bases can be categorized as either strong or weak. Strong acids and bases dissociate nearly completely into their ionized forms, thus having a very high equilibrium constant. An example is the strong acid HCl, that has an K_a of 1.3×10^6 and thus a very low pK_a value of -6. This is different from weak acids that do not fully dissociate in water. An example is acetic acid that has an K_a of 1.8×10^{-5} and a pK_a value of 4.7. As acids and bases become stronger, the conjugate bases and acids become weaker, respectively^{209,213}.

The determination of pK_a values is based on the measurement of pH as a function of a certain parameter; a common example is potentiometric titration. Potentiometric titration is a method where the pH of a sample containing the solute of interest is measured upon known additions of a titrant (commonly strong acids or bases), resulting in a characteristic sigmoid curve. An example of a titration of acetic acid, where the pH of the sample was measured upon known addition of HCl, is shown in figure 4.1^{4,209,214}.

The midpoint of the titration curve (the inflection point) is where half of the acid has dissociated into its conjugate base, i.e., where the degree of protonation

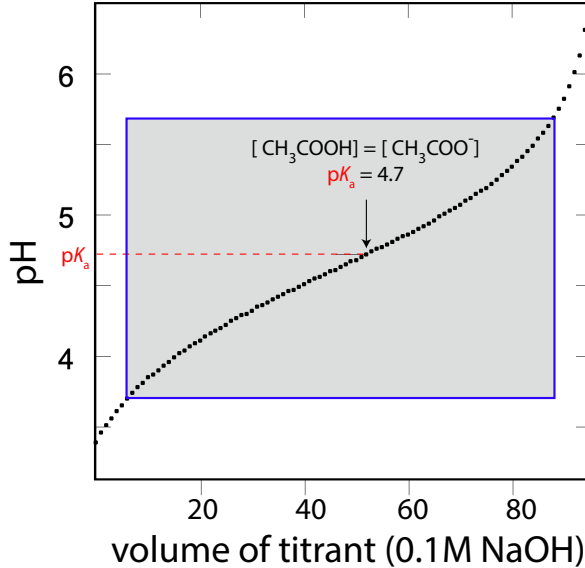


Figure 4.1: Potentiometric titration of 10 mM acetic acid. The part of the titration curve corresponding to the buffer region is marked with a gray box. The pK_a value of acetic acid corresponds to the pH value at the inflection point of the sigmoidal curve (red dashed line), where $[CH_3COOH] = [CH_3COO^-]$, or $pH = 4.7$ (this is experimental data).

is 0.5. The degree of protonation (Q) of an acid is defined as:

$$Q = \frac{[HA]}{[HA] + [A^-]} = \frac{[H^+]}{[H^+] + [K_a]} \quad (4.9)$$

The pH at the point where $Q = 0.5$ corresponds to the pK_a value of the acid.

This is expressed with the Henderson-Hasselbalch equation that gives the relationship between pH and pK_a values as well as the ratio of the acid and its conjugate base in dilute solutions²¹⁴:

$$pH = pK_a + \log \frac{[A^-]}{[HA]} \quad (4.10)$$

From equation 4.10 it can be seen that 90% of an acid is dissociated at one pH unit above the pK_a , while only 10% is dissociated at one pH unit below the pK_a .

While 99% and 1% is dissociated at 2 pH units above and below, respectively. The part of the titration curve corresponding to the resistance to pH change is referred to as the buffer region and is fundamental when making a buffer system (gray box in figure 4.1). The width of the buffer region may change in coupled systems containing more than one titrating group (cf. below).

4.1.5 pK_a values of amino acid residues

Electrostatic interactions within and between proteins are predominantly due to the titratable side chain groups (as well as the C- and N-termini). Seven of the 20 amino acids are weak acids or bases with a titratable side-chain group. Those are the acidic residues: aspartic acid (Asp, D) and glutamic acid (Glu, E); the basic residues: lysine (Lys, K), arginine (Arg, R), and histidine (His, H); the hydrophobic and hydroxyl-containing residue tyrosine (Tyr, Y); and the thiol group-containing residue cysteine (Cys, C). The N- and C-terminus of proteins also have a titratable group. For residues Asp, Glu, Tyr, and Cys, the degree of negative charge species becomes greater at pH above their pK_a value. The opposite holds for His, Lys and Arg, where the degree of positively charged species is greater at pH below their pK_a value^{4,199,213,215,216}.

Proteins are thus large heteropolymers that can consist of numerous ionizable groups. The charge state of individual titratable residues and thus the net charge of the protein is determined by their pK_a values, which are also affected by the electrostatic environment (such as pH, ionic strength, and proximity of other ions) (see chapter 4.1.6)^{199,216}. The surface of folded proteins and amyloid fibrils can thus consist of regions of different charge and hydrophobicity. Such anisotropic patterns have been found to affect protein-protein interaction, as well as result in direction-dependent inter-molecular interactions^{53,207,208}. Determination of the pK_a values of protein molecules provides valuable information and can be important for understanding their behavior, as well as getting insightful information about their electrostatic environment.

4.1.6 pK_a perturbations

Despite the pK_a value being referred to as the negative logarithm of the dissociation "constant", it can be highly influenced by the presence of other ions, the type of solvent, and temperature²¹⁴. Such changes in pK_a values are often referred to as **pK_a perturbations** or **pK_a shifts**²¹⁶. Perturbations on pK_a values of amino acid residues within proteins have been studied substantially

Table 4.1: Comparison of unperturbed and perturbed pK_a values of amino acid residues. A) Values were determined using various model compounds and corrections were done to yield pK_a values of unperturbed groups²¹⁹. B) Values were determined using uncharged alanine pentapeptide ala-ala-X-ala-ala^{215,216}. C) Values were determined using a random coil model peptide (linear tetrapeptides H-Gly-Gly-X-Ala-OH)²²⁰. D) Average values of 78 folded protein²¹⁶.

	A) Intrinsic pK_a values	B) In alanine pentapeptides	C) In random coil model peptide	D) In folded proteins
Asp	4.0	3.9	3.9 ± 0.1	3.5 ± 1.2
Glu	4.4	4.3	4.3 ± 0.1	4.2 ± 0.9
Tyr	9.6	9.8	10.3 ± 0.1	10.3 ± 1.2
Cys	9.5	8.6	–	6.8 ± 2.7
His	6.3	6.5	7.0 ± 0.1	6.6 ± 1.0
Lys	10.4	10.4	11.1 ± 0.2	10.5 ± 1.1
Arg	12	–	–	–
C-term	3.8	3.7	–	3.3 ± 0.8
N-term	7.5	8.0	–	7.7 ± 0.5

since 1924 when Linderstrøm-Lang discovered that pK_a values of amino acid can be affected by the net charge of the protein²¹⁷. This behavior was also emphasized by Tanford and Kirkwood (1957), who showed that titration curves of proteins (containing many acidic and basic side chains) are flatter or less steep compared to a mixture containing identical proportions and concentration of single amino acids²¹⁸. This behavior can be explained by differences in the electrostatic environment (electrostatic coupling) between individual residues and their pK_a values being perturbed (down-shifted or up-shifted) compared to their intrinsic pK_a values, to a different extent²¹⁸.

While studying perturbations of amino acids within proteins, it is valuable to compare apparent pK_a values to the intrinsic pK_a values. Intrinsic pK_a values can be defined as the pK_a value of a single amino acid residue that is not perturbed by any neighboring charges or changes in electrostatic environment²¹⁸. Those values are obtained from model compounds, such as an alanine pentapeptide (Ala-Ala-X-Ala-Ala) (see table 4.1). Model peptides yield values that exclude perturbations both from charge-charge interactions (from end charges and neighboring groups) as well as perturbations from burial within the protein core, while including the effects of the peptide bonds (see table 4.1)^{199,215}. As can be seen from table 4.1, the pK_a value of amino acid residues can be up-shifted or down-shifted in comparison to their intrinsic values.

The three main factors contributing to changes in electrostatic environments

and thus to pK_a perturbations are charge-charge interactions, charge-dipole interactions and dehydration, where charge-charge interactions contribute the most to pK_a perturbations on protein surfaces^{199,216}. The pK_a values of the amino acid residues in proteins can become shifted due to charge-charge interactions with neighboring ions, biomolecules, or ligands. The pK_a values of the ionizable groups in a negatively charged environment get upshifted. The close proximity between negative charges (acidic residues) is energetically unfavorable, which can result in a decreased tendency to give away a proton (being in a charge state) and, thus, up-shifts in the pK_a values. On the other hand, pK_a values of groups in the positively charged environment get downshifted, which can be explained by an increased tendency to donate a proton^{199,216}.

The degree of pK_a value perturbations of amino acid residues positioned on protein surfaces are commonly found to be within two units²²¹. An upshift of a pK_a value to 6.5 of Glu positioned at the calcium site of S100G (calbindin D9K) is an example of an upshift in a pK_a value of a surface localized residue^{222,223}. On the other hand, pK_a values of residues with lower solvent accessible surface area, often found within enzymes active sites, can be perturbed to a larger extent. Such perturbations have been found to play an essential role in their catalytic activity²²¹. pK_a perturbations due to electrostatic interactions between charges become less pronounced at higher ionic strength due to charge screening by salt, macro-molecular ions, and their counter-ions.^{51,108,224,225}

Perturbations of pK_a values have been detected within self-assembling systems, such as upon Fmoc-diphenylalanine fibers and hydrogel formation, and during the assembly of fatty acids into membranes. These pK_a perturbations can be explained by the decreased distance between molecules during self-assembly^{226–228}. This shows that studying pK_a perturbations can provide fundamental insights into the role of electrostatic interactions within various systems and provide valuable insights into protein behavior.

4.2 Electrostatic interactions and α -synuclein fibril formation

In addition to the contribution of electrostatic interactions to optimal protein function, they also play a significant role in modulating self-assembling processes, such as amyloid formation. Studies of the effect of aggregation rate as a function of pH and ionic strength have shown that aggregation kinetics and the different microscopic mechanisms can be strongly affected by changes in electrostatic interactions^{50,51,53,229,230}. Electrostatic effects on the stability of amyloid fibrils have also been documented, where manipulation of electrostatic interactions can result in fibril dissociation^{54,55,231-233}. Furthermore, fibril morphology has also been found to be affected by changes in electrostatic interaction^{43,50,230}. This part of the chapter focuses on the role of electrostatic interaction in α -synuclein aggregation.

4.2.1 The C-terminal tail

The C-terminal tail of α -synuclein is of particular focus in this thesis and central to **paper I**, **paper II** and **paper V**. The C-terminal tail is highly acidic, containing 15 acidic groups (including the C-terminal end) among its ca. 40 residues (figure 3.1 and 4.2). The tail is unstructured in both the monomeric form and fibrillar form^{31,32}. It is, therefore, not a part of the fibril core, and instead, it forms a fussy coat around the fibrils (see figures 3.1 and 4.3).

The conformation of the tails, or how much they extend from the fibril core, is dependent on solution conditions, such as pH and ionic strength, which affect its charge state and electrostatic screening. As an example, at neutral pH, the net charge of the tail itself is calculated to be -14 in the monomeric form and -13 in the fibrillar form (figure 4.2). At such conditions, where it is highly charged, it has been found to extend from the fibril core like a polymer brush due to high degree of electrostatic repulsion between the charged acidic residues (figure 4.3)^{31,32,177,178}. On the other hand, with lower charge (lower pH) or with increased screening (higher ionic strength), there is less electrostatic repulsion within and between individual tails at the fibril surface, resulting in more collapsed conformation of the tails (see figures 4.2 and 4.3)¹⁷⁸.

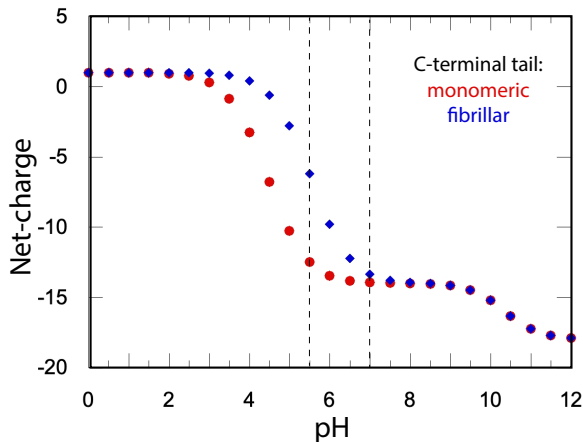


Figure 4.2: Theoretical titration curve of the C-terminal tail of α -synuclein in the monomeric (red) and fibrillar (blue) form. Previously determined pK_a values of the acidic groups of the monomers were used for the calculation in the monomeric form²²⁵. The upshift in the pK_a values of the acidic residues of the C-terminal tail upon fibril formation were taken into account in the calculation of the fibrillar form¹⁸⁰. Ionizable groups of residues between 101 to 140 were included in the calculations.

4.2.2 Electrostatic effects on the aggregation mechanism

It has been established that the aggregation rate of α -synuclein, and more specifically, the secondary nucleation rate, is highly dependent on pH. The secondary nucleation rate is about four orders of magnitudes higher at mildly acidic pH (below pH 5.8) than at neutral pH. The elongation rate is also affected by a decrease in pH, but to a lower extent, where the rate only increases about one order of magnitude^{50,195}. This pH dependence of secondary nucleation has been suggested to be linked to the neutralization of the high number of acidic residues within the C-terminal tail at mildly acidic pH⁵⁰.

The effect of a decreased density of acidic residues within the C-terminal tail on the aggregation of α -synuclein at various pH values was studied in **paper V**. The results showed that removal of negative charges from the C-terminal tail affects the aggregation profile at both mildly acidic and neutral pH.

Truncations at the C-terminal tail of α -synuclein have also been found to have profound effects on the aggregation propensity and mechanism of α -synuclein, with higher aggregation rate at neutral pH^{52,56,181,182}. At the same time, truncation mutants show opposite behavior at mildly acidic pH, with slower aggregation rates compared to wild-type^{52,56}. This can be explained by the C-terminal

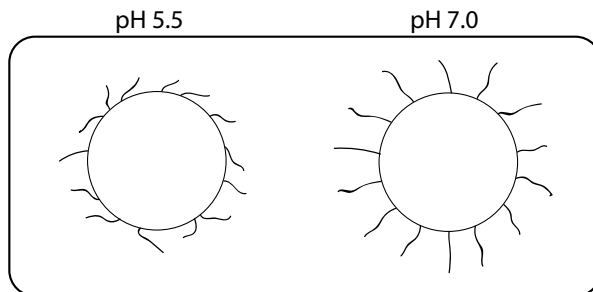


Figure 4.3: Schematic illustration of the conformation of the C-terminal tails forming a fuzzy coat around the fibril core at pH 5.5 and 7.0. The circles represent a cross-section of the core of a filament¹⁷⁸.

truncations shifting the optimal pH range for secondary nucleation towards higher pH⁵⁶.

Aggregation kinetics of α -synuclein are also highly dependent on ionic strength. Charge screening at neutral pH is linked to higher aggregation rates of α -synuclein^{52,193,234}. On the other hand, the aggregation rate of α -synuclein at pH 5.5 in the presence of seeds or anionic lipid vesicles is lower at higher ionic strength. Such anomalous behavior indicates a complex interplay between short-range attractive and long-range repulsive electrostatic interactions, highlighting the role of short-range interactions in secondary nucleation⁵³. Furthermore, interactions of divalent ions (e.g., Ca^{2+} and Mg^{2+}) and polyamines with the C-terminal tail have shown an increase in the aggregation propensity at neutral pH^{52,166,179,235,236}. Studies of the interaction of α -synuclein with Ca^{2+} suggest more specific ion effects^{166,237–239}.

Furthermore, the formation of higher-order aggregates, for example gels, has also been found to be dependent on pH and ionic strength^{50,240}.

4.2.3 pK_a upshift of acidic residues of α -synuclein

For α -synuclein, the apparent pK_a values of all groups that ionize below pH 7 have been determined by NMR²²⁵. The results showed that the ionizable residues that are part of the first 100 residues are down-shifted compared to intrinsic values and values obtained from a random coil model peptides, indicating favorable interaction between acidic and basic groups. On the other hand, the pK_a values of the residues within the C-terminal tail are measured to be up-

shifted compared to intrinsic values. The up-shifts can be explained by the high charge density of acidic residues, resulting in greater affinity for protons²²⁵. At low ionic strength, the average pK_a values of Asp and Glu, in the C-terminal tail of monomers, have been determined to be 4.2 ± 0.3 and 4.6 ± 0.2 , respectively (see intrinsic values in table 4.1)²²⁵. The pK_a values were still measured to be perturbed at physiological ionic strength (150 mM salt) but to a lower extent.

In **paper I**, we show that the consequence, or the effect on the pK_a values, is even more significant upon fibril formation, where the average pK_a value of the acidic residues gets up-shifted by 1.1 unit¹⁸⁰. The measured average up-shift can be explained by the close proximity of the acidic tails at the fibril surface.

4.2.4 Transient intra- and inter-molecular interactions of the C-terminal tail

The highly acidic C-terminal tail has been shown to play a role in the monomeric form of the protein. Transient interactions between the C-terminal tail and the N-terminal tail, as well as between the C-terminal tail and the NAC region, have been established both at neutral and low pH^{177,179,183}. Such transient contacts within the monomer result in a lower radius of gyration of α -synuclein monomers in comparison to a random coil^{179,183,241,242}. With increased ionic strength at neutral pH, the radius of gyration increases, which has been linked to faster aggregation⁵². It has thus been proposed that these transient contacts may limit interactions between NAC regions of different monomers, which might result in a lower possibility of nucleation and growth to occur¹⁷⁹.

The correlation of higher aggregation rates and the disruption of the intra-molecular transient interactions due to neutralization, removal, and shielding of the acidic residues at the C-terminal tail thus indicates that the C-terminal tail might have a protective role against α -synuclein amyloid formation at neutral pH^{179,181,243}.

In addition to intra-molecular interactions, inter-molecular interactions of the N-terminal end, of free α -synuclein monomers in solution, with the negatively charged fibril surface (presumably the negatively charged C-terminal tail) have also been established (**paper II**)^{121–123}. Interactions of the N-terminal region of monomers with the fibril surface might disrupt the "protective" N- to C-terminal transient interactions within the monomers, as well as increasing the local concentration. Additionally, the orientation of the monomers interacting with the fibril surface could potentially favor NAC-NAC interactions between

different monomers sitting at the fibril surface, which might increase the chance of interaction between different monomers occurring at the fibril surface.

Interactions of α -synuclein monomers with fibrils of two different morphologies were studied in **paper II**. There, we show that the N-terminal end of the monomers of both morphologies interacts more strongly with the fibril surface relative to the rest of the protein.

Furthermore, the interaction of the N-terminal region and the acidic surface of the amyloid fibrils can, to some extent, be compared to the interaction between α -synuclein monomers and negatively charged phospholipid vesicles^{53,124–126,244}. Studies of these systems do show attractive interactions between the N-terminal end of the monomers and the anionic lipid vesicles, and suggest that specific binding modes of the N-terminus to the phospholipid vesicles can promote interactions between the NAC regions of different monomers and thus accelerating their aggregation at low lipid to protein ratios.

Chapter 5

Stability and solubility of amyloid fibrils

Amyloid fibrils are large, non-covalent self-assemblies, and their formation is thus a reversible process²⁴⁵. As mentioned in chapter 2, if the monomer concentration exceeds the solubility limit (supersaturated solution), the system becomes unstable, and the thermodynamically most stable state consists of amyloid fibrils in dynamic equilibrium with monomers in solution. The **solubility limit** (S , or the critical concentration, c_c) can thus be defined as the monomer concentration at thermodynamic equilibrium^{68,72,77}.

At conditions where the total monomer concentration is slightly above the solubility limit (the c_{mon}/S is low), the aggregation occurs slowly and is often not detectable within the experimental time frame. This concentration range is defined as the **metastable zone**. At infinite time, a closed system will be in thermodynamic equilibrium and the monomeric concentration will equal the solubility limit (S)^{72,246}.

5.1 Relationship between solubility and stability

The chemical potential of monomer free in solution can be determined from its intrinsic energy and the activity¹⁴⁹:

$$\mu_m = \mathcal{E}_m + RT \ln(a_m) \quad (5.1)$$

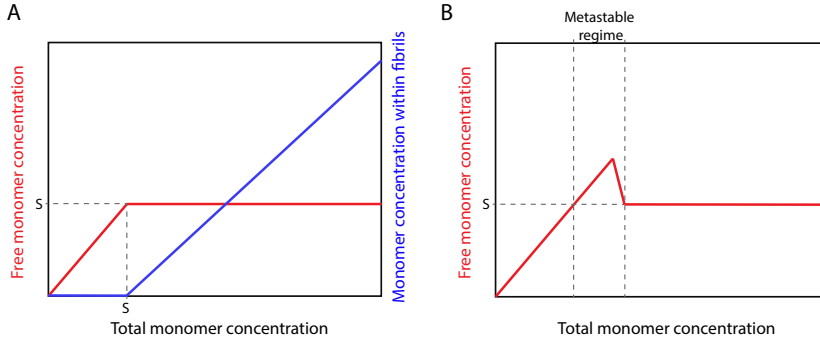


Figure 5.1: Schematic representation of solubility and the metastable zone. A) Schematic representation of solubility. Free monomer concentration (red) and monomer concentration within fibrils (blue) is shown as a function of total monomer concentration within the system. All monomers remain soluble at total monomer concentration below the solubility (S) of the protein or the critical concentration (c_c). Above the solubility of the protein, the monomer concentration (red) remains constant, and fibrils start to form (blue). B) Representation of the metastable zone. At conditions where the total monomeric concentration is below the solubility limit, the sample is thermodynamically stable and stays monomeric. At conditions where the monomeric concentration is slightly higher than the saturation concentration, the nucleation event is rare, and the solution can remain monomeric for a prolonged time. At such conditions, the solution is termed to be metastable.

where intrinsic energy of the monomers is represented by \mathcal{E}_m and the activity as a_m . At infinite dilution, the activity term approaches the concentration, $[m]$. When working with dilute solutions, it can thus be approximated to:

$$\mu_m = \mathcal{E}_m + RT \ln [m] \quad (5.2)$$

In the same way, the chemical potential of the monomers within fibrils is:

$$\mu_{mf} = \mathcal{E}_{mf} + RT \ln [mf] \quad (5.3)$$

where intrinsic energy of the monomers within fibrils is represented by \mathcal{E}_{mf} and the concentration of monomers within fibrils as $[mf]$. As mentioned earlier, amyloid fibrils can be seen as a separate solid phase⁶⁸, and in such cases, the contribution of translational energy is minimal. The chemical potential of the monomers within fibrils can, thus, be approximated to equal to:

$$\mu_{mf} = \mathcal{E}_{mf} \quad (5.4)$$

From this, we can see that the chemical potential of the monomers within fibrils is not dependent on concentration, different from the chemical potential of monomers in solution, which is concentration dependent (figure 5.2)^{121,149}.

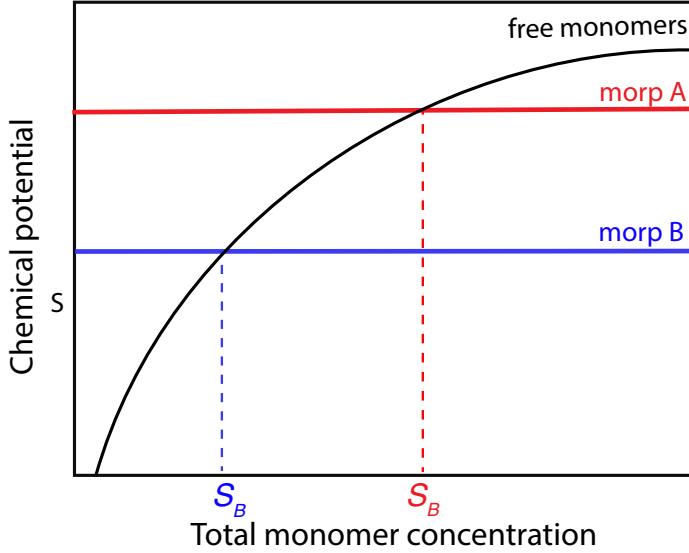


Figure 5.2: Schematic illustration showing the chemical potential as a function of the total monomeric concentration of monomer free in solution (black), amyloid fibrils of morphology A (red), and morphology B (blue). The solubility (S) is represented with dashed lines.

In a supersaturated solution (at non-equilibrium), the chemical potential of the monomers in solution (μ_m) is different from the chemical potential of the monomers within fibrils (μ_{mf}). At thermodynamic equilibrium, the chemical potential of the monomers in solution and within fibrils are equal:

$$\mu_m = \mu_{mf} \quad (5.5)$$

The monomer concentration at equilibrium $[m]$ or the solubility (S) can thus be obtained by substituting equations 5.2 and 5.4 into equation 5.5:

$$[m] = S = \exp\left(\frac{\mathcal{E}_{mf} - \mathcal{E}_m}{RT}\right) \quad (5.6)$$

Equation 5.6 shows that solubility is lower in the presence of more stable fibril (lower \mathcal{E}_{mf}). The solubility is thus dependent on the stability of the fibril (**papers II and III**)¹⁴⁹.

5.2 Kinetic versus thermodynamic stability

Theoretically, a system under **thermodynamic control** should always end up in the same state (the most stable one). All polymorphic samples should, thus, over time become monomorphic, consisting of the morphology of the highest stability and, thus, lowest solubility (unless more than two morphologies have identical stability, which is highly unlikely). Formation of two morphologies under identical conditions from identical monomers was observed in **paper II**, where the samples consisting of the less stable morphology (higher solubility) transferred into consisting of the more stable morphology (lower solubility) with time. Time-dependent structural evolution of amyloid fibrils within a closed system has also been documented for wild-type α -synuclein and mutants at other solution conditions than studied in paper II, as well as for other amyloidogenic proteins, such as IAPP^{62,230,247,248}.

The existence of more than one morphology within the same sample under identical conditions is most likely explained by the system being under **kinetic control**. This could be explained by the energy barriers for formation of the less stable morphology being similar to, or even lower than, the energy barriers for formation of the more stable morphology. The less stable morphologies can be referred to as being kinetically stable, and the corresponding concentrations of free monomers in solution, thus report on the apparent solubility limits.

This can be visualized with the help of illustrations of **free-energy landscapes** (aggregation funnels, see chapter 1.2), where different morphologies have different energy minima with energy barriers of different height (figure 5.3)^{14,16-18,43}.

Energy minima separated by high energy barriers can thus explain the sample being kinetically trapped. The less stable morphology dominating a sample for a period of time could be explained by the energy barriers for elongation and secondary nucleation being lower than for primary nucleation (see chapter 2.1.1 and figure 2.3). As mentioned earlier, primary nucleation of α -synuclein in bulk is unlikely to occur at any relevant rate. Kinetically, it is thus more favorable for the system to propagate the already existing morphology^{62,121}. Despite that, the sample will become under thermodynamic control at infinite time, consisting only of the morphology of the highest stability. This can be understood in terms of the reversibility of amyloid fibrils. With time, the monomers dissociating from the fibril ends of the less stable structure will associate with the fibril ends of the fibrils of the higher stability. Structural conversion from one morphology to another can not be excluded.

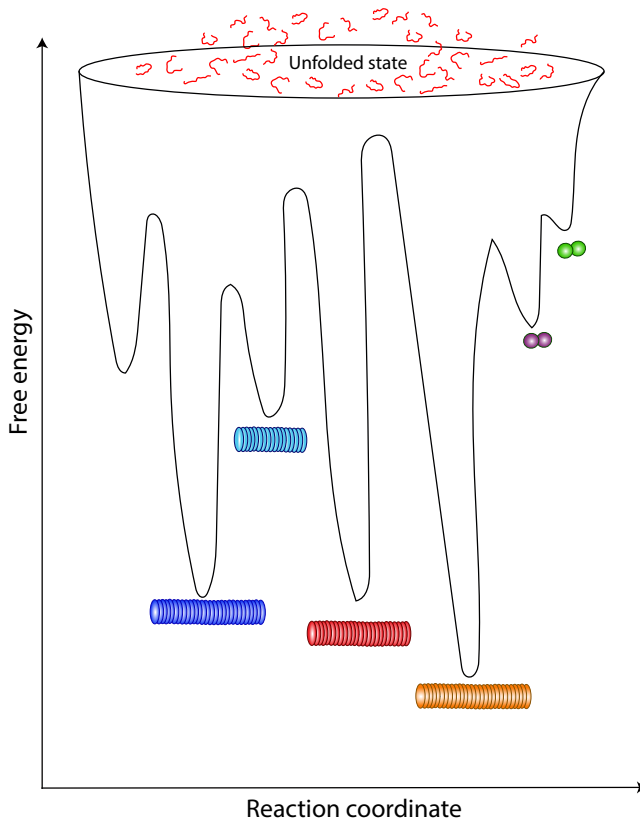


Figure 5.3: Illustrative representation of a free energy landscape consisting of different energy minima corresponding to different fibril morphologies. The fibril morphologies have free energy, and separated by energy barriers of various heights. This energy landscape would only be accessible above the critical concentration, c_c .

5.3 Relationship between solubility and reversibility

For amyloid fibrils, the association rate of monomers to fibril ends can be given by:

$$-\frac{dm(t)}{dt} = k_+ m(t) 2P(t) \quad (5.7)$$

where k_+ is the **association rate constant**, $m(t)$ is the monomer concentration, $P(t)$ is the fibril number concentration, and $2P(t)$ is the concentration of the fibril ends at any given time (t). The rate of dissociation of monomers from the fibril ends at any given time can be given by:

$$\frac{dm(t)}{dt} = k_{\text{off}}2P(t) \quad (5.8)$$

where k_{off} is the **dissociation rate constant**. The change in monomer concentration in a closed system can thus be obtained from:

$$\frac{dm(t)}{dt} = -k_+m(t)2P(t) + k_{\text{off}}2P(t) \quad (5.9)$$

At equilibrium, there is no change in free monomer concentration and the association rate of monomers at fibril ends is equal to the dissociation rate:

$$k_+m(t)2P(t) = k_{\text{off}}2P(t) \quad (5.10)$$

We also know that at equilibrium, the monomer concentration in solution is equal to the solubility (S) or the critical concentration:

$$K = k_+/k_{\text{off}} = \frac{1}{m(t)} = \frac{1}{S} \quad (5.11)$$

The solubility limit can thus also (in addition to equation 5.6) be estimated from the rate constants of association and dissociation of monomers to and from the fibril ends:

$$S = k_{\text{off}}/k_+ \quad (5.12)$$

The association and dissociation rates are not equal for a system that is not in equilibrium. As an example, for a system containing monomer concentration above the solubility limit, the association rate is higher than the dissociation rate, resulting in decreasing concentration of monomers in solution with time, or until the system has reached equilibrium^{72,246}. The opposite holds when a fibril-consisting sample is diluted to a concentration below the solubility limit, resulting in higher dissociation rates than association rates. In such cases, the free monomer concentration increases until the sample has reached equilibrium^{245,249,250}. Fibril dissociation can be very slow and, thus, consequently, difficult to detect within reasonable experimental time-frames. For a closed system, this could be explained by the dissociation rate constant k_{off} being very low relative to the association rate constant k_+ . Such a system could thus be observed as practically irreversible.

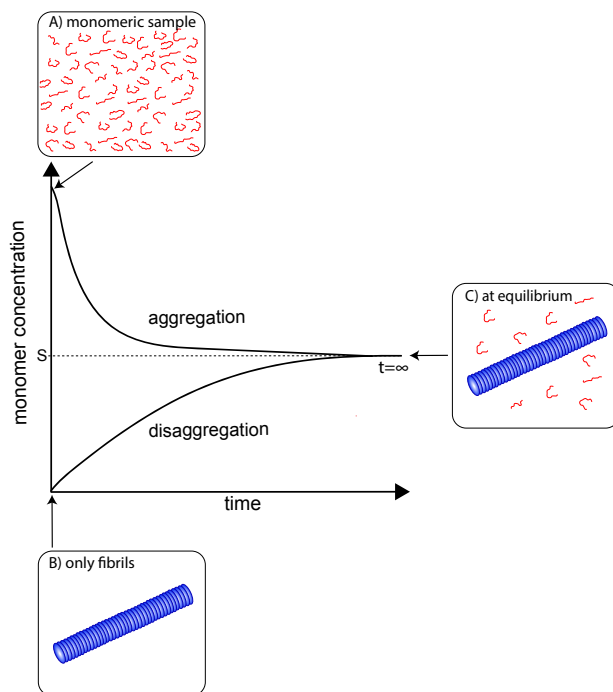


Figure 5.4: Schematic representation of aggregation and disaggregation in a closed system, where the starting point (time = 0) consists of A) a fully monomer sample or B) a sample consisting of only fibrils. In case A, monomers misfold into fibrils, where free monomeric concentration decreases with time. In case B, the monomers dissociate from the fibril ends, resulting in increased monomer concentration with time until it has reached the solubility (S). C) At infinity time, the monomer concentration has reached the same value in both cases (the solubility).

The reversibility of amyloid fibril formation can also be observed upon system change, such as by changing the pH^{34,231,232}, temperature^{251–253}, denaturant concentration^{254–256}, ionic strength^{55,233}, or pressure^{257,258}. Dissociation of α -synuclein upon pH change (titration) was encountered while developing an approach to measure pKa values of α -synuclein fibrils (see chapter 7.1 and Paper I).

5.4 Effect of chaperones on solubility

An indication of a change in solubility has been documented earlier for A β ₄₂ in the presence of JB6¹⁴⁴. In paper III, we have a strong indication of increased

solubility of α -synuclein as well as formation of co-aggregates in the presence of the chaperone JB6. An increase in solubility at thermodynamic equilibrium in the presence of chaperones could be explained by the high chemical potential of the chaperone alone¹⁴⁹; this will be presented in more detail as follows:

To our knowledge, there is no evidence of an interaction between amyloid monomers and JB6 (**paper III**)^{138,143}. Therefore, in a dilute system, we can assume that the intrinsic energy of the monomer is unaltered in the presence of JB6. The chemical potential of α -synuclein monomer in solution in the presence of the chaperone (JB6) can thus be written as:

$$\mu_{m^*} = \mathcal{E}_m + RT \ln[m^*] \quad (5.13)$$

Where m^* denotes the amyloid protein monomer in the presence of a chaperone. The chemical potential of monomers within the aggregates in the presence of a chaperone can be written as:

$$\mu_{mf^*} = \mathcal{E}_{mf^*} + RT \ln[mf^*] \quad (5.14)$$

As explained earlier (eq. 5.4), the contribution of translational energy to the chemical potential of the fibrils can be neglected, and the chemical potential of the monomers within fibrils in the presence of chaperones can, thus, be simplified to:

$$\mu_{mf^*} = \mathcal{E}_{mf^*} \quad (5.15)$$

The chemical potential of the monomers within fibrils is thus not dependent on the monomer concentration, in contrast to the chemical potential of the monomers in solution that is dependent on the monomer concentration (figure 5.5).

As explained earlier for pure fibrils (eq. 5.5), at equilibrium, the chemical potential of monomers free in solution is equal to the chemical potential of the monomers within the aggregates:

$$\mu_{m^*} = \mu_{mf^*} = \mathcal{E}_{mf^*}$$

The concentration of free monomer in solution (the solubility) in the presence of a chaperone can, thus, be written as:

$$[m^*] = S^* = \exp\left(\frac{\mathcal{E}_{mf^*} - \mathcal{E}_m}{RT}\right)$$

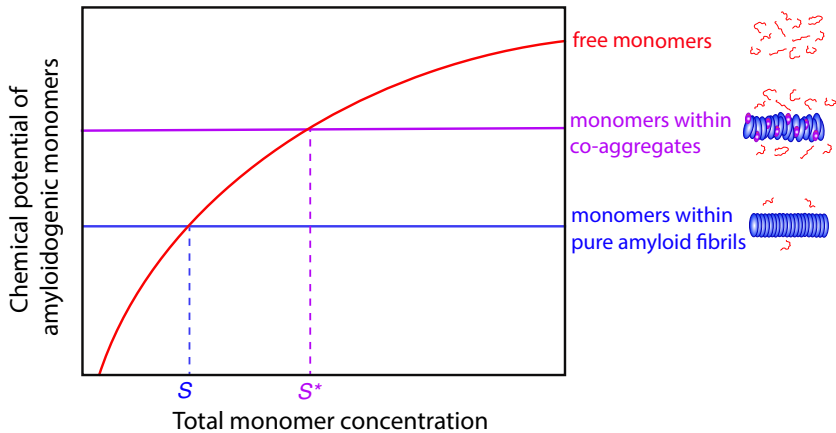


Figure 5.5: Schematic illustration showing the chemical potential of an amyloid protein as a function of the total monomer concentration for monomer free in solution (red), for monomers within aggregates in the presence of the chaperone (JB6) (Purple), and for monomers in aggregates formed from a sample consisting only of the amyloidogenic protein (blue). The chemical potential of the monomers free in solution is dependent on the total concentration of monomers. In contrast, the chemical potential of monomers within the aggregates is independent of the total monomer concentration.

The results presented in paper III, as well as by another study of $a\beta_{42}$ ¹⁴⁴, indicate that the solubility of α -synuclein and $a\beta_{42}$ increases in the presence of the chaperone (in this case JB6):

$$[m^*] > [m]$$

This suggests that the intrinsic energy of the α -synuclein monomer within the aggregates formed in the presence of the chaperone is higher than that of the α -synuclein monomer within the fibrils formed from α -synuclein alone (figure 5.5).

$$\mathcal{E}_{mf^*} > \mathcal{E}_{mf}$$

This further implies that the aggregates formed in the presence and absence of the chaperone are of different structures of different stability. This hypothesis is supported by cryo-TEM images (paper III) showing different fibrillar structures in the presence of JB6, indicating the formation of co-aggregates. Evidence of the formation of co-aggregates has also been documented with immunoblots for a system consisting of $a\beta_{42}$ in the presence of JB6^{142,144}.

The formation of co-aggregates between the amyloidogenic protein and a chaperone (α -synuclein and JB6 in this case) would minimize the free energy of

the system as a whole, where a greater decrease in the chemical potential of the chaperone would compensate for the increase in the chemical potential of α -synuclein. A system consisting of co-aggregates in equilibrium with soluble α -synuclein and JB6 would thus be energetically more stable than a system consisting of JB6 co-existing with pure α -synuclein fibrils in equilibrium with monomeric α -synuclein.

Alternatively, JB6 could bind to the surface of already-formed fibrils (coating). Such behavior has been documented for other systems, e.g., the amyloidogenic proteins A β and IAPP, in the presence of the chaperones Brichos and prefoldin, respectively^{133,259}. However, such a process would more likely result in increased stability of the fibrils and, thus, not result in an increase in solubility.

Chapter 6

Methodology

This chapter aims to present an overview of the methodology applied and developed within this thesis. Different standard methods were used and strategically combined to address our research questions. The standard methods are outlined in information boxes throughout the chapter, while the focus of the main text is on the methodology and experimental design.

6.1 Preparation of α -synuclein samples

Good control over sample preparation is fundamental and essential for obtaining reliable and reproducible data. Isolating the protein of interest from other proteins and contaminants is an example of a crucial preparation step for protein studies. Substantial errors in determining protein concentration using absorbance spectroscopy can arise in the presence of contaminants or due to increased light scattering from, e.g., aggregated species (as can be seen from Lambert-Beer's law).

Expression and purification

Wild-type human α -synuclein and the α -synuclein mutants were expressed in *Escherichia coli* (*E. coli*). Cells were harvested, sonicated, and centrifuged. Most α -synuclein does not accumulate into inclusion bodies; the supernatant can thus be collected and directly used for protein purification. One of the first steps in the purification protocol involves heating of the sample to 85°C, followed by cooling on ice and centrifugation to pellet the *E.coli* proteins. The supernatant is again collected and subjected to two steps of ion-exchange chro-

matography (box 1). All buffers are pre-cooled, and all purification steps are performed in a cold room to avoid aggregation and to limit proteolysis. At the end of each purification, the sample's correct mass and purity are confirmed using mass spectrometry and SDS-PAGE, as well as performing and comparing the aggregation kinetics to a previous batch. Samples are aliquoted and stored at -20°C . Specific steps of the expression and purification of α -synuclein are described in detail in the papers within this thesis, with extra focus in **paper III** where documentations of individual steps are presented in the supplementary information.

Column chromatography

Box I

Column chromatography is a powerful method to fractionate and isolate proteins based on, e.g., their size, charge, hydrophobicity, or binding affinity. A stationary phase (resin) is packed into a column and a mobile phase (buffer solution) flows through the column by gravity or pressure. A protein sample is loaded on top of the column, and the different components travel through the column at different speeds depending on their properties and the type of the stationary phase. **Ion-exchange chromatography (IEX)** is based on the separation of molecules according to their charge. The stationary phase consists of resins with either cationic groups (anion exchangers) or anionic groups (cation exchangers). The affinity of the protein to the resin depends on its charge state, and the elution profile can be controlled by pH and ionic strength. In anion exchangers, the negatively charged molecules travel more slowly through the column; the opposite holds for cation exchangers. **Size-exclusion chromatography (SEC)** is based on separating molecules according to their size. The stationary phase consists of cross-linked porous beads. The distance the molecules travel through the column is dependent on their size. Smaller molecules can enter more pores while larger molecules pass by. The elution time for smaller molecules is thus longer due to the longer path they travel through the column. A desalting column is a type of SEC, where the size of the pores has been optimized for separating larger molecules from small ions⁴.

Monomer preparation

When working with amyloid proteins, it is essential to ensure that the protein is in its monomeric form at the start of the experiment. Therefore, prior to each experiment presented in this paper, monomeric α -synuclein was isolated by

size exclusion chromatography (SEC) in the desired experimental buffer (box 1). Buffers were freshly prepared, filtered, and degassed at the start of a new experiment. The center of the monomeric peak was collected into low-binding tubes to minimize protein loss and the occurrence of heterogeneous primary nucleation on the external surfaces. In order to measure a change in pH upon fibril formation (**paper I**), it was essential to apply an additional step, using a HiTrap desalting column, to successfully separate α -synuclein monomers from buffer ions, and thus obtain monomeric α -synuclein in pure water.

6.2 Formation of amyloid fibrils

In this thesis, fibrils were formed mainly in two ways. When measuring fibril kinetics, the fibrils were formed under quiescent conditions in 96 well plates. For larger sample volumes and when the fibrillar state is of primary interest rather than the fibril kinetics, fibrils were prepared in 2 mL low-binding tubes with stirring. Fibril seeds were also prepared in 2 mL low-binding tubes with stirring, aliquoted, and stored at -20°C . Prior to use, the seeds were taken out, thawed, sonicated in a water sonication bath for one minute and incubated at room temperature for at least one hour.

6.3 Aggregation kinetics

The formation of amyloid fibrils or the disappearance of monomers can be followed indirectly or directly.

Indirect measurements of formation of amyloid fibrils

In **paper I, III, IV and V**, the formation of amyloid fibrils was followed indirectly by supplementing the samples with the fluorescent optical probe **thioflavin T** and the change in fluorescence intensity was monitored over time (box 2 and 3). This is the most common and convenient way to measure fibril formation kinetics, allowing multiple samples to be studied simultaneously in a plate reader (high-throughput).

Direct measurement of a decrease in monomer concentration

In **paper III** we follow the the formation of amyloid fibrils directly by NMR spectroscopy. This was done by measuring the disappearance of signals corresponding to free monomer in solution.

Direct measurements of an increase in fibril mass

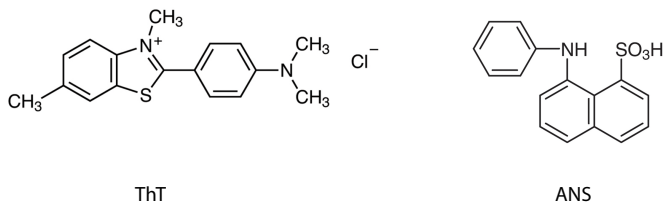
In **paper I** we measure the static light scattering during fibril formation. Formation of fibrils, results in generation of larger species and an increase in scattering. Change in static scattering, pH and ThT-fluorescence was measured simultaneously to get information about if the increase in pH during fibril formation could be directly related to the formation of fibrils.

Fluorescence spectroscopy*Box 2*

Fluorescence spectroscopy is an optical spectroscopy method. Fluorescence may occur when a fluorophore absorbs light at one wavelength and gets excited to a higher electronic level. The lifetime of the excited state is long enough for the molecule to relax to lower vibration levels within the excited electronic energy level. When the molecule spontaneously returns to the lower electronic energy level it may emit photons that are of higher wavelength than the photons of the incident light. This spontaneous emission is measured within fluorescence spectroscopy. The quantum yield is the ratio between the number of photons emitted and the number of photons absorbed. An increase in quantum yield results in greater fluorescence intensity. Fluorophores are the groups responsible for fluorescence and can be intrinsic or extrinsic. The most common intrinsic fluorophores are the aromatic residues. Extrinsic fluorophores are either covalently linked to the protein or added to the sample as non-covalent optical probes. Fluorescence spectra of the chromophores can be significantly affected upon changes in their environment, which makes it possible to study conformational changes. The high sensitivity of the method makes it highly suitable for protein studies²⁶⁰.

Non-covalent optical probes*Box 3*

Thioflavin T (ThT) and 8-Anilino-1-naphthalenesulfonic acid (ANS) are both examples of non-covalent optical probes that are useful within the studies of amyloid proteins. The binding of ThT to fibrils restricts the rotation of the carbon-carbon bond connecting the aromatic rings, which significantly affects the fluorescence quantum yield, resulting in increased fluorescence intensity^{261–264}.



ANS is a fluorescent probe, where its quantum yield is highly dependent on the hydrophobicity of its environment. When ANS binds to hydrophobic patches of proteins, such as amyloid fibril, its fluorescence intensity increases significantly^{260,265}.

6.4 Confirming the presence of fibrils

Before the experiments, the presence of fibrils within the samples was confirmed by at least one method. This was done by recording the **far-UV circular dichroism (CD) spectrum** (box 4) and/or by comparing the fluorescence of the **optical probes ThT or ANS** (box 2 and 3) before and after fibril formation.

Circular dichroism (CD) spectroscopy

Box 4

Proteins are chiral molecules and thus optically active. Optically active molecules absorb right and left hand circularly polarized light differently. This phenomenon is defined as circular dichroism (CD). When left and right hand circularly polarized light are absorbed to different extents, the resulting light becomes elliptically polarized. This is quantified in the terms of the ellipticity (θ). The primary chromophores in proteins contributing to the CD signal are the peptide bonds, aromatic side chain groups, and disulfide bonds. Each chromophore absorbs light within a certain wavelength range, and specific structural information can be obtained from different spectral regions. The peptide bond absorbs in the far-UV region (185–240 nm) and gives information about the secondary structure of the proteins, where the secondary structural units, random coil, α -helix, and β -sheets, give distinct CD signals. Absorbance by the aromatic side chain groups and the disulfide bonds contribute mainly to the signal in the near-UV region. Measuring in the far-UV region is more sensitive, where the required concentration of the sample and the path length of the cuvette are lower than while recording within the near-UV region. CD spectroscopy is a valuable method within the study of amyloid proteins as the high number of β -sheets in the core gives rise to a strong β -sheets signal. The monomeric form of the intrinsically disordered protein α -synuclein gives a strong random coil signal

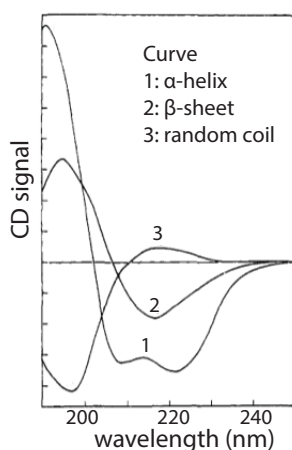


Figure 6.1: Computed CD spectra of poly-L-lysine, consisting of 100% α -helix, β -sheet, or random coil. The figure is adapted with permission from²⁶⁶. Copyright 1969, American Chemical Society.

6.5 Determining pK_a shifts upon fibril formation

The first task of the work presented in **paper I** was to find an applicable experimental approach to measure the effect of amyloid formation on the pK_a values of α -synuclein. Using established methods, the pK_a values of individual residues can be determined by NMR spectroscopy, and the average pK_a values can be determined by potentiometric titration. However, these techniques presented significant challenges when working with α -synuclein fibrils. Firstly, measuring the pK_a values of the individual ionizable groups within the fibrils remained challenging due to the fibrils being NMR invisible. Secondly, potentiometric titrations of α -synuclein fibril samples, performed in both water and low buffer strength, resulted in dissociation of the fibrils into free monomers upon change in pH. Therefore, it was not possible to obtain complete titration curves. This led us to conclude that measuring pH changes upon fibril formation might be a suitable way to access the pK_a value shifts. This approach measures the average effect in bulk but misses the more extreme local effects. The change in pH during fibril formation was measured with pH electrode, pH indicator and NMR spectroscopy. Additionally, we used a computational method (Monte Carlo simulation) to calculate the ionization states of individual residues at constant pH values.

Potentiometric pH measurements

The primary method for measuring pH changes was potentiometric measurements using a glass electrode (box 5), where isolation of α -synuclein in water was essential. In such systems, the only buffering groups are the ionizable groups of the protein, and a change in their protonation state (linked to pK_a shifts) would result in a change in the pH of the sample. The pH was measured before and after fibril formation at two concentrations (20 μ M and 70 μ M). From the measured pH value, we could calculate the shift in the apparent pK_a values upon fibril formation (see chapter 7.1).

For comparison with the wild-type, the pH change during fibril formation was also measured for an α -synuclein mutant having a lower number of acidic residues within the C-terminal tail, where five acidic residues had been substituted with non-charged polar residues (referred to as the 5Q-mutant). This was done to better understand if the up-shift in the average apparent pK_a value can be linked to the high density of acidic residues within the C-terminal tail and could be explained by the proximity of different tails extending from the fibril core.

Moreover, the pH was monitored continuously during amyloid fibril formation alongside ThT-fluorescence and static light scattering measurements using the instrument Probe Drum. This combination of techniques provides further information about whether pH changes are directly linked to the formation of amyloid fibrils.

Potentiometric pH measurements

Box 5

Ion-selective glass electrode that responds to H_3O^+ can be used to experimentally determine pH^{209,213,267}. A combined pH electrode consists of a reference electrode of a known electric potential and an indicator electrode. The combined glass electrode is then immersed into an analyte solution where the difference in chemical potential is measured. The chemical potential difference depends on the activity of H_3O^+ . This difference can be linearly related to the pH of the sample by using a pH meter connected to the electrode and calibrated by standard solutions of known pH^{209,213,214}. Calculations of dissociation constants based on potentiometric measurement using combined glass electrodes provide mixed dissociation constants, including both activity and concentration terms^{211,267}. It is, thus, important to report on solution conditions. In the same way, as for the concentration-based dissociation constant, the mixed dissociation constant approaches the thermodynamic one at infinite dilution (zero ionic strength). For dilute solutions, this difference is thus often negligible. For practical reasons, the mixed thermodynamic dissociation constant is, thus, the most commonly used in biochemical studies²¹¹.

pH indicator

Change in pH upon fibril formation can be detected using a pH indicator (box 6). The indicator resazurin was chosen as its protonation state, and thus, its spectrum changes within the pH range of interest, corresponding to a change from purple (monomeric sample) to blue (fibril dominating sample). The sample was prepared in a weak buffer system at pH 5.8. This was crucial to set the starting pH and thus being able to relate changes in pH to titration of the acidic residues. At the same time, it is essential that the concentration of the buffer component is low enough to detect pH changes. The color of the monomer samples was visually inspected and compared to the color of a sample consisting of amyloid fibrils.

pH indicator*Box 6*

Indirectly, pH can be estimated by adding a pH indicator to the analyte solution. Indicators are compounds that themselves can dissociate into acids and bases, where the different forms have different absorbance spectra. The dissociation constant of the pH indicators determines at what pH they change color or respond to pH changes^{209,213}. Therefore, picking an indicator that changes color in the pH range of interest is crucial. pH indicators exist in both soluble and solid forms. For example, pH papers contain a mixture of solid indicators with different dissociation constants. In **paper I**, we used a water soluble indicator added directly to the sample of interest to detect pH changes.

His50 as a pH sensor

Another way of detecting pH change is by monitoring the local environment around ionizable amino acids with NMR spectroscopy, where chemical shifts are measured (box 7)^{225,260,268,269}. α -synuclein contains one histidine residue at position 50 with a pK_a value of 6.78 (in 20 mM phosphate buffer, pH 7)²²⁵. Accordingly, the pH of a monomer- and fibril-dominated samples (in water) falls within the buffer region of His50, suggesting it as a potential pH reporter for our system (see equation 4.10). This was validated by performing ^{15}N - ^1H heteronuclear single quantum coherence (HSQC) NMR spectroscopy and diffusion order NMR spectroscopy (DOSY). ^{15}N - ^1H HSQC NMR spectra of an α -synuclein monomer sample and a fibril sample were almost identical, except for the chemical shift corresponding to His50 (**paper I**). Both spectra displayed characteristics typical for disordered proteins. This indicated that the signal obtained by NMR spectroscopy originates from the intrinsically disordered monomer free in solution rather than monomers within fibrils. Furthermore, DOSY NMR spectroscopy was used to distinguish between signals originating from monomers and fibrils. The highest applied gradient strength suppressed all signals in the monomeric sample. The signals in the fibrillar sample were slightly less suppressed and the 1D spectra overlapped well with the ones obtained from the monomeric sample. This indicated that signals in the fibrillar sample originate from α -synuclein monomers in solution interacting with slower diffusing species (fibrils). We concluded that the chemical shifts corresponding to His50 originate from the disordered monomers in solution both in the monomeric and fibrillar samples, and the corresponding chemical shift changes can supposedly be related to changes in the protonation state of His50, and thus to a change in the pH of the sample.

Nuclear magnetic resonance (NMR) spectroscopy*Box 7*

Nuclei that have a spin behave like small magnets. In NMR spectroscopy, the most useful nuclei are the ones with spin $1/2$, these are ^1H , ^{13}C , ^{15}N , ^{19}F , and ^{31}P . By placing the sample in a strong magnetic field, you can manipulate these spins using radiofrequency radiation and record NMR spectra. One of the main advantages of NMR spectroscopy is that it gives a signal for each individual atomic nucleus within the molecule. The signal frequency (chemical shift) depends on the surrounding nuclei and the chemical environment. With NMR spectroscopy, we can thus get site-specific information on molecular structures and also dynamics. For example, a change in pH and, thus, a change in the protonation state of ionizable groups results in a change in the chemical shift^{260,268,269}.

Expressing protein in the presence of a ^{13}C labeled carbon source and/or ^{15}N labeled nitrogen source incorporates these otherwise low abundance isotopes into the protein structure. Performing 2D NMR spectroscopy on a labeled protein simplifies the spectra by reducing overlaps between peaks. Heteronuclear single quantum coherence (HSQC) is a commonly used 2D NMR method within protein studies. Each peak in the 2D spectrum corresponds to a unique ^1H - ^{15}N heteronuclear pair, including signals from the amide groups of all amino acid residues except for proline.^{4,260,270}

NMR spectroscopy is a versatile tool that can be applied to solid and solution states. The advantage of solution-state NMR spectroscopy lies in its ability to measure native structures in solution. As molecular species increase in size, their tumbling in solution becomes slower, leading to peak broadening and lower signal intensities. This is particularly evident in the case of amyloid fibrils that are NMR-invisible. The interactions of free monomers with NMR invisible fibrils modulate their signal intensities, which can provide highly valuable information about the monomer-fibril interaction^{4,260,270}.

Simulations of individual ionization states

Metropolis Monte Carlo simulations were used to calculate the ionization states of individual residues using a coarse-grained protein model. All residues of the protein were included in the simulations and treated as single beads. Simulations of the monomer free in solution included all 140 beads connected by harmonic bonds. The simulations of monomers within fibrils were represented

by ten monomer planes, where the residues corresponding to the N- and C-terminal tails were treated as single beads connected with harmonic bonds, and the residues corresponding to the fibril core were kept fixed (according to a published structural model of α -synuclein fibrils, PDB: 2NoA). Simulations were performed at two constant pH values (5.5 and 6.5), and the ionization state of the ionizable residues was allowed to fluctuate according to the electrostatic environment. Electrostatic coupling due to the proximity of charges (within a single monomer and between different monomers within fibrils) could thus affect the ionization state of the residues. The ionization states of all titratable residues were calculated for both wild-type α -synuclein and an α -synuclein mutant and compared to experimental findings.

6.6 Detecting differences in morphology

In **paper II** we studied two structurally distinct but chemically identical morphologies, formed under the same conditions. The methods used to study their surface properties and structure will be introduced as follows.

Secondary structural content

Two morphologies studied in **paper II** showed differences in their CD-spectra. This became a valuable tool to get information about the dominant morphology within the sample and for monitoring changes in fibril morphology present within the sample over time.

Interaction of monomers with the fibril surface

In **paper II**, we used NMR spectroscopy (box 7) to study transient interactions of free monomers with the fibril surface of the two distinct morphologies. HSQC spectra were measured and the residue resolved ^{15}N - ^1H signal intensities of monomers in presence of fibrils, relative to the intensities in pure monomeric sample were calculated. Comparing signal intensities along the protein sequence provides information on how individual regions of the monomers interact with the fibril surface. Similarly, differences in these intensity patterns between various fibril morphologies can indicate a morphology-dependent interaction between monomers and the fibril surface. Distinct mode of interaction between the free monomers and fibrils of different morphology was also investigated by measuring variations in the ^{15}N transverse relaxation rates along the protein sequence.

Differences in ultrastructure

Cryo-TEM (box 8) can be used to get information about the structure of the amyloid fibrils present within the sample (**paper I**). The method was used to evaluate differences in the ultrastructure of α -synuclein fibrils of different morphologies (**paper II**), and to evaluate differences in the ultrastructure in the presence or absence of a chaperone (**paper III**).

Differences in surface properties

The fluorescence intensity of the optical probe ThT is dependent on the restriction of the carbon-carbon bond between the rings (box 3)^{261–264}. To what extent the rotation around the bond becomes restricted can differ between fibrils of different morphology and result in differences in the binding affinity and the fluorescence quantum yield^{248,271}. The binding of ThT to the two different morphologies presented in **paper II** was thus measured and compared. This was done by titrating ThT into the individual samples and recording the corresponding fluorescence emission spectra.

Cryogenic Transmission Electron Microscopy (Cryo-TEM) *Box 8*

Cryo-TEM is a popular method in the study of amyloids, and it is beneficial for getting structural information about fibril morphology and for visual inspection of the status of the sample. Electrons are transmitted through a sample and interact with the species within the sample, where they are either absorbed or scattered and from that, an image can be created. High-resolution images can be obtained by Cryo-TEM due to the short wavelength of electrons (down to picometers). Cryo-TEM provides imaging of the sample without staining. In order to avoid structural rearrangements during imaging, the sample is flash-frozen in liquid ethane (-180 degrees) as a thin liquid film on a carbon-film copper grid. This provides snapshots of the species of interest trapped in transparent amorphous ice^{272,273}.

6.7 Measuring apparent solubility

Determination of apparent solubility is a part of **papers I, II, and III**. The apparent solubility can be determined by separating free monomers from fibrils by centrifugation, followed by measuring the concentration of the monomer fraction. The concentration of free monomers can be determined by **SDS-PAGE** (box 9), where the intensity of the bands is compared to the intensity of bands of known concentrations. The concentration of free monomer in the solution can also be measured by **high-performance liquid chromatography (HPLC)**, where the absorbance of the elute is measured, and the area of the peak corresponding to the free monomers is integrated and compared to a standard curve. Furthermore, the concentration of free monomers in the supernatant can also be quantified with **mass spectrometry (MS)** by spiking the sample with isotope-labeled α -synuclein of known concentration (internal standard). The total intensity of the signals corresponding to non-labelled α -synuclein of unknown concentration is compared to signals corresponding to known concentration of ^{15}N -labelled α -synuclein peptides. Moreover, the fraction corresponding to free monomers was also analyzed by measuring absorbance at 280 nm. However, the absolute values were not reliable due to increased scattering in the supernatant compared to the free monomeric sample, which is most likely related to the presence of smaller species (e.g. oligomers) that do not successfully pellet with centrifugation.

Additionally, in **paper II**, the fraction of free monomer within the fibril-containing samples was measured by **NMR spectroscopy** (box 7). This was done by comparing the integrated ^{15}N - ^1H signal intensity of the last residue at the C-terminal end (A140) in the fibrillar sample to that of the monomeric sample. As mentioned earlier (chapter 6.5), all signals originate from free monomers. We assumed that the signal corresponding to A140 is not affected by transient interactions of the monomer with the fibril surface. The data were, thus, complemented using another method (determination of free monomer concentration using centrifugation and SDS-PAGE, see above).

SDS-PAGE*Box 9*

Sodium dodecyl sulfate-polyacrylamide gel electrophoresis (SDS-PAGE) is a useful analytic electrophoretic method used to separate and characterize proteins. It is commonly used to get information about the purity of the sample and the size and relative amount of the species present within a sample. SDS is a detergent that is a crucial component of the method. It binds to the proteins and denatures them (not always fully). The binding of SDS to proteins results in proteins being more or less uniformly negatively charged with a similar charge-to-mass ratio. SDS is a part of the samples, the gel, and the buffers. The gel consists of cross-linked acrylamide and bis-acrylamide, which form a mesh-like structure. Samples are loaded onto the polyacrylamide gel, and an electric field is applied. All the negatively charged proteins travel through the gel towards the anode. The larger molecules travel slower through the gel compared to smaller molecules, as they get more retained within the mesh. The mobility of the molecules is dependent on the net charge and friction. The shape of the proteins, thus, also affects how fast the proteins migrate through the gel. Different staining methods can be used to visualize the proteins in the gel.

6.8 Photo-induced cross-linking of unmodified proteins

Challenges are faced in the study of oligomers due to their heterogeneous and transient nature, low stability, and low abundance relative to free monomers and fibrils. Using bulk methods to obtain information on the structure and kinetics of different oligomers is thus challenging. However, advances in biophysical methods and instruments have led to improvements in oligomeric studies²⁷⁴.

Studying oligomers

Studies of oligomers can be approached in different ways. Certain methods can be used to stabilize or trap certain oligomeric structures by altering the energy landscape²⁷⁴. For example, certain kinetically favored oligomeric structures can be captured by following specific preparation protocols^{97,275}. Oligomers can also be captured by molecules, such as antibodies and small molecules, that bind to and stabilize certain structures^{91,274,276}. Intra- and intermolecular cross-linking is another way to shift the equilibrium and stabilize certain structures²⁷⁷. Other methods, such as single particle methods and radioactive labeling, can be used to get kinetic information, e.g., for following change in the total

concentration of oligomers as a function of time throughout the aggregation process^{83,278,279}. This shows how different available methods can report on different properties and characteristics of oligomers within amyloid systems, as well as being biased towards different oligomeric structures. A combination of different methods in the study of oligomers is thus optimal.

Cross-linking reactions involve the formation of covalent bonds within and between molecules. One of the most commonly used cross-linking methods within protein research involve chemical-cross-linkers that react with primary amines and thus require chemical modifications on the protein itself^{277,280}. In **paper IV**, we worked towards optimization of the cross-linking method photo-induced cross-linking of unmodified proteins (PICUP). The advantage of this method, as can be seen from its name, is that there is no need for any modification on the native structure prior to the cross-linking reaction, and thus, there is no need for a potential intervening linker arm¹⁰⁶. PICUP is a photo-reactive cross-linking method where the photo-sensitive reagent is activated by light. Without light activation, the photo-sensitive reagent is relatively inert, which makes it possible to apply the method under controlled conditions^{106,280}.

The cross-linking reaction

The photo-sensitive reagent essential for PICUP is the metal-coordinated complex ruthenium (II) tris-bipyridyldication ($\text{Ru(II)(bpy)}_3^{2+}$). The maximum absorbance of $\text{Ru(II)(bpy)}_3^{2+}$ is at 452 nm in aqueous solvents¹⁰⁶. Irradiation of the complex with light gets it into an excited state. In the excited state, the complex is capable of donating an electron to an electron-acceptor, in this case ammonium persulfate (APS), resulting in the formation of the one-electron oxidant $\text{Ru(III)(bpy)}_3^{3+}$, sulfate radical and sulfate ion. The oxidant $\text{Ru(III)(bpy)}_3^{3+}$ can now accept electrons from certain protein side-chain groups and by that forming a highly reactive protein radical that can react with other side-chain protein groups through intra- and inter molecular interactions. This process is believed to involve a proton transfer to the sulfate radical, resulting in the formation of a chemical bond between two side-chain groups. The formation of new covalent bonds can continue until the reaction is stopped, which usually involves the addition of a reducing agent (such as β -mercaptoethanol) leading to the reduction of the oxidant $\text{Ru(III)(bpy)}_3^{3+}$ to $\text{Ru(II)(bpy)}_3^{2+}$ ¹⁰⁶. Which residues become cross-linked is determined by the ability of the group to accommodate an unpaired electron (most commonly tyrosine and tryptophan) as well as the distance between the reactive groups^{106,107,281,282}.

Post-analysis

The post-analysis of cross-linked samples often involves fractionation methods such as SDS-PAGE and HPLC. Post-analyses are commonly performed by run-

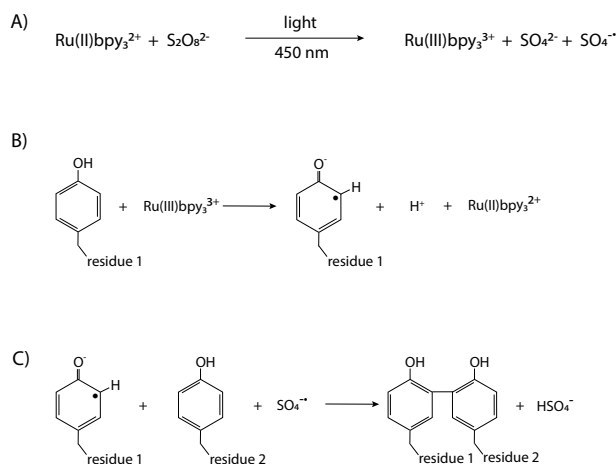


Figure 6.2: The PICUP reaction. A) Light (450 nm) is used to induce the metal-coordinated complex ruthenium (II) tris-bipyridylation ($\text{Ru(II)(bpy)}_3^{2+}$) to get it into an excited state, where it is capable of donating an electron to ammonium persulfate ($\text{S}_2\text{O}_8^{2-}$), resulting in the formation of the oxidant $\text{Ru(III)(bpy)}_3^{3+}$, a sulfate radical and a sulfate ion. B) The oxidant $\text{Ru(III)(bpy)}_3^{3+}$ can accept electrons from certain protein side-chain groups (tyrosin in the case of α -synuclein), resulting in the formation of a highly reactive protein radical. C) The reactive protein radical can react with other nearby side-chain protein groups through intra- and intermolecular interactions. This process involves a proton transfer to the sulfate radical and results in the formation of a chemical bond between two side-chain groups. The formation of new covalent bonds can continue until the reaction is stopped. This is based on a mechanistic hypotheses published by Fancy and Kodadek (1999). Copyright (1999) National Academy of Sciences, U.S.A.¹⁰⁶.

ning the samples directly on SDS-PAGE, where the oligomeric pattern of the cross-linked species can be directly visualized^{106,107,281,283}. For convenience, the solution used to stop the reaction (that generally contains the reducing agent) contains the ingredients needed to run the sample on an SDS-PAGE (SDS-loading buffer)^{106,107}. Post-analysis using a combination of fractionation methods and mass spectrometry could also be useful^{107,280}.

Advantages

One of the biggest advantages of this method is that crosslinking occurs between amino acid residues that are part of the native structure, and thus there is no need for any prior modifications of the primary structure^{106,107,281}. For the reaction to occur, the molecules need to be very close in space (within chemical bond distance), making the method more specific than, for instance, cross-linking methods using a chemical linker. Applying PICUP can thus provide information about molecular contacts^{106,281}. Additionally, the reaction time of

photo-induced chemicals is relatively shorter compared to other cross-linking methods, which further adds to the specificity of the method¹⁰⁷. Short lighting time can be an advantage within kinetic studies and studies of protein-protein interactions. Furthermore, the photo-sensitive reagent groups are relatively inert without light activation, which makes it possible to apply the method under controlled conditions¹⁰⁶. The light used for activating the reaction is within the visible range and, thus, not harmful to macromolecules or cells¹⁰⁶. Finally, PICUP has been found to work at several pH values.

Shortcomings

In an ideal case, all monomers within each oligomer would become cross-linked, and the cross-linking reaction would thus provide a perfect snapshot of the oligomeric distribution and abundance within the sample. However, that is not the case. Firstly, the cross-linking efficiency is not 100%, and the reaction might thus be biased towards smaller oligomeric species. As an example, a trimer might appear as a dimer if only two of the monomers are sufficiently cross-linked^{107,281}. Using longer lighting times can thus result in higher chances of sufficiently cross-linking together a higher number of monomers within the existing oligomers. On the other hand, using longer lighting time increases the chance of detecting cross-linked species that are not representative of the system, which can potentially be a result of cross-linking between proteins in proximity of each other. Using shorter lighting times makes it more likely that the most reactive residues will be cross-linked, which can simplify structural interpretations. This we address in **paper IV** and conclude that due to the biases of the different lighting times used, PICUP is not an optimal method for quantification of oligomers distribution and concentration. However, it can be a valuable method for comparative studies within amyloid research, e.g., by comparing changes in oligomeric pattern and concentration over time or comparing oligomeric patterns obtained by different variants. In **paper IV**, we suggest that combining shorter and longer lighting times might be optimal for comparative studies. Furthermore, the optimal distance between reactive residues might not be fulfilled within all oligomeric structures. For those reasons, PICUP could be biased towards specific oligomeric structures that can be categorized as PICUP visible oligomers.

Applications

PICUP was first established in 1999 and was presented as a method that could rapidly, efficiently, and with high yields cross-link stable protein assemblies¹⁰⁶. Since its introduction, it has been used within various studies¹⁰⁷, e.g., for studying multi-protein complexes²⁸⁴, protein-ligand interactions²⁸⁵ and for forming covalently bound dimeric antibodies²⁸⁶. PICUP has also been used to cross-

link colloidal silica-polypeptide-particles²⁸⁷. PICUP has been established as a valuable method for studies of heterogeneous mixtures of non-covalently bound oligomers formed within amyloid systems, such as $A\beta$ in Alzheimer's disease and α -synuclein in Parkinson's disease^{107,281,288–292}. It allows for studying the oligomers in their native form, where it has been used to cross-link monomers within oligomers to get information about their size distribution^{107,281,288}. The method has been used to compare the oligomer distribution of wild-type proteins and mutants under the same conditions²⁹². Furthermore, PICUP can be used to enrich concentrations of specific oligomeric structures, which can be essential for structural studies^{274,291,293}. The versatility of the method allows for diverse applications that extend beyond its original purpose. It can be adapted to various systems and other light-induced methods.

Previous experimental setups

Experimental setups have been found to vary significantly between individual research groups. The first experimental setup consisted of a light source placed within a camera box, where the lighting time was controlled by the shutter of the camera. The type of light source varied (e.g., 200-watt incandescent lamp, Xe-lamp, flashlight), and the distance from the light source ranged from 5 to 50 cm. The minimal lighting time required for sufficient cross-linking varied from 0.5 to 30 seconds^{106,107,281}. Later experimental setups have been found to consist of manually controlled blue-LED-light source within a closed chamber using a lighting time of 1 to 10 seconds^{288–290}. A standardized experimental system has thus been missing. As demonstrated in **paper IV**, precise control of the lighting time is crucial for good comparison within and between studies.

Optimization and use of PICUP within this thesis

In **paper IV**, we designed a 3D printable reaction chamber for PICUP and optimized the method for studies of α -synuclein. The chamber was designed for using a PCR tube as the sample container and using a sample volume of 20 μ L. The distance between the light source and the sample holder was kept minimal (1 mm) to maximize the intensity of light exposed to the sample. We chose to use an LED light of 450 nm close to the maximum absorbance of $\text{Ru(II)(bpy)}_3^{2+}$. The light sources and the electronics are easily fitted to the chamber. An Arduino program was written, making it possible to control light exposure times with ms accuracy. All material was made accessible for others to use.

Chapter 7

Summary of thesis work

In this chapter I will give a summary of each individual research paper presented in this thesis.

7.1 Paper I

Charge Regulation during Amyloid Formation of α -synuclein

Previous studies of α -synuclein have revealed that its rate of aggregation is highly pH dependent, where the rate of secondary nucleation is about four orders of magnitudes higher at mildly acid pH than at neutral pH. This pH dependence has been suggested to be related to the high density of the acidic residues in the C-terminal tail, which titrate at mildly acidic pH (chapter 4.2.2 and 4.2.3)⁵⁰. Studies of the pK_a values of the ionizable residues of α -synuclein in its monomeric form revealed that the pK_a values of the acidic residues in the C-terminal tail are upshifted compared to intrinsic values²²⁵.

The aim of the work presented in paper I was to investigate the effect of amyloid fibril formation on the pK_a values of α -synuclein to gain a better understanding of the role of electrostatic interactions in amyloid fibril formation.

The main finding is that there is a change in pH of almost one unit upon fibril formation of α -synuclein isolated in pure water. Based on this finding, the pK_a values of the acidic residues in the C-terminal tail of the monomers within fibrils were calculated to be upshifted by 1.1 unit compared to the monomers free in solution.

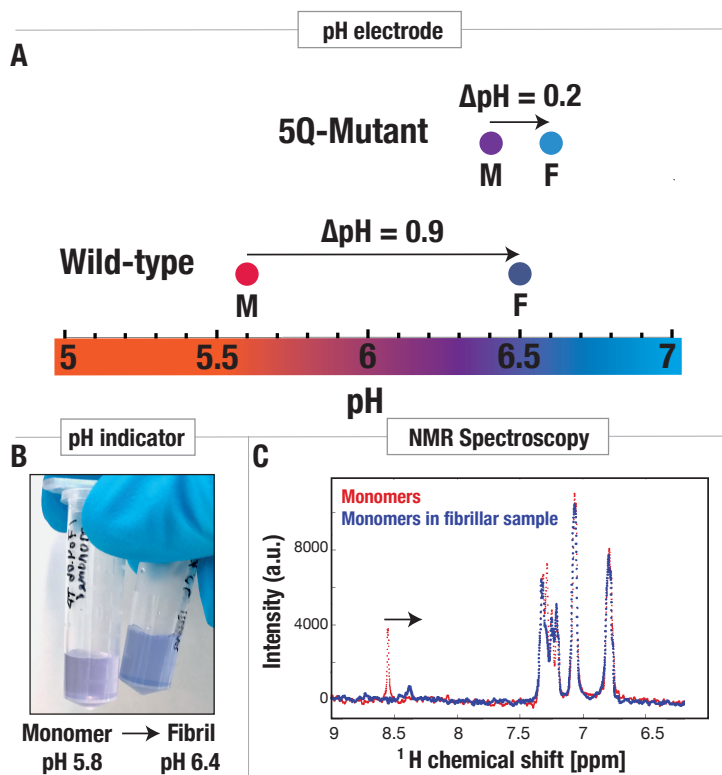


Figure 7.1: An increase in pH detected during amyloid fibril formation of α -synuclein.

A) The change in pH during amyloid fibril formation detected by pH electrode for wild-type α -synuclein and 5Q mutant. Samples were isolated in pure water (no buffer or other additional components). The pH of the sample was measured before and after fibril formation. The change in pH was measured to be on average from pH 5.6 to pH 6.5 for the wild-type α -synuclein and from pH 6.4 to pH 6.6 for the 5Q mutant. B) pH change detected using a pH indicator (resazurin). Wild-type α -synuclein was isolated in a weak buffer system. The monomeric sample gave a purple color while the sample containing fibrils gave blue color. For comparison, the pH was measured before and after aggregation, showing an increase in pH from 5.8 to 6.4. C) A change in pH detected by NMR spectroscopy, using the δ_2 proton of His₅₀ in the monomeric α -synuclein as a pH sensor. The red spectrum is recorded for a monomeric α -synuclein sample in 99.9% D₂O. The blue spectrum is recorded for the same sample after amyloid fibril formation. The decrease in the chemical shift corresponding to the δ_2 proton of His₅₀ indicates an increase in pH during fibril formation of α -synuclein.

For a system containing only the protein of interest isolated in pure water, the only buffering components within the system are the ionizable groups of the protein itself, in this case, α -synuclein. Any change in the protonation state of the ionizable residues would, thus, affect the pH of the sample. In other

words, the pK_a values of the ionizable groups of the protein determine the pH of the sample. Perturbations of the pK_a values would then result in a change in the concentration of free protons, which is measured as a change in pH. For α -synuclein in water, the pH increased upon fibril formation from 5.6 to 6.5, or by 0.9 pH units for a 20 μ M sample. The measured increase in pH upon fibril formation suggests that protons are taken up by the self-assembled protein, strongly indicating upshifts in the pK_a values.

An increase in pH upon fibril formation was measured using three complementary experimental methods: potentiometric pH measurements, pH indicator and NMR spectroscopy. The results were supported by Metropolis Monte Carlo simulations, where the ionization states of the individual ionizable residues of α -synuclein were calculated at constant pH, indicating upshifts in the apparent pK_a values upon fibril formation. Additionally, the pH was also monitored continuously during amyloid fibril formation using a pH electrode.

The calculations of the upshifts in pK_a values were performed as follows. A closed system consists of a defined number of protons, which makes it possible to calculate the change in the apparent average (pK_a) value from the measured pH change. In the initial samples, consisting of α -synuclein in pure water (no buffer), the protons are either free in solution ($\text{free}[H^+]_{\text{mono}}$) or bound to the monomers ($\text{bound}[H^+]_{\text{mono}}$). The concentration of free protons in such monomeric sample can be obtained from the measured pH of the sample according to:

$$\text{free}[H^+]_{\text{mono}} = 10^{\text{pH}_{\text{mono}}} \quad (7.1)$$

The degree of protonation of each individual ionizable group of α -synuclein monomers free in solution can be calculated according to:

$$Q = \frac{\text{free}[H^+]_{\text{mono}}}{\text{free}[H^+]_{\text{mono}} + K_a} \quad (7.2)$$

This was done by using published pK_a values of the titratable groups of monomeric α -synuclein²²⁵. The average protonation state (Q^{ave}) can be obtained from all individual protonation states. The number of protons bound ($\text{bound}[H^+]_{\text{mono}}$) to the acidic groups can thus be calculated according to:

$$\text{bound}[H^+]_{\text{mono}} = C \cdot \#\text{acidic groups} \cdot Q^{\text{ave}} \quad (7.3)$$

where C is the total concentration of the protein and "acidic groups" refers to the number of ionizable acidic groups.

The total number of protons ($\text{total}[H^+]_{\text{mono}}$) in the system can be obtained from the sum of the free and the bound:

$$\text{total}[H^+]_{\text{mono}} = \text{bound}[H^+]_{\text{mono}} + \text{free}[H^+]_{\text{mono}} \quad (7.4)$$

For a closed system, the total proton concentration in the initially monomeric sample is equal to the one in the finally fibrillar sample:

$$\text{total}[H^+]_{\text{mono}} = \text{total}[H^+]_{\text{fib}} \quad (7.5)$$

where, $\text{total}[H^+]_{\text{fib}}$ stands for the total proton concentration within the sample containing fibrils in equilibrium with monomers.

In the same way, as for the monomeric sample, the free proton concentration can be calculated from the pH of the fibril-containing sample according to:

$$\text{free}[H^+]_{\text{fib}} = 10^{\text{pH}_{\text{fib}}} \quad (7.6)$$

The total concentration of protons bound to the acidic groups within the fibrillar samples, $\text{bound}[H^+]_{\text{fib}}^{\text{tot}}$, can thus be estimated to be:

$$\text{bound}[H^+]_{\text{fib}}^{\text{tot}} = \text{total}[H^+]_{\text{fib}} - \text{free}[H^+]_{\text{fib}} \quad (7.7)$$

Within the fibrillar sample, $\text{bound}[H^+]_{\text{fib}}^{\text{tot}}$ thus refers to protons bound to both monomers free in solution and to monomers within the fibrils. The free monomer concentration in the fibrillar sample ($C_{\text{fib}}^{\text{mono}}$) has to be taken into account when estimating the concentration of protons bound to free monomers within the fibrillar sample. The $\text{p}K_{\text{a}}$ values of the acidic groups of monomers free in solution were assumed to be the same within the monomeric and fibrillar samples, and used to calculate the Q^{ave} of the monomers within the fibrillar sample. The concentration of protons bound to free monomers within the fibrillar sample, $\text{bound}[H^+]_{\text{fib}}^{\text{mono}}$, was then calculated according to:

$$\text{bound}[H^+]_{\text{fib}}^{\text{mono}} = C_{\text{fib}}^{\text{mono}} \cdot \# \text{acidic groups} \cdot Q^{\text{ave}} \quad (7.8)$$

The number of protons bound to the acidic groups of monomers within fibrils ($\text{bound}[H^+]_{\text{fib}}^{\text{fb}}$) can thus be calculated according to:

$$\text{bound}[H^+]_{\text{fib}}^{\text{fb}} = \text{bound}[H^+]_{\text{fib}}^{\text{tot}} - \text{bound}[H^+]_{\text{fib}}^{\text{mono}} \quad (7.9)$$

The concentration of ionizable groups that are not protonated ($\text{free}[P]_{\text{fib}}^{\text{fb}}$), i.e., in an ionized form, can be calculated according to:

$$\text{free}[P]_{\text{fib}}^{\text{fb}} = C_{\text{fib}}^{\text{fb}} \cdot \# \text{acidic groups} - \text{bound}[H^+]_{\text{fib}}^{\text{fb}} \quad (7.10)$$

Where $C_{\text{fib}}^{\text{fb}}$ is the concentration of monomers within fibrils, i.e. the fibril mass concentration.

The average apparent equilibrium constant K_a^{ave} for the acidic groups of the monomers within fibrils can then be calculated according to:

$$K_a^{\text{ave}} = \frac{\text{free}[H^+]_{\text{fib}} \cdot \text{free}[P]_{\text{fib}}^{\text{fb}}}{\text{bound}[H^+]_{\text{fib}}^{\text{fb}}} \quad (7.11)$$

From K_a^{ave} we can thus obtain the average apparent $\text{p}K_a$ value ($\text{p}K_a^{\text{ave}}$).

$$\text{p}K_a^{\text{ave}} = -\log_{10} K_a^{\text{ave}} \quad (7.12)$$

From the measured pH increase (the pH before and after aggregation) we could, thus, estimate that the apparent $\text{p}K_a^{\text{ave}}$ of α -synuclein shifts from 4.3 to 5.4, or by 1.1 unit, during fibril formation (figure 7.1 and table 7.1).

The role of the acidic residues in the effects on pH and $\text{p}K_a$ values was validated using a mutant with five fewer acidic groups (5Q) (see figure 7.1 and table 7.1).

Table 7.1: Comparison of the calculated apparent $\text{p}K_a^{\text{ave}}$ for monomers free in solution and monomers within fibrils. The upshift in the apparent $\text{p}K_a^{\text{ave}}$ is represented as $\Delta\text{p}K_a^{\text{ave}}$.

	$\text{p}K_a^{\text{ave}}$ monomers	$\text{p}K_a^{\text{ave}}$ fibrils	$\Delta\text{p}K_a^{\text{ave}}$
wild-type	4.3	5.4	1.1
5Q-mutant	4.2	4.7	0.5

Where do the protons come from? The results of this work show that protons are taken up during the amyloid formation of α -synuclein. However, the num-

ber of protons taken up can only partly be donated from the solvent, where the effect of auto-ionization of water would be minor. As α -synuclein itself is the major buffer component within the system (serves as an internal buffer), the majority of the protons taken up by the monomers that become a part of a fibril, thus, originate from the monomers that remain free in solution. The pK_a^{ave} of monomers in solution is not the same as the pK_a^{ave} of the monomers within the fibrils. The charge state at the end of the aggregation reaction thus differs, where the net charge and the charge of the C-terminal tail are more negative for the free monomer than the monomer within fibrils. We, thus, find that the protons taken up by the monomers that form the fibrils are donated by the monomers that remain in solution. This means that for the system as a whole to reach the lowest possible free energy, a fraction of the monomers need to remain in solution, which explains why the solubility cannot be lower than a particular value (cf. below).

The measured concentration of free monomer concentration in the fibrillar sample indeed differed between the wild-type protein and the ζ Q-mutant, where the mutant was found to have lower apparent solubility. The lower apparent solubility of the mutant, compared to the wild-type, can be related to the lower amount of protons taken up during the fibril formation of the mutant, and thus the smaller increase in apparent pK_a values of the mutant compared to the wild-type. This can be explained by the fact that there has to be enough monomers free in solution to donate enough protons to the monomers within fibrils, for the system as a whole to reach the lowest possible free energy. In the case of the wild-type, monomers within fibril have a higher affinity for protons compared to the ζ Q-mutant, and thus, a higher number of protons has to be donated from free monomers, which could explain the higher concentration of monomer left in solution at the end of the reaction.

In conclusion, the pH, of a closed system consisting of α -synuclein in water, increases during amyloid fibril formation. This implies that protons are taken up during the aggregation process, i.e., an increased affinity for protons, indicating upshifts in the pK_a values of monomers in the fibrils compared to monomers in solution. Upshifts in pK_a values of the ζ Q-mutant were lower than for the wild-type protein, indicating that the pK_a value perturbations occurring during the fibril formation are linked to the high-density of negative charges within the C-terminal tail. The uptake of protons during aggregation lowers the unfavorable electrostatic repulsion between the negatively charged tails decorating the fibril surface, which can make amyloid fibril formation thermodynamically more favorable compared to a non-titrating charged system.

7.2 Paper II

Morphology-Dependent Interactions between α -Synuclein Monomers and Fibrils

Amyloid fibrils share the characteristics of elongated and nonbranched protein self-assemblies, with a highly ordered cross- β structured core (see chapter 1.3). Despite this, the structure of amyloid fibrils, even formed from identical proteins and peptides, can vary significantly, referred to as different morphologies. The structure is highly dependent on the solution conditions, resulting in morphologies of different stability and with different surface properties (see chapter 1.4).

The aim of the work presented in paper II was to study the mode of interaction of α -synuclein monomers with the fibril surface. The presence of two structurally distinct but chemically identical morphologies formed under identical conditions provided a way to follow changes in the structure and free-monomer concentration with time, aiming to better understand the structural evolution and changes in stability as a function of time.

The main findings of this paper revealed significant differences between the two morphologies formed under identical conditions. These differences included: how monomers interact with the fibril surface, apparent solubility, structure, and surface properties.

First, two chemically identical but structurally different fibril morphologies were observed to form independently under identical conditions at neutral pH, termed morphology A and B. In other words, splitting a freshly purified monomeric sample into multiple tubes could result in the samples either consisting of morphology A or morphology B, which made it possible to study them independently (at early time points, 1-2 days). The apparent solubility was found to differ between the two morphologies, where morphology A was found to have a higher solubility than morphology B. This indicates that the stability of morphology A was lower than the stability of morphology B (figure 7.2).

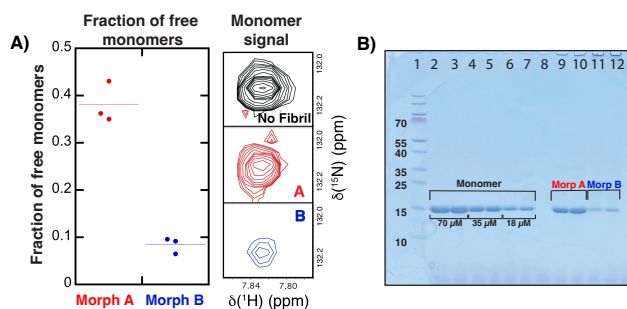


Figure 7.2: Apparent solubility of morphology A and B. A) The left panel represents the fraction of free monomers in samples consisting of fibrils of either morphology A (0.38 ± 0.04) or B (0.08 ± 0.02), corresponding to $27.7 \pm 3 \mu\text{M}$, and $6.0 \pm 1.2 \mu\text{M}$, respectively. The different dots represent individual data points, with the average shown as a line. This was obtained by comparing the integrated intensity of A_{140} in the fibril containing samples to that of a monomeric sample (right panel). B) SDS-PAGE of four independent samples consisting of a supernatant that had been separated from fibrils of morphology A (wells 9-10) and morphology B (wells 11-12) with centrifugation. The initial total protein concentration was $70 \mu\text{M}$ α -synuclein in 10 mM Tris/HCl, 0.02% NaN_3 , pH 7. For comparison with the free monomer concentration, aliquots of a monomeric sample of three different concentrations ($70 \mu\text{M}$, $35 \mu\text{M}$, and $18 \mu\text{M}$) were loaded onto wells 2-7.

By the use of NMR spectroscopy, we observed that the two morphologies have different surface properties, where the mode of interaction of the free monomer in solution with the fibril surface was found to differ significantly between the two morphologies. In the case of morphology A, only a part of the positively charged N-terminal domain of the monomers (the first 16 residues) was found to interact with the negatively charged fibril surface. In the case of morphology B, a larger part of the monomer was found to interact with the fibril surface (figure 7.3).

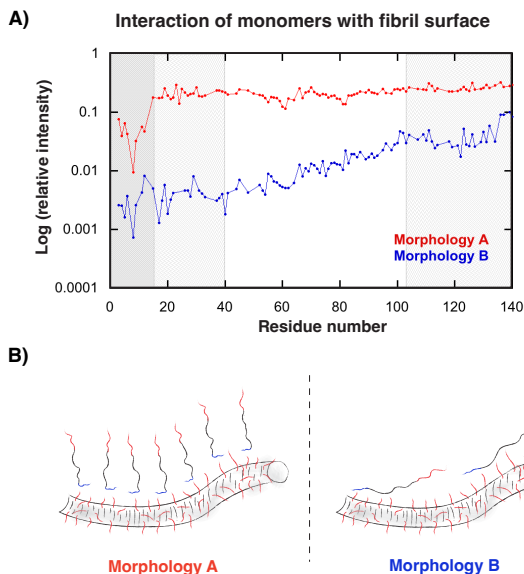


Figure 7.3: The different modes of interaction of free monomers in solution with the fibril surface of morphologies A (red) and B (blue). A) A NMR spectroscopic characterization of transient interactions of free monomers with the fibril surface of morphology A and B. The red and blue traces represent the residue-resolved signal intensities for monomers in the presence of morphology A (red) and B (blue) relative to the signal intensities in a monomeric sample. The three shaded areas correspond to residues 1-15, 16-40, and 102-140. The two different samples presented originated from identical monomeric sample in 10 mM Tris, 0.02% NaN_3 , 5% D_2O , pH 7.0. B) A schematic illustration of the different mode of interaction of monomers with the fibril surface, showing that a small part (residues 1-15) of the positive N-terminal domain interacts with the negative fibril surface of morphology A. In presence of morphology B, a large part of the sequence was found to interact with the fibril surface. The interaction can be divided into three regions. Firstly, the N-terminal domain interacts strongest with the fibril surface. Secondly, the interaction of the NAC domain gradually decreases along the sequence, towards the C-terminal tail. Lastly, the C-terminal tail might also be affected by the interaction with the fibril surface, but to a lower degree.

Fluorescence titrations showed differences in the binding of ThT to fibrils of the two morphologies, further indicating differences in surface properties. Structural differences were detected by cryo-TEM and CD spectroscopy, showing different mesoscopic structures and different CD-spectra, respectively (figure 7.4).

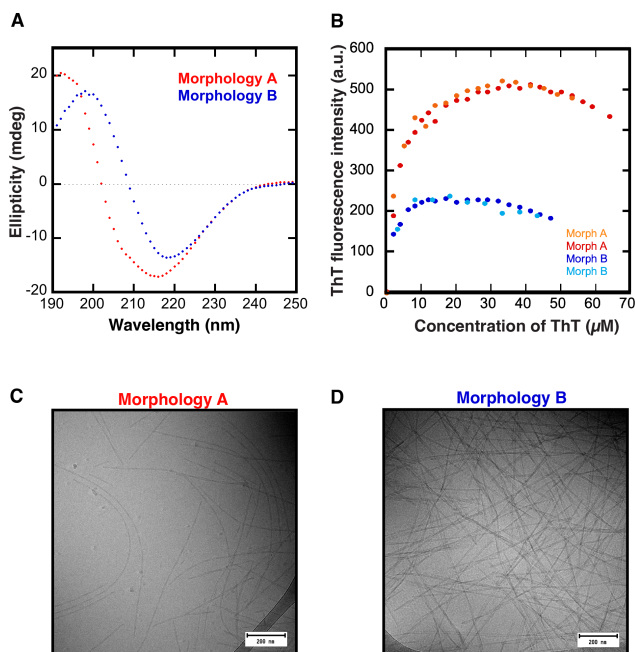


Figure 7.4: Differences in surface properties and structure between morphology A and B. A) The two morphologies gave different Far-UV CD spectra. The spectrum corresponding to morphology A (red) is more shifted towards lower wavelengths compared to the spectra corresponding to morphology B. B) Fluorescence titrations of the different morphologies with ThT. The maximum fluorescence intensity of individual emission spectra plotted against increased concentration of ThT. The maximum fluorescence of morphology A (two replicates shown) was more than two times higher than for morphology B, despite morphology A having lower fibril concentration. Lower concentration of ThT was needed to reach the maximum fluorescence intensity for B than A. C) Cryo-TEM image (40K) of sample of morphology A, consisting of thinner and more curly fibrils. D) Cryo-TEM image (40K) of morphology B, consisting of thicker and more straight fibrils.

The time evolution of the samples, containing fibrils of either morphology A or B, indicated that the samples of the lower stability and higher solubility (morphology A) gradually transit into consisting majorly of the morphology with the higher stability and lower solubility (morphology B). In other words, with time, fibrils of morphology B, take over the samples that originally consisted of morphology A (figure 7.5). This can be understood from the laws of thermodynamics, that at infinite time a system will always end up in its most energetically favorable state (chapter 5.1).

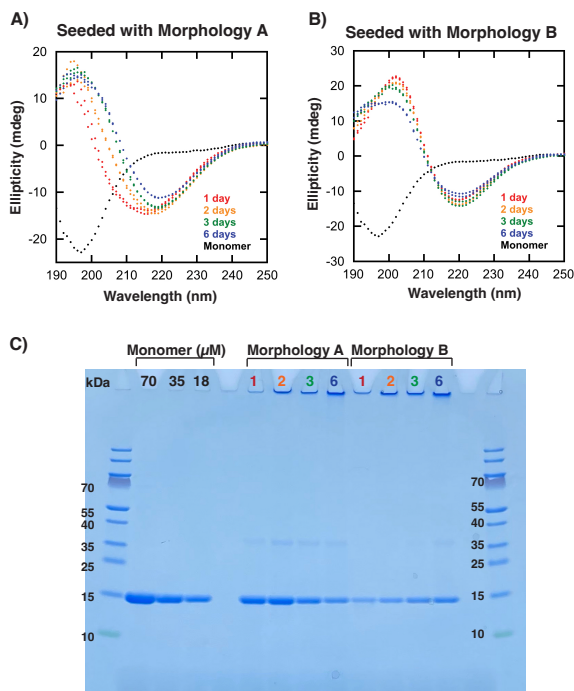


Figure 7.5: Time-evolution of morphology A and B. Identical monomeric samples were seeded with morphology A or morphology B. At early times (1–2 days), the sample seeded with morphology A gave a CD spectra corresponding to morphology A. However after longer incubation times, the CD spectra shifted towards the one corresponding to morphology B (panel A). Simultaneously the free monomer concentration decreased to a concentration in the range of the apparent solubility of morphology B (panel C). At all time points, the sample seeded with fibrils of morphology B gave CD spectra of corresponding morphology (panel B). At the end of the experiment, the free monomer concentration of both samples had equilibrated to a similar value (panel C).

How can morphology A and B form under identical conditions? Firstly, the free energy is lower for the morphology of the higher stability and the ΔG for the formation of the more stable structure is, thus, larger. Despite that, the kinetic barriers for formation of morphologies of different stability can vary, where the energy barriers for nucleation of the less stable morphology (A), can be similar and even lower than the energy barriers for forming the more stable morphology (B) (figure 7.6 and section 5.2). A system can, thus, consist of fibrils that do not have the most thermodynamically stable morphology. In such cases, the system is under kinetic control. However, at equilibrium, at infinite time, the sample should become under thermodynamic control (see chapter 5.2).

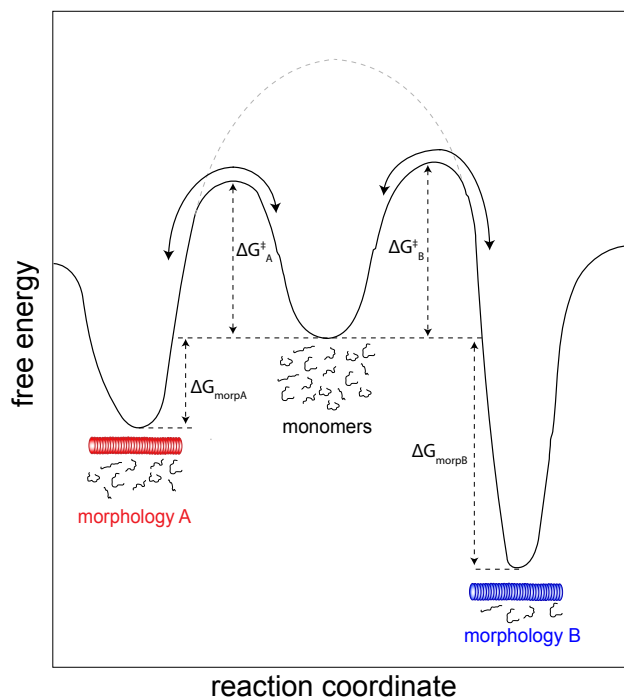


Figure 7.6: Simplified illustration of the energy landscape of two different morphologies forming at identical conditions. The energy barriers for forming the different morphologies can be of similar heights (ΔG^\ddagger). In such cases, a sample could become under kinetic control, consisting of the less stable fibrils of morphology A. The free-energy difference (ΔG) between the monomeric state and the fibrillar state is not the same for the two morphologies, where ΔG is more negative for formation of the more stable morphology. At infinite time, a sample will always end up consisting of the most thermodynamic stable morphology. This most likely occurs through dissociation of monomers from the less stable morphology and association to the fibrils of the higher stability (arrows). The energy barrier for structural conversion is probably higher, and it is thus less likely to occur through structural conversions (gray dashed lines).

How can sample become dominated by fibrils of the less stable morphology A? This can possibly be related to the energy barriers for primary nucleation of α -synuclein being much higher than the energy barriers for secondary nucleation and elongation (sections 3.3 and 2.1.1). The de-novo formation of a new morphology of higher stability could thus be less favored than the replication of an already existing morphology through secondary nucleation and elongation. This is also supported by our findings, that the fibril morphology was successfully replicated by seeding the monomer samples.

How can sample consisting of morphology A transit into a sample consisting of morphology B? This can possibly be related to the reversible nature of amyloid fibrils (section 5.3). The monomers continuously associate and dissociate to and from the fibril ends, where the rates of association and dissociation vary throughout the aggregation process. With time, the monomers that detach from the fibril ends of morphology A can attach to the growing ends of the thermodynamically more stable morphology B. At infinite time, a sample should become monomorphic, consisting only of the thermodynamically most stable morphology. A structural conversion of one morphology to another is most likely, a less favorable process.

In conclusion, the formation of fibrils of different morphologies, of different structure, surface properties, solubility, and stability, under identical conditions could be explained by the system being under kinetic control. In this work, the interaction of the free α -synuclein monomers with the fibril surface of morphology A and B were found to differ significantly, where only a small part of the N-terminal domain of the monomer was found to interact with the fibril surface of morphology A, while a larger part of the protein was found to interact with the surface of morphology B. In both cases, the N-terminal end was found to interact the strongest to the negative fibril surface. These results are in agreement with other published studies of α -synuclein indicating preferential interactions between the slightly positive N-terminal region of the monomers and the negatively charged fibril surface^{122,123}, further suggesting that favorable attractive electrostatic interactions may play a role in amyloid formation process, with possible implications for secondary nucleation (section 4.2.4).

7.3 Paper III

The role of α -synuclein-DNAJB6b co-aggregation in amyloid suppression

The impact of chaperones on the aggregation rates and mechanism of amyloid fibril formation is an active research field^{132,138,139,143–145}. Previous studies indicate that the relative stabilities of the fibrils and monomers of A β 42 are affected in the presence of the molecular chaperone JB6 (chapter 2.3)¹⁴². Formation of less stable co-aggregates could result in higher apparent solubility of amyloid proteins in the presence of chaperones (chapter 5.5)¹⁴⁹. This was further investigated in this work, focusing on the amyloidogenic protein α -synuclein and the molecular chaperone JB6.

The aim of the work presented in paper III was to investigate and get a better thermodynamic understanding of the effect of the human chaperone JB6 on the aggregation of α -synuclein.

The main findings of this study are that the aggregation of α -synuclein is suppressed in the presence of JB6, at low stoichiometric ratios at conditions where the effects on secondary nucleation are well detectable (low seed concentration, mildly acidic pH, quiescent, low binding surfaces) (figure 7.7). The results suggest that JB6 might interfere with the secondary nucleation process of α -synuclein. This was observed using two complementary methods, where the formation of amyloids was indirectly measured using ThT and where the consumption of monomers was measured directly using NMR spectroscopy.

In comparison, the half-times increased significantly less in the presence of a JB6 mutant, termed S/T18A, where 18 serine and threonine residues in the S/T-rich region had been substituted with alanine residues (figure 7.7). These results are consistent with results previously obtained for A β 42^{138,142,144} and polyglutamine peptide¹⁴³. The decreased suppression effect of the mutant compared to the wild-type JB6 could potentially be explained by the increased hydrophobicity upon removal of hydroxyl groups, which might result in a lower amount of available JB6 subunits.

The results imply an increase in the apparent solubility of α -synuclein in the presence of JB6. This was observed by analyzing the amount of α -synuclein remaining in solution at the end of an aggregation experiment using three complementary methods: SDS-PAGE, HPLC and NMR spectroscopy, where the concentration of free α -synuclein left in solution was found to positively correlate with the JB6 concentration (figure 7.7).

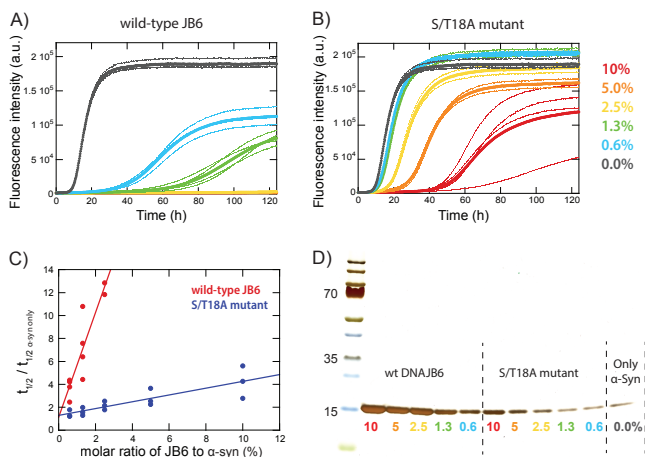


Figure 7.7: The effect of JB6 on the aggregation and solubility of α -synuclein. The aggregation kinetics of 20 μM α -synuclein at pH 5.5 in the presence of 2 μM (10% on molar basis), 1 μM (5%), 0.5 μM (2.5%), 0.25 μM (1.3%) and 0.13 μM (0.6%) (A) wild-type JB6 and (B) S/T18A mutant. The replicates are shown with smaller data points, and the average of the four replicates of each wild-type and mutant JB6 concentration are presented with larger data points. (C) The relative half-times ($t_{1/2}$) are calculated from the corresponding data and plotted against the molar ratio of JB6 to α -syn in molar percentage. The data are obtained from three individual experiments containing different combinations of batches of α -synuclein, wild-type JB6, and S/T18A mutant. Fits of straight lines to all data points for wild-type JB6 (red) and S/T18A mutant (blue) are shown. (D) The effect of wild-type JB6 and S/T18A JB6 mutant on the apparent solubility of α -synuclein. Samples were harvested at the end of the kinetic experiment and centrifuged to separate fibrils from free monomers in solution. The supernatant was collected and run on the SDS-PAGE.

Thirdly, cryo-TEM analyses, of α -synuclein in the presence and absence of JB6 show significant differences in the mesoscopic structures as well as in the amount of fibrils formed (figure 7.8). Samples of α -synuclein alone showed higher amounts of fibrils that appeared bundled up and relatively straight. The elongated fibrillar structures formed in the presence of the chaperone appear to be less bundled up, with a curly appearance and small knobs and irregularities along the fibrils. Variation in the diameter of the fibrils was more significant in the presence than in the absence of JB6. Additionally, the diameter was found to be, on average, larger in the presence of JB6.

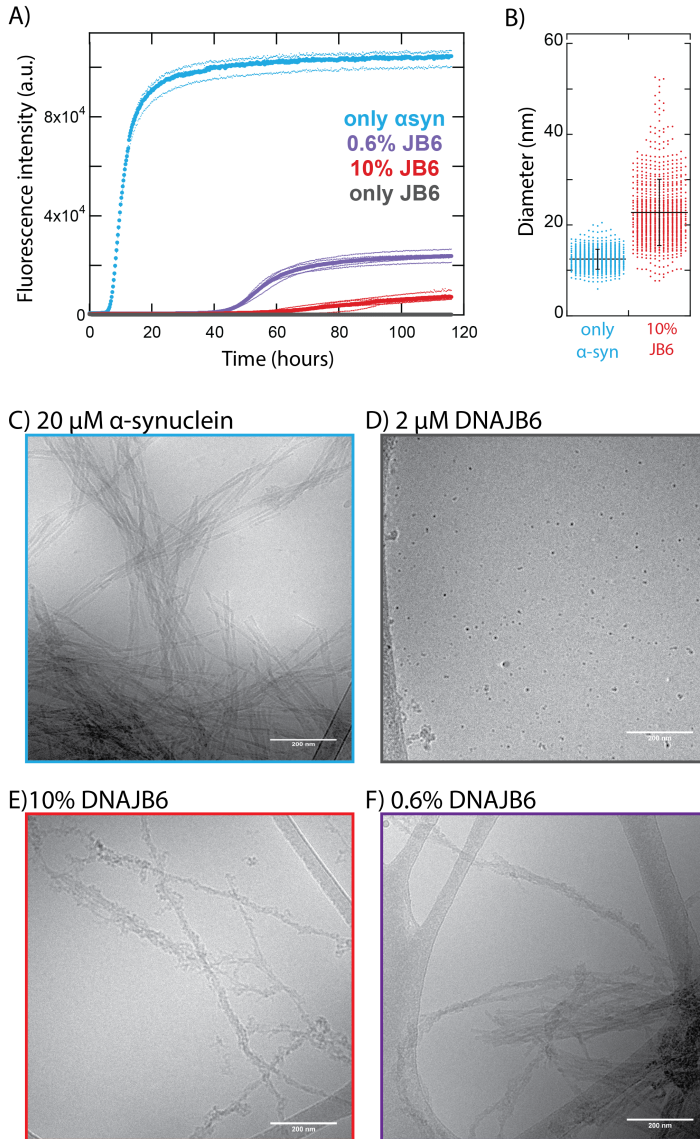


Figure 7.8: The effect of JB6 on the supra-molecular structure of α -synuclein fibrils. A) Comparison of the aggregation of 20 μ M wild-type α -synuclein at pH 4.5 in the absence and presence of 2 μ M (10%, red) and 0.13 μ M (0.6%, purple) JB6 as well as 2 μ M JB6 alone (gray). B) A scatter plot presenting the average diameter of pure α -synuclein fibrils (12.5 ± 2.2 nm, n=668) and co-aggregates of α -synuclein and JB6 (22.8 ± 7.3 nm, n=765). Individual measurements are represented with a single dot, and the average and standard deviation are shown with black lines. (C-F) Cryo-TEM images showing the ultrastructures in the samples collected at the end of the kinetic experiment for samples of C) 20 μ M α -synuclein D) 2 μ M DNAJB6, E) α -synuclein in presence of 2 μ M (10%) DNAJB6, F) α -synuclein in presence of 0.13 μ M (0.6%) DNAJB6 (F). The scale bars correspond to 200 nm.

These results strongly indicate the formation of co-aggregates of α -synuclein and JB6. The existence of ThT-negative aggregates in samples consisting of α -synuclein and JB6 in high stoichiometric ratios (5 and 10%) further supports the conclusion of the formation of co-aggregates of α -synuclein and JB6.

Why would α -synuclein form co-aggregates that are less stable (higher solubility) with respect to the amyloid protein? A thermodynamic explanation for the increase in solubility of amyloidogenic proteins in the presence of chaperones, such as JB6, has been proposed¹⁴⁹ and is also presented in detail in chapter 5.4. The presence of co-aggregates of α -synuclein and JB6 at the conditions used in this work, as well as the observed increase in the apparent solubility of α -synuclein in the presence of JB6, can plausibly be explained by a high chemical potential of the chaperone alone. Within co-aggregates, the chaperone would be energetically happier, with a lower chemical potential. The net decrease in chemical potential of the chaperone exceeding the net increase in the chemical potential of α -synuclein would result in the **system as a whole** having lower free energy in the case of co-aggregates than pure α -synuclein fibrils co-existing with the free chaperone (figure 7.9).

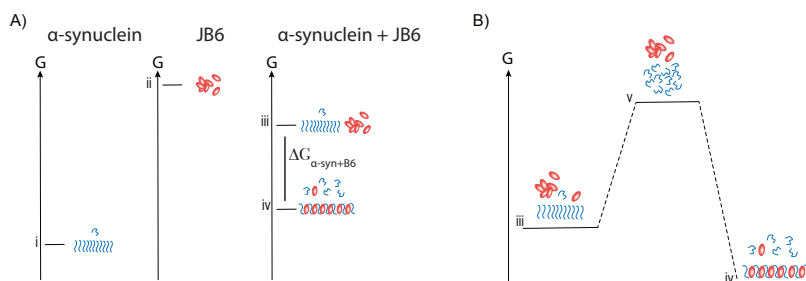


Figure 7.9: A thermodynamic explanation for the formation of co-aggregates of α -synuclein and JB6. A) Schematic illustration showing that in terms of α -synuclein, amyloid fibrils (i) are energetically more stable than co-aggregates of α -synuclein and JB6 (iv). However, due to the high chemical potential of JB6 alone (ii), the formation of co-aggregates (iv) in equilibrium with α -synuclein and free chaperone is energetically more favorable than the formation of pure α -synuclein amyloid fibrils co-existing with the unhappy chaperone (iii). B) Schematic representation of a system consisting of α -synuclein and JB6 (v), illustrating that the formation of co-aggregates of α -synuclein and JB6 (iv) results in the total free energy of the system being lower than in the case of formation of pure α -synuclein aggregates in the presence of JB6 (iii).

In conclusion, the aggregation of α -synuclein, at mildly acidic pH and with low seed concentration, is suppressed in the presence of JB6, with potential implications on secondary nucleation events of α -synuclein. Substitutions of serine

and threonine residues with alanine residues in the S/T-rich region decreased the chaperone's potency as an amyloid protein inhibitor. Further investigations are needed to understand if the decreased inhibitor efficiency may be directly linked to the removal of the hydroxyl groups or an increase in hydrophobicity that could affect the concentration of available active subunits or the rate of their release from oligomers.

The aggregation of α -synuclein in the presence of JB6 resulted in the formation of co-aggregates and an increase in the apparent solubility of α -synuclein. This indicates that the chemical potential of α -synuclein monomers is higher within the co-aggregates than in pure α -synuclein amyloid fibrils. This could potentially be explained by the high chemical potential of the chaperone alone, where the formation of co-aggregates would be thermodynamically favorable, making the total free energy of the system lower than in the case of the formation of pure α -synuclein aggregates co-existing with JB6.

7.4 Paper IV

Photo-Induced Cross-Linking of Unmodified α -Synuclein Oligomers

Oligomers have been found to play a crucial role in the pathogenesis of amyloid diseases, making them essential to study. Their transient nature, high heterogeneity, and low abundance relative to fibrillar and monomeric species have posed significant challenges in their study (chapter 2.2.1). Available methods can give different information and be biased towards different species. Combining different methods to study oligomers and performing careful data analysis can thus be crucial. PICUP is an example of an available method for studying oligomers (chapter 6.8). A standardized and well-controlled experimental setup has previously been absent. The reaction chamber has typically been constructed individually within different research groups.

The aim of the work presented in paper IV was to optimize the PICUP method for studying oligomers of amyloidogenic proteins, using α -synuclein as the model peptide. The aim was to design an experimental setup where we could accurately control crucial parameters, such as the reaction time and the distance from the light source, as well as being able to limit the lighting time. We wanted to increase our understanding of the factors affecting the reaction and make the optimized setup available for others, with the aim of increasing reproducibility, accessibility, and comparability.

The main findings of the first part of the work presented in paper IV show that the PICUP reaction is highly sensitive to exposure time and that precise control of the reaction time is crucial for reproducibility and relative comparison between samples. We started the work by designing a standardized 3D printable reaction chamber for the PICUP reaction (figure 7.10), allowing for accurate control over the geometry and lighting time down to ms accuracy (see more details in chapter 6.8).

The PICUP reaction of α -synuclein within the newly designed reaction chamber was optimized in regards to exposure time, stopping reagents, and ThT concentration. Only monomers are detected on an SDS-PAGE without irradiation (no PICUP reaction). On the other hand, a light-exposure time of one ms was sufficient for detecting cross-linked species corresponding to the size of a dimer within a freshly prepared α -synuclein sample (figure 7.11). This highlights the sensitivity of the method for detecting oligomers that only exist as a small fraction of the total protein concentration. These results also show that oligomeric species can be detected within a freshly prepared α -synuclein sample

(run through a size-exclusion column and kept on ice for 0.5 -1 h). Moreover, the results show that small errors in lighting time can significantly affect the number of cross-linked species, highlighting the importance of precise control of the lighting time in comparative studies.

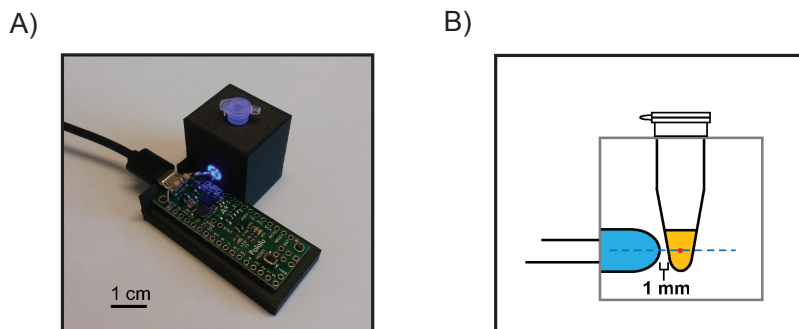


Figure 7.10: The design of the PICUP reaction chamber. A) Photograph of the experimental setup: the reaction chamber and the led-light source connected to a board that is controlled with an Arduino program. B) Schematic illustration of the reaction chamber, showing that the center of the LED light source (blue) and the center of the sample (orange) are aligned.

Furthermore, we show that the reaction is not sensitive to variations in the time interval between the end of the irradiation and addition of the stopping buffer. This is most likely explained by illumination continuously activating the reagents that only stay active for a very short time. We found that in the case of α -synuclein, adding SDS is enough to prohibit further cross-linking reaction from occurring, and in such cases, the addition of β -mercapethanol can, thus, be avoided. This might be due to the oligomers not being SDS-resistant (the fibrils formed at these conditions are not SDS-resistant) and/or due to SDS affecting the reagent.

The aim of the second part of the project was to apply the optimized method to get information on oligomer formation as a function of time during the aggregation process of α -synuclein at mildly acidic pH, where secondary nucleation is the dominating microscopic nucleation mechanism. In parallel, we analyzed all samples with and without PICUP using two different lighting times.

The highest oligomer concentration was detected at the start of the aggregation process, showing a correlation between the disappearance of oligomers and an increase in fibril mass. This indicates that the PICUP visible oligomers detected under these conditions originate from the monomers. This is interesting as

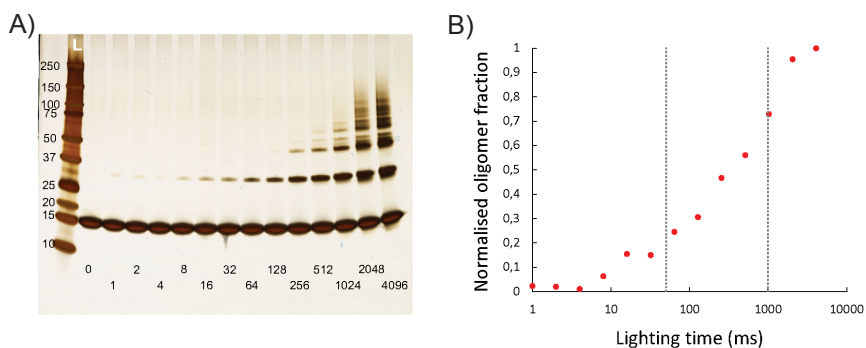


Figure 7.11: Photo-induced cross-linking of monomeric α -synuclein with different lighting times. A) Samples of freshly purified α -synuclein monomers were cross-linked using different irradiation times (0 to 4096 ms). Samples were run on SDS-PAGE, silver stained, and analyzed with ImageJ. The concentration of oligomers relative to the total protein concentration was calculated and normalized to the highest oligomer fraction. B) Normalised values at different lighting times plotted on a logarithmic time-scale.

secondary nucleation has been found to be the main process for generation of oligomers. One potential explanation could be that individual methods can be biased towards the detection of different oligomeric species (see chapter 6.8). The number and variety of oligomers present within the system could thus be much greater than is detected by PICUP under these conditions. This could be explained by the method being favored towards certain oligomeric species with optimal covalent bond distance between reactive residues as well as the reaction being favored towards detection of smaller oligomeric structures (see chapter 6.8).

Another potential explanation could be that the detachment of the oligomers that form at the fibril surface through secondary nucleation is slow, resulting in large part of the oligomers not being detected. Recent studies by Xu et al. (2024)¹⁹⁶ demonstrate that the measured concentration of oligomers formed through secondary nucleation (in PBS, pH 7.4) is highly dependent on the detachment of the oligomers from the fibril surface. They show that the concentration of oligomers detected in solution increases significantly upon shaking. It would thus be interesting to perform the experiments present in our work with mild agitation as a function of time, to further investigate the effect of concentration and distribution of oligomers throughout the aggregation process.

Furthermore, we detect two bands with a molecular weight around 30 kDa at the end of the aggregation, but those bands also appear without the PICUP reaction and are thus not a product of the cross-linking reaction. Additionally, sep-

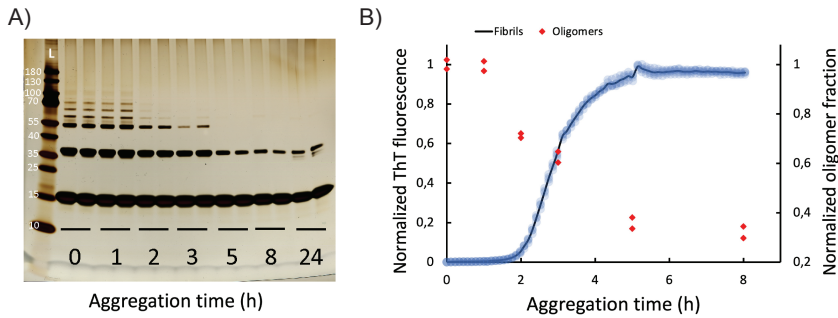


Figure 7.12: PICUP at different time-points during the amyloid formation of α -synuclein. Samples taken at different time-points (0, 1, 2, 3, 5, 8, and 24 h) were cross-linked and analysed with SDS-PAGE. A) silver-stained gel of samples that were cross-linked using lighting time of 1 s. B) Normalised ThT fluorescence intensity of 6 replicates (blue) where the average is shown as a black line. Red dots correspond to the the normalised intensity of the oligomeric bands relative to all bands in the same lane at each time point.

aration of free monomers and fibrils by centrifugation, shows that these species follow the fibril fraction.

The origin of these bands may be linked to secondary nucleation, indicating that oligomers are attached to the fibril surface. This further suggests that the oligomer distribution detected under quiescent conditions does not represent the oligomeric distribution of the system as a whole, due to majority of the oligomers being stuck on the fibril surface, which could be linked to the low net charge of the fibril surface at pH 5.5. This is consistent with cryo-TEM images of fibrils formed at pH 5.5, showing fibrils that are bundled (**paper I and III**).

Could PICUP capture random diffusion of monomers into proximity of one another? This was addressed by performing PICUP under the same conditions but on a non-oligomeric protein. The protein of choice, human lysozyme, is of similar molecular weight as α -synuclein and has four tyrosine residues positioned on the surface of the protein, which potentially could allow for cross-linking between diffusing species. The results showed no detectable cross-linked oligomers with light exposure time of 4 s. As previously mentioned, no cross-linking was observed in the presence of SDS, which might further support the conclusion that the cross-linked species result from transient interactions between different monomers. Additionally (not part of the published paper), we have done experiments where α -synuclein at different concentrations was cross-linked. The relative number of oligomers was similar within samples of different

monomer concentrations, further indicating that the PICUP visible oligomers are not a result of random cross-linking between adjacent monomers in solution.

In conclusion, we designed an 3D printable reaction chamber for the PICUP reaction, allowing for accurate controls of the lighting time and the geometry of the experimental setup. All material was made accessible for others to use and can be easily adjusted towards other sample containers. We conclude that PICUP can be a method of choice for comparative studies, where a combination of different lighting times can be optimal. We believe this work provides good fundamental grounds that can be further built upon and linked to other methods and systems of choice.

7.5 Paper V

On the role of α -synuclein C-terminal acidic residues

The primary structure of α -synuclein is highly polar, with a basic N-terminus, hydrophobic central region, and a highly acidic C-terminal tail. In its free form, transient interactions between termini within the monomer have been found protective against aggregation^{179,181,242,243}. Transient interactions between the C-terminal tails at the fibril surface and the N-terminal tail of the free monomer have been documented and suggested to play a role in secondary nucleation (**paper II**)^{121–123}. The aggregation of wild-type α -synuclein is highly pH dependent^{50,53}, where the rate of aggregation is higher at pH below six than above due to the presence of secondary nucleation at mildly acidic pH. The slower aggregation of α -synuclein at neutral pH is believed to be related to the highly negative C-terminal tail and the high net negative charge of the protein^{52,56,181,182}.

The aim of the work presented in paper V was to get better insights into the role of the high density of acidic residues within the C-terminal tail and better understand the pH dependence of α -synuclein aggregation. This was done by studying a series of mutants, where up to eight acidic residues (Asp and Glu) in the C-terminal tail had been mutated to non-charged polar residues (Asn and Gln) (termed 1Q to 8Q). This provides a way to study the charge effect on the aggregation by keeping the length of the tail intact. The aggregation was followed by thioflavin T fluorescence at different pH values (ranging from pH 4 to 7). Self-seeding (mutant seeds) was compared to cross-seeding (wild-type seeds) to get insight into the ability of the monomer to nucleate at the fibril surface and attach to fibril ends.

The main findings of the study are that the number of acidic groups within the C-terminal tail affects the rate and the pH dependence of α -synuclein aggregation. The change in the behavior differed between mildly acidic pH and neutral pH (figure 7.13). The pH optimum for secondary nucleation (at mildly acidic pH) was found to shift to a lower pH with an increasing number of mutations (figure 7.13 and 7.14). This can be linked to the pK_a values of the acidic residues of the mutants becoming less upshifted upon fibril formation compared to wild-type (**Paper I**).

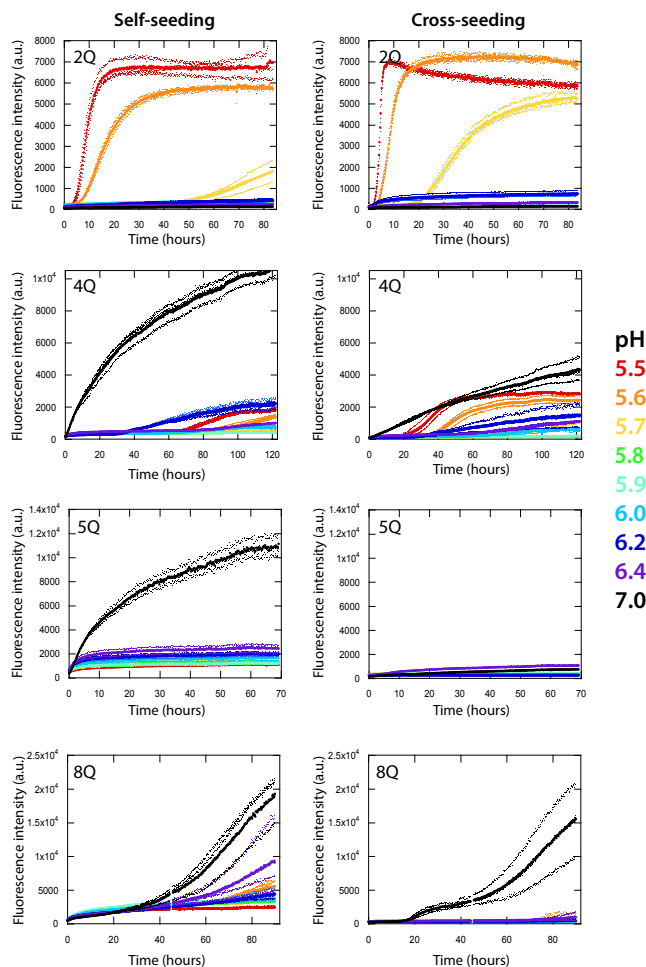


Figure 7.13: Self-seeding versus cross-seeding of 2Q, 4Q, 5Q and 8Q at pH 5.5-7.0. 20 μM monomer was seeded with 1% of their own seeds or 1% of the wild-type seeds. The aggregations of individual mutants were studied at the same time, in the same plate. All mutants were studied in 10 mM MES/NaOH.

At neutral pH, the aggregation was found to occur faster upon charge mutations, which is presumably related to the tail becoming gradually less charged at neutral pH with an increasing number of mutations. The effect of self-seeding (mutant seeds) and cross-seeding (wild-type seeds) differed between the individual mutants and varied between pH values. Cross-seeding of 2Q and 4Q was more efficient than self-seeding, which could be explained by the surface of the wild-type fibrils being less charged and thus easier for the mutant monomers to access and nucleate on the fibril surface. In contrast, our results indicate that the

4Q mutant self-elongates better than cross-elongates at neutral pH. This could be explained by the mutant being less negatively charged at neutral pH compared to wild-type, and thus experiencing less repulsive interactions between fibril ends and free monomer.

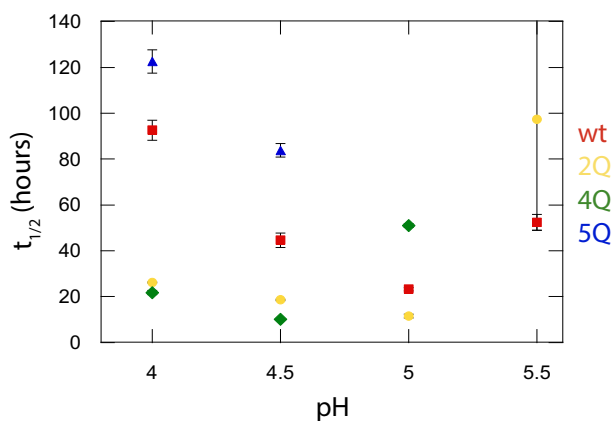


Figure 7.14: Comparison of half-times for wt, 2Q, 4Q and 5Q at pH 4.0, 4.5, 5.0 and 5.5. All experiments were performed in 20 mM PB with 0.02% NaN_3 .

Could a change in the number of acidic groups within the C-terminal tail affect transient interactions? The aggregation is dependent on various internal (within the monomer) and external (monomer-monomer, monomer-fibril, fibril-fibril) transient contacts, which are mediated by distinct interactions, e.g., short-range and long-range electrostatic interactions, hydrophobic interactions, short-range π - π interactions, and steric repulsions. The relative contribution of such interactions can for example be modulated by changing the charge state of the protein, which can be achieved by a change in pH or by charge mutations.

How can the removal of acidic residues from the C-terminal tail result in the tail becoming more negatively charged at mildly acidic pH? This may sound counterintuitive; however, in **paper I**, we showed that the $\text{p}K_a$ values of the acidic residues become upshifted upon fibril formation due to the proximity of the acidic tails decorating the fibril core. We also showed that the $\text{p}K_a$ value upshift is less for the 5Q mutant. This affects the net charge of the protein, where the pI value of the mutant is lower than for the wild-type. The pH value for minimal electrostatic repulsion between the fibril surface and monomers in solution is thus at a lower pH for the mutant than the wild-type. This may explain why the optimal pH for secondary nucleation shifts towards a lower pH with an increasing number of mutations.

How could the number of acidic residues relate to the protective role of the C-terminal tail? A decrease in the number of acidic residues results in faster aggregation at neutral pH. This could both be related to less protective transient intermolecular contacts between the N-terminus and the C-terminus of the free monomer, as well as being related to the less repulsions between the fibrils and the free monomers. In contrast, removing acidic residues from the C-terminal tail results in slower aggregation at mildly acidic pH, where the optimal pH for secondary nucleation shifts to lower pH. The results thus indicate that a higher number of acidic residues is more protective at neutral pH, opposite to pH 5.5, where it may be less protective.

In conclusion, the results from this work demonstrate that the pH dependent aggregation of α -synuclein is highly linked to the number of acidic residues in its C-terminal tail. This work highlights how modulations of electrostatic interactions by pH change and charge mutations can affect the amyloid fibril formation of α -synuclein.

Chapter 8

Conclusion

The polar protein α -synuclein, characterized by its basic N-terminal end, hydrophobic core, and highly acidic C-terminal tail, is the protein under investigation in all papers presented within this thesis. The results presented in **papers I, II and V** support the conclusion that the polar and intrinsic nature of α -synuclein is a key factor influencing its aggregation behavior. A significant portion of my studies has been centered around investigating the contributions of electrostatic interactions in the amyloid formation of α -synuclein, with particular emphasis on the role of the C-terminal tail. Another significant part of my work explores the different aspects of amyloid fibril stability and solubility.

The work presented in **paper I** involved developing an approach to measure the pK_a values of monomers within fibrils. From this work, we learned that protons are taken up by the monomers upon fibril formation, indicating that the pK_a values of the acidic groups become upshifted when monomers misfold into fibrils. Because of this upshift the stability of the fibrils is higher than would otherwise be the case. We also show that the upshift is significantly less for a mutant with fewer acidic residues within the tail, indicating that the pK_a upshift can be linked to the high density of acidic groups within the C-terminal tail.

In the same study, we show that the apparent solubility (in water) is higher for wild-type α -synuclein than for the mutant. This can be explained by the protein itself being the main buffering component and, thus, the main proton donor within the system. Free monomers in solution thus donate protons to the monomers that misfold into fibrils. In the case of the wild-type protein, a higher concentration of free monomers is needed to provide enough protons for

the monomers within fibrils. The fraction of monomer left in solution, i.e., the solubility, thus increases with the number of protons that need to be taken up per monomer and this criterion needs to be fulfilled for the system to reach the lowest possible free energy. The difference in solubility thus further supports the conclusion that the pK_a upshift is dependent on the density of the acidic residues within the C-terminal tail.

In **paper V**, we also show how the aggregation rate and pH dependence of α -synuclein is affected by a change in the number of acidic residues within tail. The results suggest that the optimal pH for secondary nucleation is shifted to a lower pH upon a decrease in the acidity of the tail. This behavior aligns with the findings in **paper I**, where the direction of this change can presumably be related to less increase in pK_a values for the less acidic variants upon fibril formation.

The net charge of the protein at mildly acidic pH increases upon removal of acidic residues, which may significantly alter the relative contribution of different interactions that play a role in the amyloid formation of α -synuclein, such as the balance between short-range attractive and long-range repulsive electrostatic interactions. The optimal conditions for secondary nucleation occur at mildly acidic pH, or when the net charge of the protein approaches zero, resulting in minimized repulsions and maximized attractions between monomers and fibril surfaces.

The intricate balance between the different interactions governing monomer-fibril interactions may thus be tuned by alterations in the net charge of the protein. Understanding these interactions requires consideration of not only the overall net charge but also the charge distribution across different regions of the protein. This is in line with the studies presented in **paper II**, showing that the polarity of the sequence governs electrostatic interactions between monomer and fibrils, where the positively charged N-terminus was found to be attracted to the negatively charged fibrils. This mode of interaction was observed for two chemically identical but structurally distinct fibril morphologies, where the extent of the sequence from the N-terminal end being attracted to the fibril surface varied.

The two fibril morphologies studied in **paper II** were found to form independently under identical conditions. This could be related to the energy barriers for the primary nucleation of the individual morphologies being similar. The energy barriers for elongation and secondary nucleation are much lower than for primary nucleation, and the propagation of the already existing structure could thus be kinetically more favorable than the de-novo formation of a new structure. The solubility of the fibrils was also found to differ, indicating a dif-

ference in their stability. The independent formation of each structure made it possible to capture and study samples predominantly consisting of either one of the fibril morphologies. Due to the reversible nature of amyloid fibrils, the monomer will dissociate from the less stable structure and attach to and propagate the more stable structure. This is consistent to our results that show that with time, the samples transit into consisting of the more stable structure.

Following the investigation of fibril solubility in a pure α -synuclein system, **paper III** explores how the apparent solubility is affected by the presence of the molecular chaperone DNAJB6b (JB6). Firstly, the results show that JB6 suppresses α -synuclein aggregation in a concentration-dependent manner at sub-stoichiometric ratios. Cryo-TEM analyses of the samples at the end of the aggregation reactions strongly indicate the formation of co-aggregates between α -synuclein and JB6. This is further supported by the apparent solubility of α -synuclein being higher in the presence of JB6. Higher solubility indicates that the chemical potential of α -synuclein is higher within co-aggregates than pure α -synuclein aggregates. This could be explained by a high chemical potential of the chaperone alone driving the system as a whole into the energetically most favorable state, where the decrease in the chemical potential of the chaperone upon formation of co-aggregates would be greater than the increase in chemical potential of α -synuclein.

Lastly, in **paper IV**, we optimized the method PICUP for the study of α -synuclein. We show that a precise control of lighting time is crucial for comparison within and between studies. We designed and built a reaction chamber and made it available for others to rebuild. The improvements in the method may serve as a good starting point for studying various systems. As an example, it would be interesting to apply the method to the various system described in this thesis and compare oligomeric patterns obtained for α -synuclein at different solution conditions, for α -synuclein mutants, different morphologies, and in the absence and presence of molecular chaperones.

The work presented in this thesis has taught me a lot about α -synuclein, its intrinsic nature, and how aggregation is highly dependent on various intrinsic and extrinsic factors. However, as always, answering one question brings you to many more. I look forward to continuing to work towards an increased understanding of the system and being exposed to new questions as they arise. Science is fun!

References

- [1] Harold Hartley. Origin of the Word "Protein". *Nature*, 168:244, 1951.
- [2] Hubert Bradford Vickery. The origin of the word protein. *Yale Journal of Biology and Medicine*, 22(5), 1950.
- [3] Carl Branden and John Tooze. *Introduction to Protein Structure*. Garland Scienc, Taylor & Francis groups, New Trj, 2 edition, 1998.
- [4] David L. Nelson and Michael M. Cox. *Lehninger Principles of Biochemistry*. W. H. Freeman and Company, New York, 5th edition, 2008.
- [5] Ken A. Dill. Dominant Forces in Protein Folding. *Journal of the American Chemical Society*, 29(31):7133–7155, 1990.
- [6] Peter E. Wright and H. Jane Dyson. Intrinsically disordered proteins in cellular signalling and regulation. *Nature Reviews Molecular Cell Biology*, 16(1):18–29, 2015.
- [7] Max A Eisenberg and Georg W Schwert. The reversible heat denaturation of chymotrypsinogen. *The Journal of General Physiology*, 34(5), 1951.
- [8] Timothy O. Street, Naomi Courtemanche, and Doug Barrick. Protein Folding and Stability Using Denaturants. *Methods in Cell Biology*, 84(07):295–325, 2008.
- [9] Joachim Seelig and Anna Seelig. Protein Stability—Analysis of Heat and Cold Denaturation without and with Unfolding Models. *Journal of Physical Chemistry B*, 127(15):3352–3363, 2023.
- [10] Alan Cooper. Thermal stability of tropocollagens—Are hydrogen bonds really important? *Journal of Molecular Biology*, 55(1):123–127, 1971.
- [11] Kalyani Sanagavarapu, Tanja Weiffert, Niamh Ní Mhurchú, David O’Connell, and Sara Linse. Calcium binding and disulfide bonds regulate the stability of Secretagogin towards thermal and urea denaturation. *PLoS ONE*, 11(11):1–22, 2016.
- [12] Charles Tanford and Kirk C. Aune. Thermodynamics of the Denaturation of Lysozyme by Guanidine Hydrochloride. III. Dependence on Temperature. *Biochemistry*, 9(2):206–211, 1970.

- [13] Karen L. Maxwell, David Wildes, Arash Zarrine-Afsar, Miguel A. De Los Rios, Andrew G. Brown, Claire T. Friel, Linda Hedberg, Jia-Cherng Horng, Diane Bona, Erik J. Miller, Alexis Vallée-Bélisle, Ewan R.G. Main, Francesco Bemporad, Linlin Qiu, Kaare Teilum, Ngoc-Diep Vu, Aled M. Edwards, Ingo Ruczinski, Flemming M. Poulsen, Birthe B. Kragelund, Stephen W. Michnick, Fabrizio Chiti, Yawen Bai, Stephen J. Hagen, Luis Serrano, Mikael Oliveberg, Daniel P. Raleigh, Pernilla Wittung-Stafshede, Sheena E. Radford, Sophie E. Jackson, Tobin R. Sosnick, Susan Marqusee, Alan R. Davidson, and Kevin W. Plaxco. Protein folding: Defining a “standard” set of experimental conditions and a preliminary kinetic data set of two-state proteins. *Protein Science*, 14(3):602–616, 2005.
- [14] Christopher M Dobson. Protein folding and misfolding. *Nature*, 426(18/25):884–890, 2003.
- [15] Sara Linse and Tuomas Knowles. Amyloids and protein aggregation. *Chemical Science*, 14(24):6491–6492, 2023.
- [16] Patricia L. Clark. Protein folding in the cell: Reshaping the folding funnel. *Trends in Biochemical Sciences*, 29(10):527–534, 2004.
- [17] F. Ulrich Hartl and Manajit Hayer-Hartl. Converging concepts of protein folding in vitro and in vivo. *Nature Structural and Molecular Biology*, 16(6):574–581, 2009.
- [18] Pu Chun Ke, Ruhong Zhou, Louise C. Serpell, Roland Riek, Tuomas P.J. Knowles, Hilal A. Lashuel, Ehud Gazit, Ian W. Hamley, Thomas P. Davis, Marcus Fändrich, Daniel Erik Otzen, Matthew R. Chapman, Christopher M. Dobson, David S. Eisenberg, and Raffaele Mezzenga. Half a century of amyloids: Past, present and future. *Chemical Society Reviews*, 49(15):5473–5509, 2020.
- [19] Joseph T Jarrett, Elizabeth P Berger, and Peter T Lansbury. The carboxy terminus of the beta amyloid protein is critical for the seeding of amyloid formation: implications for the pathogenesis of Alzheimer’s disease. *Biochemistry*, 32(18):4693–4697, 1993.
- [20] Dennis J. Selkoe. Cell biology of protein misfolding: The examples of Alzheimer’s and Parkinson’s diseases. *Nature Cell Biology*, 6(11):1054–1061, 2004.
- [21] Claudio Soto. Unfolding the role of protein misfolding in neurodegenerative diseases. *Nature Reviews Neuroscience*, 4(1):49–60, 2003.
- [22] Fabrizio Chiti and Christopher M. Dobson. Protein misfolding, functional amyloid, and human disease. *Annual Review of Biochemistry*, 75:333–366, 2006.
- [23] Peter T. Lansbury and Hilal A. Lashuel. A century-old debate on

- protein aggregation and neurodegeneration enters the clinic. *Nature*, 443(7113):774–779, 2006.
- [24] Jean D. Sipe, Merrill D. Benson, Joel N. Buxbaum, Shu Ichi Ikeda, Giampaolo Merlini, Maria J.M. Saraiva, and Per Westermark. Amyloid fibril protein nomenclature: 2012 recommendations from the Nomenclature Committee of the International Society of Amyloidosis. *Amyloid*, 19(4):167–170, 2012.
- [25] Fabrizio Chiti and Christopher M. Dobson. Protein misfolding, amyloid formation, and human disease: A summary of progress over the last decade. *Annual Review of Biochemistry*, 86:27–68, 2017.
- [26] H. Puchtler, F. Sweat, and M. Levine. On the binding of congo red by amyloid. *Journal of Histochemistry & Cytochemistry*, 10(3):355–364, 1962.
- [27] H. Puchtler and F. Sweat. A review of early concepts of amyloid in context with contemporary chemical literature from 1839 to 1859. *The journal of histochemistry and cytochemistry*, 14(2):123–134, 1966.
- [28] Dobson C.M. Protein misfolding, evolution and disease. *Trends in Biochemical sciences*, 24(9):329–332, 1999.
- [29] Margaret Sunde and Colin Blake. The structure of amyloid fibrils by electron microscopy and x-ray diffraction. *Advances in Protein Chemistry*, 50:123–159, 1997.
- [30] Thomas R. Jahn, O. Sumner Makin, Kyle L. Morris, Karen E. Marshall, Pei Tian, Pawel Sikorski, and Louise C. Serpell. The Common Architecture of Cross- β Amyloid. *Journal of Molecular Biology*, 395(4):717–727, 2010.
- [31] Charyl Del Mar, Eric A. Greenbaum, Leland Mayne, S. Walter Englander, and Virgil L. Woods. Structure and properties of α -synuclein and other amyloids determined at the amino acid level. *Proceedings of the National Academy of Sciences of the United States of America*, 102(43):15477–15482, 2005.
- [32] Ani Der-Sarkissian, Christine C. Jao, Jeannie Chen, and Ralf Langen. Structural Organization of α -Synuclein Fibrils Studied by Site-Directed Spin Labeling. *Journal of Biological Chemistry*, 278(39):37530–37535, 2003.
- [33] Ricardo Guerrero-Ferreira, Nicholas M.I. Taylor, Ana Andrea Arteni, Pratibha Kumari, Daniel Mona, Philippe Ringler, Markus Britschgi, Matthias E. Lauer, Ali Makky, Joeri Verasdock, Roland Riek, Ronald Melki, Beat H. Meier, Anja Böckmann, Luc Bousset, and Henning Stahlberg. Two new polymorphic structures of human full-length alpha-synuclein fibrils solved by cryo-electron microscopy. *eLife*, 8:1–24, 2019.
- [34] L. Lutter, Christopher J. Serpell, Mick F. Tuite, and Wei Feng Xue. The molecular lifecycle of amyloid – Mechanism of assembly, mesoscopic or-

- ganisation, polymorphism, suprastructures, and biological consequences. *Biochimica et Biophysica Acta - Proteins and Proteomics*, (11):526–536, 2019.
- [35] Yaowang Li, Chunyu Zhao, Feng Luo, Zhenying Liu, Xinrui Gui, Zhipu Luo, Xiang Zhang, Dan Li, Cong Liu, and Xueming Li. Amyloid fibril structure of α -synuclein determined by cryo-electron microscopy. *Cell Research*, 28(9):897–903, 2018.
- [36] Binsen Li, Peng Ge, Kevin A. Murray, Phorum Sheth, Meng Zhang, Gayatri Nair, Michael R. Sawaya, Woo Shik Shin, David R. Boyer, Shulin Ye, David S. Eisenberg, Z. Hong Zhou, and Lin Jiang. Cryo-EM of full-length α -synuclein reveals fibril polymorphs with a common structural kernel. *Nature Communications*, 9(1):1–10, 2018.
- [37] Marcus D. Tuttle, Gemma Comellas, Andrew J. Nieuwkoop, Dustin J. Covell, Deborah A. Berthold, Kathryn D. Kloepper, Joseph M. Courtney, Jae K. Kim, Alexander M. Barclay, Amy Kendall, William Wan, Gerald Stubbs, Charles D. Schwieters, Virginia M.Y. Lee, Julia M. George, and Chad M. Rienstra. Solid-state NMR structure of a pathogenic fibril of full-length human α -synuclein. *Nature Structural and Molecular Biology*, 23(5):409–415, 2016.
- [38] Marçal Vilar, Hui Ting Chou, Thorsten Lührs, Samir K. Maji, Dominique Riek-Loher, Rene Verel, Gerard Manning, Henning Stahlberg, and Roland Riek. The fold of α -synuclein fibrils. *Proceedings of the National Academy of Sciences of the United States of America*, 105(25):8637–8642, 2008.
- [39] Robert Silvers, Michael T. Colvin, Kendra K. Frederick, Angela C. Jaccavone, Susan Lindquist, Sara Linse, and Robert G. Griffin. Aggregation and Fibril Structure of A β M01-42 and A β I-42. *Biochemistry*, 56(36):4850–4859, 2017.
- [40] Louise C. Serpell, Paul E. Fraser, and Margaret Sunde. X-Ray Fiber Diffraction of Amyloid Fibrils. *Methods in Enzymology*, 309(1986):526–536, 1999.
- [41] Christopher M. Dobson. The amyloid phenomenon and its links with human disease. *Cold Spring Harbor Perspectives in Biology*, 9(6):1–14, 2017.
- [42] Michael R. Sawaya, Michael P. Hughes, Jose A. Rodriguez, Roland Riek, and David S. Eisenberg. The expanding amyloid family: Structure, stability, function, and pathogenesis. *Cell*, 184(19):4857–4873, 2021.
- [43] Lukas Frey, Dhiman Ghosh, Bilal M Qureshi, David Rhyner, Ricardo Guerrero-Ferreira, Aditya Pokharna, Witek Kwiatkowski, Tetiana Serdiuk, Paola Picotti, Roland Riek, and Jason Greenwald. On the pH-dependence of α -synuclein amyloid polymorphism and the role of sec-

- ondary nucleation in seed-based amyloid propagation. *eLife*, 12:1–29, 2024.
- [44] Veronica Lattanzi, Ingemar André, Urs Gasser, Marija Dubackic, Ulf Olsson, and Sara Linse. Amyloid β 42 fibril structure based on small-angle scattering. *Proceedings of the National Academy of Sciences*, 118(48), 2021.
- [45] Michael T. Colvin, Robert Silvers, Birgitta Frohm, Yongchao Su, Sara Linse, and Robert G. Griffin. High Resolution Structural Characterization of A β 42 Amyloid Fibrils by Magic Angle Spinning NMR. *Journal of the American Chemical Society*, 137(23):7509–7518, 2015.
- [46] Marielle Aulikki Wälti, Francesco Ravotti, Hiromi Arai, Charles G. Glabe, Joseph S. Wall, Anja Böckmann, Peter Güntert, Beat H. Meier, and Roland Riek. Atomic-resolution structure of a disease-relevant A β (1–42) amyloid fibril. *Proceedings of the National Academy of Sciences of the United States of America*, 113(34):E4976–E4984, 2016.
- [47] Binsen Li, Peng Ge, Kevin A. Murray, Phorum Sheth, Meng Zhang, Gayatri Nair, Michael R. Sawaya, Woo Shik Shin, David R. Boyer, Shulin Ye, David S. Eisenberg, Z. Hong Zhou, and Lin Jiang. Cryo-EM of full-length α -synuclein reveals fibril polymorphs with a common structural kernel. *Nature Communications*, 9(1):1–10, 2018.
- [48] Anthony W. Fitzpatrick, Tuomas P.J. Knowles, Christopher A. Waudby, Michele Vendruscolo, and Christopher M. Dobson. Inversion of the Balance between Hydrophobic and Hydrogen Bonding Interactions in Protein Folding and Aggregation. *PLoS Computational Biology*, 7(10), 2011.
- [49] K. Tsemekhman, L. Goldschmidt, D. Eisenberg, and D. Baker. Cooperative hydrogen bonding in amyloid formation. *Protein Science*, 16(4):761–764, 2007.
- [50] A. K. Buell, C. Galvagnion, R. Gaspar, E. Sparr, M. Vendruscolo, T. P. J. Knowles, S. Linse, and C. M. Dobson. Solution conditions determine the relative importance of nucleation and growth processes in α -synuclein aggregation. *Proceedings of the National Academy of Sciences*, 111(21):7671–7676, 2014.
- [51] Georg Meisl, Xiaoting Yang, Christopher M. Dobson, Sara Linse, and Tuomas P.J. Knowles. Modulation of electrostatic interactions to reveal a reaction network unifying the aggregation behaviour of the A β 42 peptide and its variants. *Chemical Science*, 8(6):4352–4362, 2017.
- [52] Wolfgang Hoyer, Dmitry Cherny, Vinod Subramaniam, and Thomas M Jovin. Impact of the Acidic C-Terminal Region Comprising Amino Acids 109–140 on α -Synuclein Aggregation in Vitro. *Biochemistry*, 43(51):16233–16242, 2004.

- [53] Ricardo Gaspar, Mikael Lund, Emma Sparr, and Sara Linse. Anomalous Salt Dependence Reveals an Interplay of Attractive and Repulsive Electrostatic Interactions in α -synuclein Fibril Formation. *QRB Discovery*, 1(e2):1–11, 2020.
- [54] Sarah L. Shammas, Tuomas P.J. Knowles, Andrew J. Baldwin, Cait E. MacPhee, Mark E. Welland, Christopher M. Dobson, and Glyn L. Delvin. Perturbation of the Stability of Amyloid Fibrils through Alteration of Electrostatic Interactions. *Biophysical Journal*, 100(11):2783–2791, 2011.
- [55] Bakthisaran Raman, Eri Chatani, Miho Kihara, Tadato Ban, Miyo Sakai, Kazuhiro Hasegawa, Hironobu Naiki, Ch Mohan Rao, and Yuji Goto. Critical balance of electrostatic and hydrophobic interactions is required for β 2-microglobulin amyloid fibril growth and stability. *Biochemistry*, 44(4):1288–1299, 2005.
- [56] Ingrid M. Van Der Wateren, Tuomas P.J. Knowles, Alexander K. Buell, Christopher M. Dobson, and Céline Galvagnion. C-terminal truncation of α -synuclein promotes amyloid fibril amplification at physiological pH. *Chemical Science*, 9(25):5506–5516, 2018.
- [57] Michael R. Sawaya. Amyloid Atlas 2024: <https://people.mbi.ucla.edu/sawaya/amyloidatlas/>, 2024.
- [58] Aneta T. Petkova, Richard D. Leapman, Zhihong Guo, Wai-Ming Yau, Mark P. Mattson, and Robert Tycko. Self-Propagating , Molecular-Level Polymorphism in Alzheimer ' s β -Amyloid Fibrils. *Science*, 307(5707):262–266, 2005.
- [59] Matthew G. Iadanza, Matthew P. Jackson, Eric W. Hewitt, Neil A. Ranson, and Sheena E. Radford. A new era for understanding amyloid structures and disease. *Nature Reviews Molecular Cell Biology*, 19(12):755–773, 2018.
- [60] Anthony W.P. Fitzpatrick, Benjamin Falcon, Shaoda He, Alexey G. Murzin, Garib Murshudov, Holly J. Garringer, R. Anthony Crowther, Bernardino Ghetti, Michel Goedert, and Sjors H.W. Scheres. Cryo-EM structures of tau filaments from Alzheimer's disease. *Nature*, 547(7662):185–190, 2017.
- [61] René Verel, Ivan T. Tomka, Carlo Bertozzi, Riccardo Cadalbert, Richard A. Kammerer, Michel O. Steinmetz, and Beat H. Meier. Polymorphism in an amyloid-like fibril-forming model peptide. *Angewandte Chemie - International Edition*, 47(31):5842–5845, 2008.
- [62] Martin Wilkinson, Yong Xu, Dev Thacker, Alexander I.P. Taylor, Declan G. Fisher, Rodrigo U. Gallardo, Sheena E. Radford, and Neil A. Ranson. Structural evolution of fibril polymorphs during amyloid assembly. *Cell*, 186(26):5798–5811, 2023.

- [63] Samuel I.A. Cohen, Michele Vendruscolo, Mark E. Welland, Christopher M. Dobson, Eugene M. Terentjev, and Tuomas P.J. Knowles. Nucleated polymerization with secondary pathways. I. Time evolution of the principal moments. *Journal of Chemical Physics*, 135(6), 2011.
- [64] Samuel I.A. Cohen, Michele Vendruscolo, Christopher M. Dobson, and Tuomas P.J. Knowles. From macroscopic measurements to microscopic mechanisms of protein aggregation. *Journal of Molecular Biology*, 421(2-3):160–171, 2012.
- [65] Paolo Arosio, Tuomas P.J. Knowles, and Sara Linse. On the lag phase in amyloid fibril formation. *Physical Chemistry Chemical Physics*, 17(12):7606–7618, 2015.
- [66] Georg Meisl, Julius B. Kirkegaard, Paolo Arosio, Thomas C.T. Michaels, Michele Vendruscolo, Christopher M. Dobson, Sara Linse, and Tuomas P.J. Knowles. Molecular mechanisms of protein aggregation from global fitting of kinetic models. *Nature Protocols*, 11(2):252–272, 2016.
- [67] Tuomas P.J. Knowles, Christopher A. Waudby, Glyn L. Devlin, Samuel I.A. Cohen, Adriano Aguzzi, Michele Vendruscolo, Eugene M. Terentjev, Mark E. Welland, and Christopher M. Dobson. An analytical solution to the kinetics of breakable filament assembly. *Science*, 326(5959):1533–1537, 2009.
- [68] Thomas C.T. Michaels, Daoyuan Qian, Andela Šarić, Michele Vendruscolo, Sara Linse, and Tuomas P.J. Knowles. Amyloid formation as a protein phase transition. *Nature Reviews Physics*, 5(7):379–397, 2023.
- [69] Paolo Arosio, Risto Cukalevski, Birgitta Frohm, Tuomas P.J. Knowles, and Sara Linse. Quantification of the concentration of A β ₄₂ propagons during the lag phase by an amyloid chain reaction assay. *Journal of the American Chemical Society*, 136(1):219–225, 2014.
- [70] Georg Meisl, Xiaoting Yang, Birgitta Frohm, Tuomas P.J. Knowles, and Sara Linse. Quantitative analysis of intrinsic and extrinsic factors in the aggregation mechanism of Alzheimer-associated A β -peptide. *Scientific Reports*, 6:18728:1–12, 2016.
- [71] Thomas C.T. Michaels, Andela Šarić, Johnny Habchi, Sean Chia, Georg Meisl, Michele Vendruscolo, Christopher M. Dobson, and Tuomas P.J. Knowles. Chemical Kinetics for Bridging Molecular Mechanisms and Macroscopic Measurements of Amyloid Fibril Formation. *Annual Review of Physical Chemistry*, 69:273–298, 2018.
- [72] Veronica Lattanzi, Katja Bernfur, Emma Sparr, Ulf Olsson, and Sara Linse. Solubility of A β ₄₀ peptide. *Journal of Colloid and Interface Science Open*, 4:0–5, 2021.
- [73] Silvia Campioni, Guillaume Carret, Sophia Jordens, Lucrece Nicoud,

- Raffaele Mezzenga, and Roland Riek. The presence of an air-water interface affects formation and elongation of α -synuclein fibrils. *Journal of the American Chemical Society*, 136(7):2866–2875, 2014.
- [74] Sean Chia, Patrick Flagmeier, Johnny Habchi, Veronica Lattanzi, Sara Linse, Christopher M. Dobson, Tuomas P.J. Knowles, and Michele Vendruscolo. Monomeric and fibrillar α -synuclein exert opposite effects on the catalytic cycle that promotes the proliferation of A β ₄₂ aggregates. *Proceedings of the National Academy of Sciences of the United States of America*, 114(30):8005–8010, 2017.
- [75] Robert Vácha, Sara Linse, and Mikael Lund. Surface effects on aggregation kinetics of amyloidogenic peptides. *Journal of the American Chemical Society*, 136(33):11776–11782, 2014.
- [76] Mattias Törnquist, Thomas C.T. Michaels, Kalyani Sanagavarapu, Xiaoting Yang, Georg Meisl, Samuel I.A. Cohen, Tuomas P.J. Knowles, and Sara Linse. Secondary nucleation in amyloid formation. *Chemical Communications*, 54(63):8667–8684, 2018.
- [77] V. I. Kalikmanov. *Nucleation Theory*. Springer, Heidelberg, 1 edition, 2013.
- [78] Marie Grey, Christopher J. Dunning, Ricardo Gaspar, Carl Grey, Patrik Brundin, Emma Sparr, and Sara Linse. Acceleration of α -synuclein aggregation by exosomes. *Journal of Biological Chemistry*, 290(5):2969–2982, 2015.
- [79] Wojciech P. Lipiński, Brent S. Visser, Irina Robu, Mohammad A.A. Fakhree, Saskia Lindhoud, Mireille M.A.E. Claessens, and Evan Spruijt. Biomolecular condensates can both accelerate and suppress aggregation of α -synuclein. *Science Advances*, 8(48), 2022.
- [80] Jeremy Pronchik, Xianglan He, Jason T. Giurleo, and David S. Talaga. In vitro formation of amyloid from α -synuclein is dominated by reactions at hydrophobic interfaces. *Journal of the American Chemical Society*, 132(28):9797–9803, 2010.
- [81] Céline Galvagnion, Alexander K. Buell, Georg Meisl, Thomas C.T. Michaels, Michele Vendruscolo, Tuomas P.J. Knowles, and Christopher M. Dobson. Lipid vesicles trigger α -synuclein aggregation by stimulating primary nucleation. *Nature Chemical Biology*, 11(3):229–234, 2015.
- [82] Michael Rabe, Alice Soragni, Nicholas P. Reynolds, Dorinel Verdes, Ennio Liverani, Roland Riek, and Stefan Seeger. On-surface aggregation of α -synuclein at nanomolar concentrations results in two distinct growth mechanisms. *ACS Chemical Neuroscience*, 4(3):408–417, 2013.
- [83] Samuel I.A. Cohen, Sara Linse, Leila M. Luheshi, Erik Hellstrand, Duncan A. White, Luke Rajah, Daniel E. Otzen, Michele Vendruscolo,

- Christopher M. Dobson, and Tuomas P.J. Knowles. Proliferation of amyloid- β_{42} aggregates occurs through a secondary nucleation mechanism. *Proceedings of the National Academy of Sciences of the United States of America*, 110(24):9758–9763, 2013.
- [84] Manuela R. Zimmermann, Subhas C. Bera, Georg Meisl, Sourav Dasadhikari, Shamasree Ghosh, Sara Linse, Kanchan Garai, and Tuomas P.J. Knowles. Mechanism of Secondary Nucleation at the Single Fibril Level from Direct Observations of A β_{42} Aggregation. *Journal of the American Chemical Society*, 143(40):16621–16629, 2021.
- [85] Mattias Törnquist, Risto Cukalevski, Ulrich Weininger, Georg Meisl, Tuomas P.J. Knowles, Thom Leiding, Anders Malmendal, Mikael Akke, and Sara Linse. Ultrastructural evidence for self-replication of alzheimer-associated A β_{42} amyloid along the sides of fibrils. *Proceedings of the National Academy of Sciences of the United States of America*, 117(21):11265–11273, 2020.
- [86] Joseph T. Jarrett and Peter T. Lansbury. Amyloid Fibril Formation Requires a Chemically Discriminating Nucleation Event: Studies of an Amyloidogenic Sequence from the Bacterial Protein OsmB. *Biochemistry*, 31(49):12345–12352, 1992.
- [87] Samuel I.A. Cohen, Risto Cukalevski, Thomas C.T. Michaels, A. Šarić, Mattias Törnquist, Michele Vendruscolo, Christopher M. Dobson, Alexander K. Buell, Tuomas P.J. Knowles, and Sara Linse. Distinct thermodynamic signatures of oligomer generation in the aggregation of the amyloid- β peptide. *Nature Chemistry*, 10(5):523–531, 2018.
- [88] Rakesh Kumar, Luis Enrique Arroyo-García, Shaffi Manchanda, Laurène Adam, Giusy Pizzirusso, Henrik Biverstål, Per Nilsson, André Fisahn, Jan Johansson, and Axel Abelein. Molecular Mechanisms of Amyloid- β Self-Assembly Seeded by In Vivo-Derived Fibrils and Inhibitory Effects of the BRICHOS Chaperone. *ACS Chemical Neuroscience*, 14(8):1503–1511, 2023.
- [89] Rebecca Frankel, Mattias Törnquist, Georg Meisl, Oskar Hansson, Ulf Andreasson, Henrik Zetterberg, Kaj Blennow, Birgitta Frohm, Tommy Cedervall, Tuomas P.J. Knowles, Thom Leiding, and Sara Linse. Autocatalytic amplification of Alzheimer-associated A β_{42} peptide aggregation in human cerebrospinal fluid. *Communications Biology*, 2(1):1–11, 2019.
- [90] Denis Gebauer and Helmut Cölfen. Prenucleation clusters and non-classical nucleation. *Nano Today*, 6(6):564–584, 2011.
- [91] Rakez Kaye, Elizabeth Head, Jennifer L. Thompson, Theresa M. McIntire, Saskia C. Milton, Carl W. Cotman, and Charles G. Glabe. Com-

- mon structure of soluble amyloid oligomers implies common mechanism of pathogenesis. *Science*, 300(5618):486–489, 2003.
- [92] Christofer Lendel, Morten Bjerring, Anatoly Dubnovitsky, Robert T. Kelly, Andrei Filippov, Oleg N. Antzutkin, Niels Chr Nielsen, and Torleif Härd. A hexameric peptide barrel as building block of amyloid- β protofibrils. *Angewandte Chemie - International Edition*, 53(47):12756–12760, 2014.
- [93] Magnus Kjaergaard, Alexander J. Dear, Franziska Kundel, Seema Qamar, Georg Meisl, Tuomas P.J. Knowles, and David Klenerman. Oligomer Diversity during the Aggregation of the Repeat Region of Tau. *ACS Chemical Neuroscience*, 9(12):3060–3071, 2018.
- [94] Ji Eun Lee, Jason C. Sang, Margarida Rodrigues, Alexander R. Carr, Mathew H. Horrocks, Suman De, Marie N. Bongiovanni, Patrick Flagmeier, Christopher M. Dobson, David J. Wales, Steven F. Lee, and David Klenerman. Mapping Surface Hydrophobicity of α -Synuclein Oligomers at the Nanoscale. *Nano Letters*, 18(12):7494–7501, 2018.
- [95] Alexander J. Dear, Georg Meisl, Anđela Šarić, Thomas C.T. Michaels, Magnus Kjaergaard, Sara Linse, and Tuomas P.J. Knowles. Identification of on- And off-pathway oligomers in amyloid fibril formation. *Chemical Science*, 11(24):6236–6247, 2020.
- [96] Alexander J. Dear, Thomas C.T. Michaels, Georg Meisl, David Klenerman, Si Wu, Sarah Perrett, Sara Linse, Christopher M. Dobson, and Tuomas P.J. Knowles. Kinetic diversity of amyloid oligomers. *Proceedings of the National Academy of Sciences of the United States of America*, 117(22):28–31, 2020.
- [97] Serene W. Chen, Srdja Drakulic, Emma Deas, Myriam Ouberaï, Francesco A. Aprile, Rocío Arranz, Samuel Ness, Cintia Roodveldt, Tim Guilliams, Erwin J. De-Genst, David Klenerman, Nicholas W. Wood, Tuomas P.J. Knowles, Carlos Alfonso, Germán Rivas, Andrey Y. Abramov, José María Valpuesta, Christopher M. Dobson, and Nunilo Cremades. Structural characterization of toxic oligomers that are kinetically trapped during α -synuclein fibril formation. *Proceedings of the National Academy of Sciences of the United States of America*, 112(16):E1994–E2003, 2015.
- [98] Thomas C.T. Michaels, Anđela Šarić, Samo Curk, Katja Bernfur, Paolo Arosio, Georg Meisl, Alexander J. Dear, Samuel I.A. Cohen, Christopher M. Dobson, Michele Vendruscolo, Sara Linse, and Tuomas P.J. Knowles. Dynamics of oligomer populations formed during the aggregation of Alzheimer’s A β 42 peptide. *Nature Chemistry*, 12(5):445–451, 2020.
- [99] Diana C. Rodriguez Camargo, Sean Chia, Joseph Menzies, Benedetta

- Mannini, Georg Meisl, Martin Lundqvist, Christin Pohl, Katja Bernfur, Veronica Lattanzi, Johnny Habchi, Samuel I.A. Cohen, Tuomas P.J. Knowles, Michele Vendruscolo, and Sara Linse. Surface-Catalyzed Secondary Nucleation Dominates the Generation of Toxic IAPP Aggregates. *Frontiers in Molecular Biosciences*, 8:757425:1–11, 2021.
- [100] Dominic M. Walsh, Igor Klyubin, Julia V. Fadeeva, William K. Cullen, Roger Anwyl, Michael S. Wolfe, Michael J. Rowan, and Dennis J. Selkoe. Naturally secreted oligomers of amyloid β protein potently inhibit hippocampal long-term potentiation in vivo. *Nature*, 416(6880):535–539, 2002.
- [101] Giuliana Fusco, Serene W. Chen, Philip T.F. Williamson, Roberta Cascella, Michele Perni, James A. Jarvis, Cristina Cecchi, Michele Vendruscolo, Fabrizio Chiti, Nunilo Cremades, Liming Ying, Christopher M. Dobson, and Alfonso De Simone. Structural basis of membrane disruption and cellular toxicity by α -synuclein oligomers. *Science*, 358(6369):1440–1443, 2017.
- [102] Nunilo Cremades, Samuel I.A. Cohen, Emma Deas, Andrey Y. Abramov, Allen Y. Chen, Angel Orte, Massimo Sandal, Richard W. Clarke, Paul Dunne, Francesco A. Aprile, Carlos W. Bertocini, Nicholas W. Wood, Tuomas P.J. Knowles, Christopher M. Dobson, and David Klenerman. Direct observation of the interconversion of normal and toxic forms of α -synuclein. *Cell*, 149(5):1048–1059, 2012.
- [103] Shin Jung C. Lee, Eunju Nam, Hyuck Jin Lee, Masha G. Savelieff, and Mi Hee Lim. Towards an understanding of amyloid- β oligomers: Characterization, toxicity mechanisms, and inhibitors. *Chemical Society Reviews*, 46(2):310–323, 2017.
- [104] Karin M. Danzer, Dorothea Haasen, Anne R. Karow, Simon Moussaïd, Matthias Habeck, Armin Giese, Hans Kretzschmar, Bastian Hengerer, and Marcus Kostka. Different species of α -synuclein oligomers induce calcium influx and seeding. *Journal of Neuroscience*, 27(34):9220–9232, 2007.
- [105] Patrick Flagmeier, Suman De, David C. Wirthensohn, Steven F. Lee, Cécile Vincke, Serge Muyldermans, Tuomas P.J. Knowles, Sonia Gandhi, Christopher M. Dobson, and David Klenerman. Ultrasensitive Measurement of Ca^{2+} Influx into Lipid Vesicles Induced by Protein Aggregates. *Angewandte Chemie - International Edition*, 56(27):7750–7754, 2017.
- [106] David A. Fancy and Thomas Kodadek. Chemistry for the analysis of protein-protein interactions: Rapid and efficient cross-linking triggered by long wavelength light. *Proceedings of the National Academy of Sciences of the United States of America*, 96(11):6020–6024, 1999.

- [107] Gal Bitan. Structural Study of Metastable Amyloidogenic Protein Oligomers by Photo-Induced Cross-Linking of Unmodified Proteins. *Methods in Enzymology*, 413(1995):217–236, 2006.
- [108] D. Fennell Evans and Håkan Wennerström. *The Colloidal Domain: Where Physics, Chemistry, Biology, and Technology Meet*. Wiley-VCH, New York, 2 edition, 1999.
- [109] Yi Shen, Anqi Chen, Wenyun Wang, Yinan Shen, Francesco Simone Ruggeri, Stefano Aime, Zizhao Wang, Seema Qamar, Jorge R Espinosa, Adiran Garaizar, Peter St George-Hyslop, Rosana Colleparado-Guevara, David A Weitz, Daniele Vigolo, and Thomas P J Knowles. The liquid-to-solid transition of FUS is promoted by the condensate surface. *Proceedings of the National Academy of Sciences*, 120(33):8, 2023.
- [110] P.A. Albertsson. Partition of cell particles and macromolecules in polymer two-phase systems. *Archives of Biochemistry and Biophysics*, 24:309–341, 1970.
- [111] Mika Kobayashi and Hajime Tanaka. The reversibility and first-order nature of liquid-liquid transition in a molecular liquid. *Nature Communications*, 7:4–6, 2016.
- [112] Stephanie C. Weber and Clifford P. Brangwynne. Getting RNA and protein in phase. *Cell*, 149(6):1188–1191, 2012.
- [113] Anthony A Hyman and Kai Simons. Beyond Oil and Water - Phase Transitions in Cells. *Science*, 337:1047–1049, 1998.
- [114] Yongdae Shin and Clifford P. Brangwynne. Liquid phase condensation in cell physiology and disease. *Science*, 357(6357), 2017.
- [115] Salman F. Banani, Hyun O. Lee, Anthony A. Hyman, and Michael K. Rosen. Biomolecular condensates: Organizers of cellular biochemistry. *Nature Reviews Molecular Cell Biology*, 18(5):285–298, 2017.
- [116] Soumik Ray, Nitu Singh, Rakesh Kumar, Komal Patel, Satyaprakash Pandey, Debalina Datta, Jaladhar Mahato, Rajlaxmi Panigrahi, Ambuja Navalkar, Surabhi Mehra, Laxmikant Gadhe, Debdeep Chatterjee, Ajay Singh Sawner, Siddhartha Maiti, Sandhya Bhatia, Juan Atilio Gerez, Arindam Chowdhury, Ashutosh Kumar, Ranjith Padinhateeri, Roland Riek, G. Krishnamoorthy, and Samir K. Maji. α -Synuclein aggregation nucleates through liquid-liquid phase separation. *Nature Chemistry*, 12(8):705–716, 2020.
- [117] Cécile Mathieu, Rohit V. Pappu, and J. Paul Taylor. Beyond aggregation: Pathological phase transitions in neurodegenerative disease. *Science*, 370(6512):56–60, 2020.
- [118] Jitao Wen, Liu Hong, Georg Krainer, Qiong Qiong Yao, Tuomas P.J. Knowles, Si Wu, and Sarah Perrett. Conformational Expansion of Tau in

- Condensates Promotes Irreversible Aggregation. *Journal of the American Chemical Society*, 143(33):13056–13064, 2021.
- [119] Semanti Mukherjee, Arunima Sakunthala, Laxmikant Gadhe, Manisha Poudyal, Ajay Singh Sawner, Pradeep Kadu, and Samir K. Maji. Liquid-liquid Phase Separation of α -Synuclein: A New Mechanistic Insight for α -Synuclein Aggregation Associated with Parkinson's Disease Pathogenesis. *Journal of Molecular Biology*, 435(1):167713, 2023.
- [120] Samuel T Dada, Maarten C. Hardenber, Zenon Toprakcioglu, Lena K. Mrugalla, Mariana P. Cali, Mollie O. McKeon, Ewa Klimont, Thomas C.T. Michaels, Tuomas P.J. Knowles, and Michele Vendruscolo. Spontaneous nucleation and fast aggregate-dependent proliferation of α -synuclein aggregates within liquid condensates at neutral pH. *Proceedings of the National Academy of Sciences*, 120(9):9, 2023.
- [121] Tinna Pálmadóttir, Christopher A. Waudby, Katja Bernfur, John Christodoulou, Sara Linse, and Anders Malmendal. Morphology-Dependent Interactions between α -Synuclein Monomers and Fibrils. *International Journal of Molecular Sciences*, 24(6), 2023.
- [122] Xue Yang, Baifan Wang, Cody L. Hoop, Jonathan K. Williams, and Jean Baum. NMR unveils an N-terminal interaction interface on acetylated- α -synuclein monomers for recruitment to fibrils. *Proceedings of the National Academy of Sciences of the United States of America*, 118(18), 2021.
- [123] Pratibha Kumari, Dhiman Ghosh, Agathe Vanas, Yanick Fleischmann, and Thomas Wiegand. Structural insights into α -synuclein monomer – fibril interactions. *Proceedings of the National Academy of Sciences*, 118(10):1–8, 2021.
- [124] Christina R. Bodner, Christopher M. Dobson, and Ad Bax. Multiple Tight Phospholipid-Binding Modes of α -Synuclein Revealed by Solution NMR Spectroscopy. *Journal of Molecular Biology*, 390(4):775–790, 2009.
- [125] Christina R. Bodner, Alexander S. Maltsev, Christopher M. Dobson, and Ad Bax. Differential phospholipid binding of α -synuclein variants implicated in Parkinson's disease revealed by solution NMR spectroscopy. *Biochemistry*, 49(5):862–871, 2010.
- [126] Giuliana Fusco, Alfonso De Simone, Tata Gopinath, Vitaly Vostrikov, Michele Vendruscolo, Christopher M. Dobson, and Gianluigi Veglia. Direct observation of the three regions in α -synuclein that determine its membrane-bound behaviour. *Nature Communications*, 5:3827:1–8, 2014.
- [127] Sukyeong Lee and Francis T.F. Tsai. Molecular chaperones in protein quality control. *Journal of Biochemistry and Molecular Biology*, 38(3):259–265, 2005.

- [128] Bernd Bukau, Jonathan Weissman, and Arthur Horwich. Molecular Chaperones and Protein Quality Control. *Cell*, 125(3):443–451, 2006.
- [129] Leonardo Cortez and Valerie Sim. The therapeutic potential of chemical chaperones in protein folding diseases. *Prion*, 8(2):197–202, 2014.
- [130] Tessa Sinnige, Anan Yu, and Richard I. Morimoto. Challenging Proteostasis: Role of the Chaperone Network to Control Aggregation-Prone Proteins in Human Disease. *Advances in Experimental Medicine and Biology*, 1243:53–68, 2020.
- [131] Kriti Chaplot, Timothy S. Jarvela, and Iris Lindberg. Secreted Chaperones in Neurodegeneration. *Frontiers in Aging Neuroscience*, 12:268, 2020.
- [132] Francesco A. Aprile, Emma Källstig, Galina Limorenko, Michele Vendruscolo, David Ron, and Christian Hansen. The molecular chaperones DNAJB6 and Hsp70 cooperate to suppress α -synuclein aggregation. *Scientific Reports*, 7(1):1–11, 2017.
- [133] Ricarda Törner, Tatsiana Kupreichyk, Lothar Gremer, Elisa Colas Dbled, Daphna Fenel, Sarah Schemmert, Pierre Gans, Dieter Willbold, Guy Schoehn, Wolfgang Hoyer, and Jerome Boisbouvier. Structural basis for the inhibition of IAPP fibril formation by the co-chaperonin prefoldin. *Nature Communications*, 13(1):1–13, 2022.
- [134] Istvan Horvath, Stéphanie Blockhuys, Darius Šulskis, Stellan Holgersson, Ranjeet Kumar, Björn M. Burmann, and Pernilla Wittung-Stafshede. Interaction between Copper Chaperone Atox1 and Parkinson’s Disease Protein α -Synuclein Includes Metal-Binding Sites and Occurs in Living Cells. *ACS Chemical Neuroscience*, 10(11):4659–4668, 2019.
- [135] Jurre Hageman, Maria A. Rujano, Maria A.W.H. van Waarde, Vaishali Kakkar, Ron P. Dirks, Natalia Govorukhina, Henderika M.J. Oosterveld-Hut, Nicolette H. Lubsen, and Harm H. Kampinga. A DNAJB Chaperone Subfamily with HDAC-Dependent Activities Suppresses Toxic Protein Aggregation. *Molecular Cell*, 37(3):355–369, 2010.
- [136] Laurène Adam, Rakesh Kumar, Luis Enrique Arroyo-Garcia, Willem Hendrik Molenkamp, Jan Stanislaw Nowak, Hannah Klute, Azad Farzadfard, Rami Alkenayeh, Janni Nielsen, Henrik Biverstål, Daniel E. Otzen, Jan Johansson, and Axel Abelein. Specific inhibition of α -synuclein oligomer generation and toxicity by the chaperone domain Briz BRICHOS. *Protein Science*, 33(8):1–17, 2024.
- [137] Ricardo Gaspar, Tommy Garting, and Anna Stradner. Eye lens crystallin proteins inhibit the autocatalytic amyloid amplification nature of mature α -synuclein fibrils. *PLoS ONE*, 15(6):1–14, 2020.
- [138] Nicklas Österlund, Martin Lundqvist, Leopold L. Ilag, Astrid Gräslund, and Cecilia Emanuelsson. Amyloid- β oligomers are captured by the

- DNAJB6 chaperone: Direct detection of interactions that can prevent primary nucleation. *Journal of Biological Chemistry*, 295(24):8135–8144, 2020.
- [139] Nicklas Österlund, Rebecca Frankel, Andreas Carlsson, Dev Thacker, Maja Karlsson, Vanessa Matus, Astrid Gräslund, Cecilia Emanuelsson, and Sara Linse. The C-terminal domain of the anti-amyloid chaperone DNAJB6 binds to amyloid- β peptide fibrils and inhibits secondary nucleation. *Journal of Biological Chemistry*, 299(11):105317, 2023.
- [140] Judith Gillis, Sabine Schipper-Krom, Katrin Juenemann, Anna Gruber, Silvia Coolen, Rian Van Den Nieuwendijk, Henk Van Veen, Hermen Overkleeft, Joachim Goedhart, Harm H. Kampinga, and Eric A. Reits. The DNAJB6 and DNAJB8 protein chaperones prevent intracellular aggregation of polyglutamine peptides. *Journal of Biological Chemistry*, 288(24):17225–17237, 2013.
- [141] Erik Chorell, Emma Andersson, Margery L. Evans, Neha Jain, Anna Götheson, Jörgen Aden, Matthew R. Chapman, Fredrik Almqvist, and Pernilla Wittung-Stafshede. Bacterial chaperones CsgE and CsgC differentially modulate human α -Synuclein amyloid formation via transient contacts. *PLoS ONE*, 10(10):1–11, 2015.
- [142] Cecilia Månsson, Paolo Arosio, Rasha Hussein, Harm H. Kampinga, Reem M. Hashem, Wilbert C. Boelens, Christopher M. Dobson, Thomas P.J. Knowles, Sara Linse, and Cecilia Emanuelsson. Interaction of the molecular chaperone DNAJB6 with growing amyloid-beta 42 ($A\beta_{42}$) aggregates leads to sub-stoichiometric inhibition of amyloid formation. *Journal of Biological Chemistry*, 289(45):31066–31076, 2014.
- [143] Cecilia Månsson, Vaishali Kakkar, Elodie Monsellier, Yannick Sourigues, Johan Härmärk, Harm H. Kampinga, Ronald Melki, and Cecilia Emanuelsson. DNAJB6 is a peptide-binding chaperone which can suppress amyloid fibrillation of polyglutamine peptides at substoichiometric molar ratios. *Cell Stress and Chaperones*, 19(2):227–239, 2014.
- [144] Cecilia Månsson, Remco T.P. Van Cruchten, Ulrich Weininger, Xiaoting Yang, Risto Cukalevski, Paolo Arosio, Christopher M. Dobson, Thomas Knowles, Mikael Akke, Sara Linse, and Cecilia Emanuelsson. Conserved S/T Residues of the Human Chaperone DNAJB6 Are Required for Effective Inhibition of $A\beta_{42}$ Amyloid Fibril Formation. *Biochemistry*, 57(32):4891–4892, 2018.
- [145] Paolo Arosio, Thomas C.T. Michaels, Sara Linse, Cecilia Månsson, Cecilia Emanuelsson, Jenny Presto, Jan Johansson, Michele Vendruscolo, Christopher M. Dobson, and Thomas P.J. Knowles. Kinetic analysis reveals the diversity of microscopic mechanisms through which molecular

- chaperones suppress amyloid formation. *Nature Communications*, 7:1–9, 2016.
- [146] Krzysztof Liberek, Agnieszka Lewandowska, and Szymon Zietkiewicz. Chaperones in control of protein disaggregation. *EMBO Journal*, 27(2):328–335, 2008.
- [147] Xuechao Gao, Marta Carroni, Carmen Nussbaum-Krammer, Axel Mogk, Nadinath B. Nillegoda, Anna Szlachcic, D. Lys Guilbride, Helen R. Saibil, Matthias P. Mayer, and Bernd Bukau. Human Hsp70 Disaggregase Reverses Parkinson’s-Linked α -Synuclein Amyloid Fibrils. *Molecular Cell*, 59(5):781–793, 2015.
- [148] Nadinath B. Nillegoda, Janine Kirstein, Anna Szlachcic, Mykhaylo Berynskyy, Antonia Stank, Florian Stengel, Kristin Arnsburg, Xuechao Gao, Annika Scior, Ruedi Aebersold, D. Lys Guilbride, Rebecca C. Wade, Richard I. Morimoto, Matthias P. Mayer, and Bernd Bukau. Crucial HSP70 co-chaperone complex unlocks metazoan protein disaggregation. *Nature*, 524(7564):247–251, 2015.
- [149] Sara Linse, Kyrre Thalberg, and Tuomas P.J. Knowles. The unhappy chaperone. *QRB Discovery*, 2, 2021.
- [150] X. B. Qiu, Y. M. Shao, S. Miao, and L. Wang. The diversity of the DnaJ/Hsp40 family, the crucial partners for Hsp70 chaperones. *Cellular and Molecular Life Sciences*, 63(22):2560–2570, 2006.
- [151] P. F. Durrenberger, M. D. Filiou, L. B. Moran, G. J. Michael, S. Novoselov, M. E. Cheetham, P. Clark, R. K.B. Pearce, and Manuel B. Graeber. DnaJB6 is present in the core of Lewy bodies and is highly up-regulated in Parkinsonian astrocytes. *Journal of Neuroscience Research*, 87(1):238–245, 2009.
- [152] Jónvá Hentze, Jonas Folke, Susana Aznar, Pia Nyeng, Tomasz Brudek, and Christian Hansen. DNAJB6 is expressed in neurons and oligodendrocytes of the human brain. *Glia*, 72(12):1–14, 2024.
- [153] Christina Zarouchlioti, David A. Parfitt, Wenwen Li, Lauren M. Gittings, and Michael E. Cheetham. DNAJ Proteins in neurodegeneration: Essential and protective factors. *Philosophical Transactions of the Royal Society B: Biological Sciences*, 373(1738), 2018.
- [154] Sara Linse. High-Efficiency Expression and Purification of DNAJB6b Based on the pH-Modulation of Solubility and Denaturant-Modulation of Size. *Molecules*, 27(2), 2022.
- [155] Nicklas Österlund, Rebecca Frankel, Andreas Carlsson, Dev Thacker, Maja Karlsson, Vanessa Matus, Astrid Gräslund, Cecilia Emanuelsson, and Sara Linse. The C-terminal domain of the anti-amyloid chaperone

- DNAJB6 binds to amyloid- β peptide fibrils and inhibits secondary nucleation. *Journal of Biological Chemistry*, 299(11):105317, 2023.
- [156] Andreas Carlsson, Ulf Olsson, and Sara Linse. On the micelle formation of DNAJB6b. *QRB Discovery*, 4:1–7, 2023.
- [157] Theodoros K. Karamanos, Vitali Tugarinov, and G. Marius Clore. Unraveling the structure and dynamics of the human DNAJB6b chaperone by NMR reveals insights into Hsp40-mediated proteostasis. *Proceedings of the National Academy of Sciences of the United States of America*, 116(43):21529–21538, 2019.
- [158] Christopher A.G. Söderberg, Cecilia Månsson, Katja Bernfur, Gudrun Rutsdottir, Johan Härmark, Sreekanth Rajan, Salam Al-Karadaghi, Morten Rasmussen, Peter Höjrup, Hans Hebert, and Cecilia Emanuelsson. Structural modelling of the DNAJB6 oligomeric chaperone shows a peptide-binding cleft lined with conserved S/T-residues at the dimer interface. *Scientific Reports*, 8(1):1–15, 2018.
- [159] Vaishali Kakkar, Cecilia Månsson, Eduardo P. de Mattos, Steven Bergink, Marianne van der Zwaag, Maria A.W.H. van Waarde, Niels J. Kloosterman, Ronald Melki, Remco T.P. van Cruchten, Salam Al-Karadaghi, Paolo Arosio, Christopher M. Dobson, Tuomas P.J. Knowles, Gillian P. Bates, Jan M. van Deursen, Sara Linse, Bart van de Sluis, Cecilia Emanuelsson, and Harm H. Kampinga. The S/T-Rich Motif in the DNAJB6 Chaperone Delays Polyglutamine Aggregation and the Onset of Disease in a Mouse Model. *Molecular Cell*, 62(2):272–283, 2016.
- [160] Natasja Deshayes, Sertan Arkan, and Christian Hansen. The molecular chaperone DNAJB6, but Not DNAJB1, suppresses the seeded aggregation of alpha-synuclein in cells. *International Journal of Molecular Sciences*, 20(18):1–13, 2019.
- [161] Sertan Arkan, Mårten Ljungberg, Deniz Kirik, and Christian Hansen. DNAJB6 suppresses alpha-synuclein induced pathology in an animal model of Parkinson's disease. *Neurobiology of Disease*, 158:105477:105477, 2021.
- [162] Jacqueline Burré. The synaptic function of α -synuclein. *Journal of Parkinson's Disease*, 5(4):699–713, 2015.
- [163] Jacqueline Burré, Manu Sharma, Theodoros Tsetsenis, Vladimir Buchman, Mark R. Etherton, and Thomas C. Südhof. α -Synuclein promotes SNARE-complex assembly in vivo and in vitro. *Science*, 329(5999):1663–1667, 2010.
- [164] Katarzyna Makasewicz, Sara Linse, and Emma Sparr. Interplay of α -synuclein with Lipid Membranes: Cooperative Adsorption, Membrane Remodeling and Coaggregation. *JACS Au*, 4(4):1250–1262, 2024.

- [165] Céline Galvagnion, Daniel Topgaard, Katarzyna Makasewicz, Alexander K. Buell, Sara Linse, Emma Sparr, and Christopher M. Dobson. Lipid Dynamics and Phase Transition within α -Synuclein Amyloid Fibrils. *Journal of Physical Chemistry Letters*, 10(24):7872–7877, 2019.
- [166] Janin Lautenschläger, Amberley D. Stephens, Giuliana Fusco, Florian Ströhl, Nathan Curry, Maria Zacharopoulou, Claire H. Michel, Romain Laine, Nadezhda Nespovitaya, Marcus Fantham, Dorothea Pinotsi, Wagner Zago, Paul Fraser, Anurag Tandon, Peter St George-Hyslop, Eric Rees, Jonathan J. Phillips, Alfonso De Simone, Clemens F. Kaminski, and Gabriele S. Kaminski Schierle. C-terminal calcium binding of α -synuclein modulates synaptic vesicle interaction. *Nature Communications*, 9(1), 2018.
- [167] Furong Cheng, Giorgio Vivacqua, and Shun Yu. The role of alpha-synuclein in neurotransmission and synaptic plasticity. *Journal of Chemical Neuroanatomy*, 42(4):242–248, 2011.
- [168] Iris N. Serratos, Elizabeth Hernández-Pérez, Carolina Campos, Michael Aschner, and Abel Santamaría. An Update on the Critical Role of α -Synuclein in Parkinson’s Disease and Other Synucleinopathies: from Tissue to Cellular and Molecular Levels. *Molecular Neurobiology*, 59(1):620–642, 2022.
- [169] Luis D. Bernal-Conde, Rodrigo Ramos-Acevedo, Mario A. Reyes-Hernández, Andrea J. Balbuena-Olvera, Ishbelt D. Morales-Moreno, Rubén Argüero-Sánchez, Birgitt Schüle, and Magdalena Guerra-Crespo. Alpha-Synuclein Physiology and Pathology: A Perspective on Cellular Structures and Organelles. *Frontiers in Neuroscience*, 13:1399:1–22, 2020.
- [170] Jacob T. Bendor, Todd P. Logan, and Robert H. Edwards. The function of α -synuclein. *Neuron*, 79(6):1044–1066, 2013.
- [171] Seung Jae Lee, Hyesung Jeon, and Konstantin V. Kandror. α -Synuclein is localized in a subpopulation of rat brain synaptic vesicles. *Acta Neurobiologiae Experimentalis*, 68(4):509–515, 2008.
- [172] David F. Clayton and Julia M. George. Synucleins in synaptic plasticity and neurodegenerative disorders. *Journal of Neuroscience Research*, 58(1):120–129, 1999.
- [173] Michel Goedert. Alpha-synuclein and neurodegenerative diseases. *Nature Reviews Neuroscience*, 2(7):492–501, 2001.
- [174] David F. Clayton and Julia M. George. The synucleins: A family of proteins involved in synaptic function, plasticity, neurodegeneration and disease. *Trends in Neurosciences*, 21(6):249–254, 1998.
- [175] L. Maroteaux, J. T. Campanelli, and R. H. Scheller. Synuclein: A neuron-

- specific protein localized to the nucleus and presynaptic nerve terminal. *Journal of Neuroscience*, 8(8):2804–2815, 1988.
- [176] Kenji Uéda, Hisashi Fukushima, Eliezer Masliah, Yu Xia, Akihiko Iwai, Makoto Yoshimoto, Deborah A.C. Otero, Jun Kondo, Yasuo Ihara, and Tsunao Saitoh. Molecular cloning of cDNA encoding an unrecognized component of amyloid in Alzheimer disease. *Proceedings of the National Academy of Sciences of the United States of America*, 90(23):11282–11286, 1993.
- [177] Sebastian McClendon, Carla C. Rospigliosi, and David Eliezer. Charge neutralization and collapse of the C-terminal tail of alpha-synuclein at low pH. *Protein Science*, 18(7):1531–1540, 2009.
- [178] Kim K.M. Sweers, Kees O. Van Der Werf, Martin L. Bennink, and Vinod Subramaniam. Atomic force microscopy under controlled conditions reveals structure of c-terminal region of α -synuclein in amyloid fibrils. *ACS Nano*, 6(7):5952–5960, 2012.
- [179] Carlos W. Bertonecini, Young Sang Jung, Claudio O. Fernandez, Wolfgang Hoyer, Christian Griesinger, Thomas M. Jovin, and Markus Zweckstetter. Release of long-range tertiary interactions potentiates aggregation of natively unstructured α -synuclein. *Proceedings of the National Academy of Sciences of the United States of America*, 102(5):1430–1435, 2005.
- [180] Tinna Pálmadóttir, Anders Malmendal, Thom Leiding, Mikael Lund, and Sara Linse. Charge Regulation during Amyloid Formation of α -Synuclein. *Journal of the American Chemical Society*, 143(20):7777–7791, 2021.
- [181] Katerina Levitan, David Chereau, Samuel I A Cohen, Tuomas P J Knowles, Christopher M Dobson, Anthony L Fink, John P Anderson, Jason M Goldstein, and Glenn L Millhauser. Conserved C-terminal Charge Exerts a Profound Influence on the Aggregation Rate of α -synuclein. *Journal of Molecular Biology*, 411(2):329–333, 2012.
- [182] Azad Farzadfard, Jannik Nedergaard Pedersen, Georg Meisl, Arun Kumar Somavarapu, Parvez Alam, Louise Goksøyr, Morten Agertoug Nielsen, Adam Frederik Sander, Tuomas P.J. Knowles, Jan Skov Pedersen, and Daniel Erik Otzen. The C-terminal tail of α -synuclein protects against aggregate replication but is critical for oligomerization. *Communications Biology*, 5(1), 2022.
- [183] Pau Bernadó, Carlos W. Bertonecini, Christian Griesinger, Markus Zweckstetter, and Martin Blackledge. Defining long-range order and local disorder in native α -synuclein using residual dipolar couplings. *Journal of the American Chemical Society*, 127(51):17968–17969, 2005.
- [184] Aditya Iyer, Steven J. Roeters, Vladimir Kogan, Sander Woutersen,

- Mireille M.A.E. Claessens, and Vinod Subramaniam. C-Terminal Truncated α -Synuclein Fibrils Contain Strongly Twisted β -Sheets. *Journal of the American Chemical Society*, 139(43):15392–15400, 2017.
- [185] W. Sean Davidson, Ana Jonas, David F. Clayton, and Julia M. George. Stabilization of α -Synuclein secondary structure upon binding to synthetic membranes. *Journal of Biological Chemistry*, 273(16):9443–9449, 1998.
- [186] Paul H. Weinreb, Weiguo Zhen, Anna W. Poon, Kelly A. Conway, and Peter T. Lansbury. NACP, a protein implicated in Alzheimer’s disease and learning, is natively unfolded. *Biochemistry*, 35(43):13709–13715, 1996.
- [187] Tobias S. Ulmer, Ad Bax, Nelson B. Cole, and Robert L. Nussbaum. Structure and Dynamics of Micelle-bound Human α -Synuclein. *The Journal of Biological Chemistry*, 280(10):9595–9603, 2005.
- [188] Sandra Rocha, Ranjeet Kumar, Bengt Nordén, and Pernilla Wittung-Stafshede. Orientation of α -Synuclein at Negatively Charged Lipid Vesicles: Linear Dichroism Reveals Time-Dependent Changes in Helix Binding Mode. *Journal of the American Chemical Society*, 143(45):18899–18906, 2021.
- [189] Céline Galvagnion, Abigail Barclay, Katarzyna Makasewicz, Frederik Ravnkilde Marlet, Martine Moulin, Juliette M. Devos, Sara Linse, Anne Martel, Lionel Porcar, Emma Sparr, Martin Cramer Pedersen, Felix Roosen-Runge, Lise Arleth, and Alexander K. Buell. Structural characterisation of α -synuclein-membrane interactions and the resulting aggregation using small angle scattering. *Physical Chemistry Chemical Physics*, 26(14):10998–11013, 2024.
- [190] Alexandra Andersson, Marco Fornasier, Katarzyna Makasewicz, Tinna Pálmadóttir, Sara Linse, Emma Sparr, and Peter Jönsson. Single-vesicle intensity and colocalization fluorescence microscopy to study lipid vesicle fusion, fission, and lipid exchange. *Frontiers in Molecular Neuroscience*, 15:1007699:1–13, 2022.
- [191] Katarzyna Makasewicz, Stefan Wennmalm, Sara Linse, and Emma Sparr. α -Synuclein-induced deformation of small unilamellar vesicles. *QRB Discovery*, 3:1–9, 2022.
- [192] Katarzyna Makasewicz, Stefan Wennmalm, Björn Stenqvist, Marco Fornasier, Alexandra Andersson, Peter Jönsson, Sara Linse, and Emma Sparr. Cooperativity of α -Synuclein Binding to Lipid Membranes. *ACS Chemical Neuroscience*, 12(12):2099–2109, 2021.
- [193] Robert I. Horne, Michael A. Metrick, Wing Man, Dillon J. Rinauro, Z. Faidon Brotzakis, Sean Chia, Georg Meisl, and Michele Vendruscolo. Secondary Processes Dominate the Quiescent, Spontaneous Aggregation

- of α -Synuclein at Physiological pH with Sodium Salts. *ACS Chemical Neuroscience*, 14(17):3125–3131, 2023.
- [194] He Jin Lee, Chan Choi, and Seung Jae Lee. Membrane-bound α -synuclein has a high aggregation propensity and the ability to seed the aggregation of the cytosolic form. *Journal of Biological Chemistry*, 277(1):671–678, 2002.
- [195] Ricardo Gaspar, Georg Meisl, Alexander K. Buell, Laurence Young, Clemens F. Kaminski, Tuomas P.J. Knowles, Emma Sparr, and Sara Linse. Acceleration of α -synuclein aggregation. *Amyloid*, 24(51):20–21, 2017.
- [196] Catherine K Xu, Georg Meisl, Ewa Andrzejewska, Georg Krainer, Alexander J Dear, Marta Castellana Cruz, Soma Turi, Raphael Jacquat, William E Arter, Michele Vendruscolo, Sara Linse, and Tuomas P J Knowles. α -Synuclein oligomers form by secondary nucleation. *Nature Communications*, 15(1):7083, 2024.
- [197] Mikael Akke and Sture Forsén. Protein stability and electrostatic interactions between solvent exposed charged side chains. *Proteins: Structure, Function, and Bioinformatics*, 8(1):23–29, 1990.
- [198] Brian W. Matthews. Structural and genetic analysis of protein stability. *Annual Review of Biochemistry*, 62:139–160, 1993.
- [199] C. Nick Pace, Gerald R. Grimsley, and J. Martin Scholtz. Protein Ionizable Groups: pK Values and Their Contribution to Protein Stability and Solubility. *Journal of Biological Chemistry*, 284(20):13285–13289, 2009.
- [200] Sandeep Kumar and Ruth Nussinov. Close-range electrostatic interactions in proteins. *ChemBioChem*, 3(7):604–617, 2002.
- [201] Juami Hermine Mariama Van Gils, Erik Van Dijk, Alessia Peduzzo, Alexander Hofmann, Nicola Vettore, Marie P. Schützmann, Georg Groth, Halima Mouhib, Daniel E. Otzen, Alexander K. Buell, and Sanne Abeln. The hydrophobic effect characterises the thermodynamic signature of amyloid fibril growth. *PLoS Computational Biology*, 16(5):1–25, 2020.
- [202] M F Perutz. Electrostatic Effects in Proteins. *Science*, 201:1187–1191, 1978.
- [203] Rebecca C. Wade, Razif R. Gabdouliline, Susanna K. Lüdemann, and Valère Lounnas. Electrostatic steering and ionic tethering in enzyme-ligand binding: Insights from simulations. *Proceedings of the National Academy of Sciences of the United States of America*, 95(11):5942–5949, 1998.
- [204] C. Nick Pace. Single surface stabilizer. *Nature Structural Biology*, 7(5):345–346, 2000.
- [205] S. Kumar and R. Nussinov. How do thermophilic proteins deal with heat? *Cellular and Molecular Life Sciences*, 58(9):1216–1233, 2001.

- [206] Weimin Li, Björn A. Persson, Maxim Morin, Manja A. Behrens, Mikael Lund, and Malin Zackrisson Oskolkova. Charge-induced patchy attractions between proteins. *Journal of Physical Chemistry B*, 119(2):503–508, 2015.
- [207] Weimin Li, Björn A. Persson, Mikael Lund, Johan Bergenholtz, and Malin Zackrisson Oskolkova. Concentration-Induced Association in a Protein System Caused by a Highly Directional Patch Attraction. *Journal of Physical Chemistry B*, 120(34):8953–8959, 2016.
- [208] Weimin Li, Maxim Morin, Emil Gustafsson, Björn A. Persson, Mikael Lund, and Malin Zackrisson Oskolkova. Strings and stripes formed by a protein system interacting via a single-patch attraction. *Soft Matter*, 12(46):9330–9333, 2016.
- [209] Theodore E. Brown, H. Eugene LeMay, and Bruce E. Bursten. *Chemistry: The Central Science*. Pearson Prentice Hall, Upper Saddle River, New Jersey, 10 edition, 2006.
- [210] Roger G. Bates. Determination of pH : theory and practice. In *Determination of pH : theory and practice*, page 435. John Wiley and Sons, Inc., New York, 1964.
- [211] Kennedy C. D. Ionic Strength and the Dissociation of Acids. *Biochemical Education*, 18(1):35–40, 1990.
- [212] Adrien Albert and E. P. Serjeant. *The Determination of Ionization Constants*. Chapman and Hall, New York, 3 edition, 1984.
- [213] Douglas A. Skoog, Donald M. West, F. James Holler, and Stanley R. Crouch. *Analytical Chemistry: An Introduction*. Brooks/Cole, Belmont, 7 edition, 2000.
- [214] Jetse Reijenga, Arno van Hoof, Antonie van Loon, and Bram Teunissen. Development of methods for the determination of pKa values. *Analytical Chemistry Insights*, 8(1):53–71, 2013.
- [215] Richard L. Thurlkill, Gerald R. Grimsley, J. Martin Scholtz, and C. Nick Pace. pK values of the ionizable groups of proteins. *Protein Science*, 15(5):1214–1218, 2006.
- [216] Gerald R. Grimsley, J. Martin Scholtz, and C. Nick Pace. A summary of the measured pK values of the ionizable groups in folded proteins. *Protein Science*, 18(1):247–251, 2009.
- [217] K.U. Linderstrøm-Lang. On the ionisation of proteins. *Comptes rendus des travaux du Laboratoire Carlsberg*, 15:1–29, 1924.
- [218] Charles Tanford, John G. Kirkwood, and Charles Tanford. Theory of Protein Titration Curves. I. General Equations for Impenetrable Spheres. *Journal of the American Chemical Society*, 79(20):5333–5339, 1957.
- [219] Yasuhiko Nozaki and Charles Tanford. Acid-Base titrations in con-

- centrated guanidine hydrochloride. Dissociation constants of the guanidinium ion and of some amino acids. *Journal of the American Chemical Society*, 89(4):736–742, 1967.
- [220] Arno Bundi and Kurt Wuthrich. ^1H -NMR Parameters of the Common Amino Acid Residues Measured in Aqueous Solutions of the Linear Tetrapeptides H-Gly-Gly-X-L-Ala-OH. *Biopolymers*, 18:285–297, 1979.
- [221] Thomas K. Harris and George J. Turner. Structural Basis of Perturbed pKa Values of Catalytic Groups in Enzyme Active Sites. *IUBMB Life*, pages 85–98, 2002.
- [222] Tõnu Kesvatera, Bo Joandnsson, Eva Thulin, and Sara Linse. Focusing of the electrostatic potential at EF-hands of calbindin D9k: Titration of acidic residues. *Proteins: Structure, Function and Genetics*, 45(2):129–135, 2001.
- [223] Sara Linse, Peter Brodin, Charlotta Johansson, Eva Thulin, Thomas Grundström, and Sture Forsén. The role of protein surface charges in ion binding. *Nature*, 335(6191):651–652, 1988.
- [224] Stina Lindman, Sara Linse, Frans A.A. Mulder, and Ingemar André. Electrostatic contributions to residue-specific protonation equilibria and proton binding capacitance for a small protein. *Biochemistry*, 45(47):13993–14002, 2006.
- [225] R. L. Croke, S. M. Patil, J. Quevreaux, D. a. Kendall, and a. T. Alexandrescu. NMR determination of pKa values in α -synuclein. *Protein Science*, 20(2):256–269, 2011.
- [226] J. R. Kanicky, A.F. Poniatowski, N. R. Mehta, and Shahm D. O. Cooperativity among Molecules at Interfaces in Relation to Various Technological Processes: Effect of Chain Length on the pKa of Fatty Acid Salt Solutions. *Langmuir*, 16(1):172–177, 2000.
- [227] Claire Tang, Andrew M. Smith, Richard F. Collins, Rein V. Ulijn, and Alberto Saiani. Fmoc-Diphenylalanine Self-Assembly Mechanism Induces Apparent pK a Shifts. *Langmuir*, 25(16):9447–9453, 2009.
- [228] Carlo Diaferia, Giancarlo Morelli, and Antonella Accardo. Fmoc-diphenylalanine as a suitable building block for the preparation of hybrid materials and their potential applications. *Journal of Materials Chemistry B*, 7(34):5142–5155, 2019.
- [229] Alexander K. Buell, Peter Hung, Xavier Salvatella, Mark E. Welland, Christopher M. Dobson, and Tuomas P J Knowles. Electrostatic Effects in Filamentous Protein Aggregation. *Biophysical Journal*, 104(5):1116–1126, 2013.
- [230] Axel Abelein, Jüri Jarvet, Andreas Barth, Astrid Gräslund, and Jens Danielsson. Ionic Strength Modulation of the Free Energy Landscape

- of A β ₄₀ Peptide Fibril Formation. *Journal of the American Chemical Society*, 138(21):6893–6902, 2016.
- [231] Ulyana Shimanovich, Aviad Levin, Dror Eliaz, Thomas Michaels, Zenon Toprakcioglu, Birgitta Frohm, Erwin De Genst, Sara Linse, Karin S. Åkerfeldt, and Tuomas P.J. Knowles. pH-Responsive Capsules with a Fibril Scaffold Shell Assembled from an Amyloidogenic Peptide. *Small*, 17(26):1–9, 2021.
- [232] Kevin W. Tipping, Theodoros K. Karamanos, Toral Jakhria, Matthew G. Iadanza, Sophia C. Goodchild, Roman Tuma, Neil A. Ranson, Eric W. Hewitt, and Sheena E. Radford. pH-induced molecular shedding drives the formation of amyloid fibril-derived oligomers. *Proceedings of the National Academy of Sciences of the United States of America*, 112(18):E5691–E5696, 2015.
- [233] Harish Shukla, Ranjeet Kumar, Amit Sonkar, Kalyan Mitra, Md Sohail Akhtar, and Timir Tripathi. Salt-regulated reversible fibrillation of Mycobacterium tuberculosis isocitrate lyase: Concurrent restoration of structure and activity. *International Journal of Biological Macromolecules*, 104:89–96, 2017.
- [234] Wolfgang Hoyer, Thomas Antony, Dmitry Cherny, Gudrun Heim, Thomas M. Jovin, and Vinod Subramaniam. Dependence of α -synuclein aggregate morphology on solution conditions. *Journal of Molecular Biology*, 322(2):383–393, 2002.
- [235] Claudio O. Fernández, Wolfgang Hoyer, Maricus Zweckstetter, Elizabeth A. Jares-Erijman, Vinod Subramaniam, Christian Griesinger, and Thomas M. Jovin. NMR of α -synuclein-polyamine complexes elucidates the mechanism and kinetics of induced aggregation. *EMBO Journal*, 23(10):2039–2046, 2004.
- [236] Thomas Antony, Wolfgang Hoyer, Dmitry Cherny, Gudrun Heim, Thomas M. Jovin, and Vinod Subramaniam. Cellular polyamines promote the aggregation of α -synuclein. *Journal of Biological Chemistry*, 278(5):3235–3240, 2003.
- [237] Maria Zacharopoulou, Neeleema Seetaloo, James Ross, Amberley D Stephens, Thomas M Mccoy, Wenyue Dai, Ioanna Mela, Ana Fernandez Ville, Anne Martel, Alexander F Routh, Alfonso De Simone, Jonathan J Phillips, and Gabriele S Kaminski Schierle. Local ionic conditions modulate the aggregation propensity and influence the structural polymorphism of alpha-synuclein. *bioRxiv*, 2024.
- [238] Rachel Lowe, Dean L. Pountney, Poul Henning Jensen, Wei Ping Gai, and Nicolas H. Voelcker. Calcium(II) selectively induces α -synuclein

- annular oligomers via interaction with the C-terminal domain. *Protein Science*, 13(12):3245–3252, 2004.
- [239] Rafael Ramis, Joaquín Ortega-Castro, Bartolomé Vilanova, Miquel Adrover, and Juan Frau. Cu²⁺, Ca²⁺, and methionine oxidation expose the hydrophobic α -synuclein NAC domain. *International Journal of Biological Macromolecules*, 169:251–263, 2021.
- [240] Brett H. Pogostin, Sara Linse, and Ulf Olsson. Fibril Charge Affects α -Synuclein Hydrogel Rheological Properties. *Langmuir*, 35(50):16536–16544, 2019.
- [241] Kuen Phon Wu, Daniel S. Weinstock, Chitra Narayanan, Ronald M. Levy, and Jean Baum. Structural Reorganization of α -Synuclein at Low pH Observed by NMR and REMD Simulations. *Journal of Molecular Biology*, 391(4):784–796, 2009.
- [242] Matthew M. Dedmon, Kresten Lindorff-Larsen, John Christodoulou, Michele Vendruscolo, and Christopher M. Dobson. Mapping long-range interactions in α -synuclein using spin-label NMR and ensemble molecular dynamics simulations. *Journal of the American Chemical Society*, 127(2):476–477, 2005.
- [243] Caroline M. Ritchie and Philip J. Thomas. Alpha-synuclein truncation and disease. *Health*, 04(11):1167–1177, 2012.
- [244] Giuliana Fusco, Alfonso De Simone, Paolo Arosio, Michele Vendruscolo, Gianluigi Veglia, and Christopher M. Dobson. Structural Ensembles of Membrane-bound α -Synuclein Reveal the Molecular Determinants of Synaptic Vesicle Affinity. *Scientific Reports*, 6:1–9, 2016.
- [245] Joseph T. Jarrett, Philip R. Costa, Robert G. Griffin, and Peter T. Lansbury. Models of the β Protein C-Terminus: Differences] in Amyloid Structure May Lead to Segregation of “Long” and “Short” Fibrils. *Journal of the American Chemical Society*, 116(21):9741–9742, 1994.
- [246] Max Lindberg, Emil Axell, Emma Sparr, and Sara Linse. A label-free high-throughput protein solubility assay and its application to A β ₄₀. *Biophysical Chemistry*, 307(January), 2024.
- [247] Sofia Lövestam, David Li, Jane L. Wagstaff, Abhay Kotecha, Dari Kimanius, Stephen H. McLaughlin, Alexey G. Murzin, Stefan M.V. Freund, Michel Goedert, and Sjors H.W. Scheres. Disease-specific tau filaments assemble via polymorphic intermediates. *Nature*, 625(7993):119–125, 2024.
- [248] Arshdeep Sidhu, Ine Segers-Nolten, Vincent Raussens, Mireille M.A.E. Claessens, and Vinod Subramaniam. Distinct Mechanisms Determine α -Synuclein Fibril Morphology during Growth and Maturation. *ACS Chemical Neuroscience*, 8(3):538–547, 2017.

- [249] Ronald Wetzel. Kinetics and thermodynamics of amyloid fibril assembly. *Accounts of Chemical Research*, 39(9):671–679, 2006.
- [250] Brian O’Nuallain, Shankaramma Shivaprasad, Indu Kheterpal, and Ronald Wetzel. Thermodynamics of A β (1-40) amyloid fibril elongation. *Biochemistry*, 44(38):12709–12718, 2005.
- [251] Tatsuya Ikenoue, Young Ho Lee, József Kardos, Miyu Saiki, Hisashi Yagi, Yasushi Kawata, and Yuji Goto. Cold denaturation of α -synuclein amyloid fibrils. *Angewandte Chemie - International Edition*, 53(30):7799–7804, 2014.
- [252] József Kardos, András Micsonai, Henriett Pál-Gábor, Éva Petrik, László Gráf, János Kovács, Young Ho Lee, Hironobu Naiki, and Yuji Goto. Reversible heat-induced dissociation of β 2-microglobulin amyloid fibrils. *Biochemistry*, 50(15):3211–3220, 2011.
- [253] Rasmus K. Norrild, Nicola Vettore, Alberto Coden, Wei Feng Xue, and Alexander K. Buell. Thermodynamics of amyloid fibril formation from non-equilibrium experiments of growth and dissociation. *Biophysical Chemistry*, 271(January), 2021.
- [254] Azad Farzadfard, Antonin Kunka, Thomas Oliver Mason, Jacob Aunstrup Larsen, Rasmus Krogh Norrild, Elisa Torrescasana Dominguez, Soumik Ray, and Alexander K. Buell. Thermodynamic characterization of amyloid polymorphism by microfluidic transient incomplete separation. *Chemical Science*, 15(7):2528–2544, 2024.
- [255] Nicola Vettore and Alexander K. Buell. Thermodynamics of amyloid fibril formation from chemical depolymerization. *Physical Chemistry Chemical Physics*, 21(47):26184–26194, 2019.
- [256] Tomas Sneideris, Katażyna Milto, and Vytautas Smirnovas. Polymorphism of amyloid-like fibrils can be defined by the concentration of seeds. *PeerJ*, 3, 2015.
- [257] Nasrollah Rezaei-Ghaleh, Mehriar Amininasab, Sathish Kumar, Jochen Walter, and Markus Zweckstetter. Phosphorylation modifies the molecular stability of β -amyloid deposits. *Nature Communications*, 7:1–9, 2016.
- [258] Débora Foguel, Marisa C. Suarez, Astria D. Ferrão-Gonzales, Thais C.R. Porto, Leonardo Palmieri, Carla M. Einsiedler, Leonardo R. Andrade, Hilal A. Lashuel, Peter T. Lansbury, Jeffery W. Kelly, and Jerson L. Silva. Dissociation of amyloid fibrils of α -synuclein and transthyretin by pressure reveals their reversible nature and the formation of water-excluded cavities. *Proceedings of the National Academy of Sciences of the United States of America*, 100(17):9831–9836, 2003.
- [259] Samuel I.A. Cohen, Paolo Arosio, Jenny Presto, Firoz Roshan Kurundenkandy, Henrik Biverstål, Lisa Dolfe, Christopher Dunning, Xiaot-

- ing Yang, Birgitta Frohm, Michele Vendruscolo, Jan Johansson, Christopher M. Dobson, André Fisahn, Tuomas P.J. Knowles, and Sara Linse. A molecular chaperone breaks the catalytic cycle that generates toxic A β oligomers. *Nature Structural and Molecular Biology*, 22(3):207–213, 2015.
- [260] Charles R. Cantor and Paul R. Schimmel. *Biophysical Chemistry: Part II: Techniques for the Study of Biological Structure and Function*. W. H. Freeman and Company, San Francisco, 1 edition, 1980.
- [261] Matthew Biancalana, Koki Makabe, Akiko Koide, and Shohei Koide. Molecular Mechanism of Thioflavin-T Binding to the Surface of β -Rich Peptide Self-Assemblies. *Journal of Molecular Biology*, 385(4):1052–1063, 2009.
- [262] Matthew Biancalana and Shohei Koide. Molecular Mechanism of Thioflavin-T Binding to Amyloid Fibrils. *Biochimica et Biophysica Acta*, 1804(7):1405–1412, 2010.
- [263] E. S. Voropai, M. P. Samtsov, K. N. Kaplevskii, A. A. Maskevich, V. I. Stepuro, O. I. Povarova, I. M. Kuznetsova, K. K. Turoverov, A. L. Fink, and V. N. Uverskii. Spectral properties of thioflavin T and its complexes with amyloid fibrils. *Journal of Applied Spectroscopy*, 70(6):868–874, 2003.
- [264] Hironobu Naiki, Keiichi Higuchi, Masanori Hosokawa, and Toshio Takeda. Fluorometric determination of amyloid fibrils in vitro using the fluorescent dye, thioflavine T. *Analytical Biochemistry*, 177(2):244–249, 1989.
- [265] Nadine D. Younan and John H. Viles. A Comparison of Three Fluorophores for the Detection of Amyloid Fibers and Prefibrillar Oligomeric Assemblies. ThT (Thioflavin T); ANS (1-Anilinonaphthalene-8-sulfonic Acid); and bisANS (4,4'-Dianilino-1,1'-binaphthyl-5,5'-disulfonic Acid). *Biochemistry*, 54(28):4297–4306, 2015.
- [266] Norma Greenfield and Gerald D. Fasman. Computed Circular Dichroism Spectra for the Evaluation of Protein Conformation. *Biochemistry*, 8(10):4108–4116, 1969.
- [267] Helmut Sigel, Andreas D. Zuberbühler, and Osamu Yamauchi. Comments on potentiometric pH titrations and the relationship between pH-meter reading and hydrogen ion concentration. *Analytica Chimica Acta*, 255(1):63–72, 1991.
- [268] John L. Markley. Observation of Histidine Residues in Proteins by Means of Nuclear Magnetic Resonance Spectroscopy. *Accounts of Chemical Research*, 8(2):70–80, 1975.
- [269] D.H. Sachs, A.N. Schechter, and J.S. Cohen. Nuclear Magnetic Resonance Titration Curves of Histidine Ring Protons. I. Influence of Neigh-

- boring Charged Groups. *Journal of Biological Chemistry*, 246(21):6576–6580, 1971.
- [270] K.J. Leidler, J.H. Meiser, and B.C. Sanctuary. *Physical Chemistry*. Houghton Mifflin Company, Boston, 2003.
- [271] Alessia Peduzzo, Sara Linse, and Alexander K. Buell. The Properties of α -Synuclein Secondary Nuclei Are Dominated by the Solution Conditions Rather than the Seed Fibril Strain. *ACS Chemical Neuroscience*, 11(6):909–918, 2020.
- [272] Rafael Fernandez-Leiro and Sjors H.W. Scheres. Unravelling biological macromolecules with cryo-electron microscopy. *Nature*, 537(7620):339–346, 2016.
- [273] R Henderson and P.N.T. Unwin. Three-dimensional model of purple membrane obtained by electron microscopy. *Nature*, 257:28–32, 1975.
- [274] Emma E. Cawood, Theodoros K. Karamanos, Andrew J. Wilson, and Sheena E. Radford. Visualizing and trapping transient oligomers in amyloid assembly pathways. *Biophysical Chemistry*, 268:106505:106505, 2021.
- [275] Asad Jan, Dean M. Hartley, and Hilal A. Lashuel. Preparation and characterization of toxic $\alpha\beta$ aggregates for structural and functional studies in alzheimer’s disease research. *Nature Protocols*, 5(6):1186–1209, 2010.
- [276] Erwin De Genst, Anne Messer, and Christopher M. Dobson. Antibodies and protein misfolding: From structural research tools to therapeutic strategies. *Biochimica et Biophysica Acta - Proteins and Proteomics*, 1844(11):1907–1919, 2014.
- [277] Shan S. Wong and Lee Jun C. Wong. Chemical crosslinking and the stabilization of proteins and enzymes. *Enzyme and Microbial Technology*, 14(11):866–874, 1992.
- [278] Francesco Simone Ruggeri, Johnny Habchi, Andrea Cerreta, and Giovanni Dietler. AFM-Based Single Molecule Techniques: Unraveling the Amyloid Pathogenic Species. *Current Pharmaceutical Design*, 22(26):3950–3970, 2016.
- [279] Mathew H. Horrocks, Laura Tosatto, Alexander J. Dear, Gonzalo A. Garcia, Marija Iljina, Nunilo Cremades, Mauro Dalla Serra, Tuomas P.J. Knowles, Christopher M. Dobson, and David Klenerman. Fast Flow Microfluidics and Single-Molecule Fluorescence for the Rapid Characterization of α -Synuclein Oligomers. *Analytical Chemistry*, 87(17):8818–8826, 2015.
- [280] Andrea Sinz. Chemical cross-linking and mass spectrometry for mapping three-dimensional structures of proteins and protein complexes. *Journal of Mass Spectrometry*, 38(12):1225–1237, 2003.
- [281] Gal Bitan, Aleksey Lomakin, and David B. Teplow. Amyloid β -protein

- oligomerization: Prenucleation interactions revealed by photo-induced cross-linking of unmodified proteins. *Journal of Biological Chemistry*, 276(37):35176–35184, 2001.
- [282] George W. Preston and Andrew J. Wilson. Photo-induced covalent cross-linking for the analysis of biomolecular interactions. *Chemical Society Reviews*, 42(8):3289–3301, 2013.
- [283] Farid Rahimi, Panchanan Maiti, and Gal Bitan. Photo-induced cross-linking of unmodified proteins (PICUP) applied to amyloidogenic peptides. *Journal of Visualized Experiments*, (23):10–12, 2009.
- [284] Karine Deville, Vicki A.M. Gold, Alice Robson, Sarah Whitehouse, Richard B. Sessions, Stephen A. Baldwin, Sheena E. Radford, and Ian Collinson. The oligomeric state and arrangement of the active bacterial translocon. *Journal of Biological Chemistry*, 286(6):4659–4669, 2011.
- [285] H. J. Lin and Thomas Kodadek. Photo-induced oxidative cross-linking as a method to evaluate the specificity of protein-ligand interactions. *Journal of Peptide Research*, 65(2):221–228, 2005.
- [286] Reema Piparia, David Ouellette, W. Blaine Stine, Christine Grinnell, Edit Tarcsa, Czeslaw Radziejewski, and Ivan Correia. A high throughput capillary electrophoresis method to obtain pharmacokinetics and quality attributes of a therapeutic molecule in circulation. *mAbs*, 4(4):521–531, 2012.
- [287] Cornelia Rosu, Rafael Cueto, and Paul S. Russo. Poly(colloid)s: "polymerization" of Poly(l -tyrosine)-silica Composite Particles through the Photoinduced Cross-Linking of Unmodified Proteins Method. *Langmuir*, 32(33):8392–8402, 2016.
- [288] Winny Ariesandi, Chi Fon Chang, Tseng Erh Chen, and Yun Ru Chen. Temperature-Dependent Structural Changes of Parkinson's Alpha-Synuclein Reveal the Role of Pre-Existing Oligomers in Alpha-Synuclein Fibrillization. *PLoS ONE*, 8(1), 2013.
- [289] Wei Ting Chen, Yi Hung Liao, Hui Ming Yu, Irene H. Cheng, and Yun Ru Chen. Distinct effects of Zn²⁺, Cu²⁺, Fe³⁺, and Al³⁺ on amyloid- β stability, oligomerization, and aggregation: Amyloid- β destabilization promotes annular protofibril formation. *Journal of Biological Chemistry*, 286(11):9646–9656, 2011.
- [290] Yu Jen Chang and Yun Ru Chen. The coexistence of an equal amount of Alzheimer's amyloid- β 40 and 42 forms structurally stable and toxic oligomers through a distinct pathway. *FEBS Journal*, 281(11):2674–2687, 2014.
- [291] Kenjiro Ono, Margaret M. Condrón, and David B. Teplow. Structure-neurotoxicity relationships of amyloid β -protein oligomers. *Proceed-*

- ings of the National Academy of Sciences of the United States of America*, 106(35):14745–14750, 2009.
- [292] Kenjiro Ono, Tokuhei Ikeda, Jun ichi Takasaki, and Masahito Yamada. Familial Parkinson disease mutations influence α -Synuclein assembly. *Neurobiology of Disease*, 43(3):715–724, 2011.
- [293] Eric Y. Hayden, Joseph L. Conovaloff, Ashley Mason, Gal Bitan, and David B. Teplow. Preparation of pure populations of covalently stabilized amyloid β -protein oligomers of specific sizes. *Analytical Biochemistry*, 518:78–85, 2017.

Scientific publications

